October 2000 Flood Reconstruction Using Precipitation, Indirect, Satellite, and Geomorphic Information

Report submitted to:

Flood Control District of Maricopa County

FCD2000C013, Assignment No. 8

Report prepared by

JE FULLER
HYDROLOGY & GEOMORPHOLOGY, INC.

6101 S. Rural Road, Suite 110
Tempe, AZ 85283
www.jefuller.com

In association with:

Larry Mayer, Ph.D.
University of Arizona

Arizona Geological Survey

February 2002

October 2000 Flood Reconstruction Using Precipitation, Indirect, Satellite, and Geomorphic Information

Property of
Flood Control District of MC Library
Please Return to
2801 W. Durango
Phoenix, AZ 85009

Report submitted to

Flood Control District of Maricopa County

for

FCD2000C013, Assignment No. 8

Registered Professional Engineer (Civil)
CERTIFICATE NO.
35895
TED W.
LEHMAN
Date Signed 2-26-02
ARIZONA U.S.A.

Submitted by

JE FULLER
HYDROLOGY & GEOMORPHOLOGY, INC.

6101 S. Rural Road, Suite 110
Tempe, AZ 85283
(480) 752-2124 voice
(480) 839-2193 fax
www.jefuller.com

in association with

Dr. Larry Mayer
University of Arizona

Arizona Geological Survey

February 2002

Table of Contents

1. INTRODUCTION 1

1.1 PURPOSE/BACKGROUND 1

2. STORM RAINFALL RECONSTRUCTION 3

2.1 DEPTHS 3

2.1.1 Radar 3

2.1.2 ALERT gages 6

2.2 AREA 7

2.2.1 Depth-Area Relationships 7

2.3 TEMPORAL DISTRIBUTIONS 10

2.3.1 Oct. 21-22, 2000 10

2.3.2 Oct. 27, 2000 11

2.3.3 Comparison to "100-year storm" 12

2.4 STATISTICAL ANALYSES 13

2.4.1 Results 15

3. STORM RUNOFF RECONSTRUCTION 16

3.1 STREAM GAGE DATA 16

3.2 HEC-1 MODEL RECONSTRUCTIONS 16

3.2.1 Modifications to FIS model 16

3.2.2 October 21-22 Storm 18

3.2.3 October 27 Storm 21

3.2.4 Summary 24

3.3 INDIRECT DISCHARGE ESTIMATES 24

3.3.1 Physiographic Description 24

3.3.2 FCDMC Indirect Estimates 30

3.3.3 USGS Indirect Estimates 31

3.3.4 JEF Indirect Estimates 31

3.4 STATISTICAL ANALYSIS 35

3.4.1 Non-Exceedence Analysis 37

3.4.2 Results 40

4. LANDSAT BASED FLOOD DETECTION 40

5. GEOMORPHIC ANALYSIS 42

6. FLOOD INUNDATION LIMITS 45

6.1 LANDSAT VS. AERIAL PHOTO ANALYSIS 45

6.2 AERIAL PHOTO VS. FIS 100-YEAR ANALYSIS 48

7. CONCLUSIONS 51

8. REFERENCES 52

Registered Professional Engineer (Civil)
CERTIFICATE NO.
35895
TED W.
LEHMAN
Date Signed 2-26-02
ARIZONA U.S.A.

List of Figures

Figure 1. Vicinity map of the study area: Jackrabbit Wash watershed....1
Figure 2. Locations of indirect discharge estimates....2
Figure 3. October 21, 2000 NEXRAD image showing the area of highest rainfall....4
Figure 4. October 27, 2000 NEXRAD image showing the area of highest rainfall....5
Figure 5. FCDMC rain gage locations near the Jackrabbit Wash watershed....6
Figure 6. Isopluvial plots for the October 27 NEXRAD storm map....8
Figure 7. Comparison of FCDMC 6-hr Depth-Area Reduction Factors and Depth-Area Relation for 10-27-00 Storm....9
Figure 8. Comparison of Rainfall Depth vs. Drainage Area for FIS models, reconstructed HEC-1 models, and Isopluvials interpreted from NEXRAD. The red circles highlight the comparison points discussed. 10
Figure 9. Cumulative rainfall for FCDMC ALERT stations near Jackrabbit Wash watershed, Oct. 21-22, 2000....11
Figure 10. Cumulative rainfall for FCDMC ALERT stations near Jackrabbit Wash watershed, Oct. 27, 2000....12
Figure 11. Normalized comparison of temporal distributions....13
Figure 12. New sub-basin and split flow location....17
Figure 13. 30-day prior cumulative rainfall for FCDMC gages shown in Figure 5....18
Figure 14. Physiographic sub-basin delineation....25
Figure 15. Soil hydraulic conductivity for sub-basins A, B, and C....26
Figure 16. Location of stock tanks within sub-basin A....27
Figure 18. Distribution of percent bedrock outcrop for sub-basins A, B, and C....28
Figure 19. Sub-basin drainage densities....29
Figure 21. Channel reach locations of JEF indirect discharge estimates....32
Figure 22. Plot comparison of JEF cross-section 1 with FCDMC cross-section 9....33
Figure 23. Plot comparison of JEF cross-section 3 with FCDMC cross-section 8....33
Figure 24. Flood frequency analysis for gage data through Water Year 2000....36
Figure 25. Flood frequency analysis for gage data through Water Year 2001....36
Figure 24. Cross-section 7 from FCDMC December 2000 survey showing Ql non-exceedence surface....37
Figure 25. Probability distribution plot from FLDFRQ3 analysis including non-exceedence information....39
Figure 26. Peak discharge verses drainage area envelope curves for the U.S. and the lower Colorado River region (House and Baker, 2001)....40
Figure 27. Jackrabbit Wash Landsat change image taken after the October 2000 flood....41
Figure 30. Surficial geologic map of Jackrabbit Wash at the Vulture Mine Road crossing....43
Figure 29. Area with minor adjustments to Landsat flood inundation limits....46
Figure 30. Area requiring greater adjustment to Landsat flood inundation limits....47
Figure 31. Example of flood inundation limits exceeding the FIS floodplain limits....49
Figure 32. FCDMC high water marks in comparison with FIS 100-year limits....50

Registered Professional Engineer (Civil)
CERTIFICATE NO.
35895
TED W.
LEHMAN
Date Signed 2-26-02
ARIZONA U.S.A.

List of Tables

Table 1. Total cumulative rainfall for October 21 and 27 storms 7
Table 2. Maximum point rainfall from FCDMC rain gage data 14
Table 3. Maximum point rainfall from NEXRAD radar data 14
Table 4. Weighted average sub-basin rainfall 14
Table 5. Equivalent point rainfall and estimated return period for rain gage storm duration 14
Table 6. Depth-duration frequency matrix for Jackrabbit Wash 15
Table 7. "Dry" condition HEC-1 comparison for October 21-22 storm 19
Table 8. "Normal" condition HEC-1 comparison for the October 21 storm 20
Table 9. "Dry" condition HEC-1 comparison for the October 27, 2000 storm 21
Table 10. Comparison of "normal" condition HEC-1 for the October 27, 2000 storm 22
Table 11. Comparison of "wet" condition HEC-1 models for the October 27, 2000 storm 23
Table 12. Results for the SCS IIA distribution in the FIS HEC-1 model 23
Table 13. NEH seasonal rainfall limits for antecedent moisture conditions 24
Table 14. Summary of the hydrologic characteristics analyzed 30
Table 16. Individual results of physiographic analysis in comparison with indirect estimates 30
Table 17. Cross-section comparison of FCDMC and JEF indirect data 34
Table 18. Comparison summary of FCDMC and JEF indirects 34
Table 19. Comparison of discharge estimates for Jackrabbit Wash *(statistical data is shaded)* 35
Table 20. FLDFRQ3 results for non-exceedence analysis 38

Appendices

Appendix A. Indirect Discharge Estimates
Appendix B. *Landsat based flood detection in the jackrabbit Wash Are, Maricopa County, Arizona*
By: Larry Mayer, Ph.D., University of Arizona
Appendix C. *Geomorphologic Assessment of the October 2000 Flood on Jackrabbit Wash, Maricopa County, Arizona*
By: Philip A. Pearthree and Ann Youberg, Arizona Geologic Survey
Appendix D. FLDFRQ3 input and output files
Appendix E. CD-ROM containing – HEC-1 models for October 2000 storms and other digital data from this study

Primary Authors

JE Fuller Hydrology & Geomorphology, Inc.
-Ted Lehman, P.E., M.A.
-Mike Kellogg, M.S.

Arizona Geological Survey
-Philip A. Pearthree, Ph.D.
-Ann Youberg, M.S.

Larry Mayer, Ph.D.
University of Arizona
Dept. of Geosciences

1. Introduction

This report was prepared by a team consisting of JE Fuller/ Hydrology & Geomorphology, Inc. (JEF), the Arizona Geological Survey (AZGS), and Dr. Larry Mayer of the University of Arizona for the Flood Control District of Maricopa County (FCDMC) under contract FCD 2000C013, Assignment No. 8. Dr. Mayer and the AZGS produced separate reports for their parts of the study, which are included in their entirety as Appendices. The important aspects and conclusions of their reports are summarized in the main body of the report.

1.1 Purpose/background

The purpose of this report was to investigate the characteristics of a very large flood that occurred in October 2000 on Jackrabbit Wash in western Maricopa County, Arizona (Figure 1).

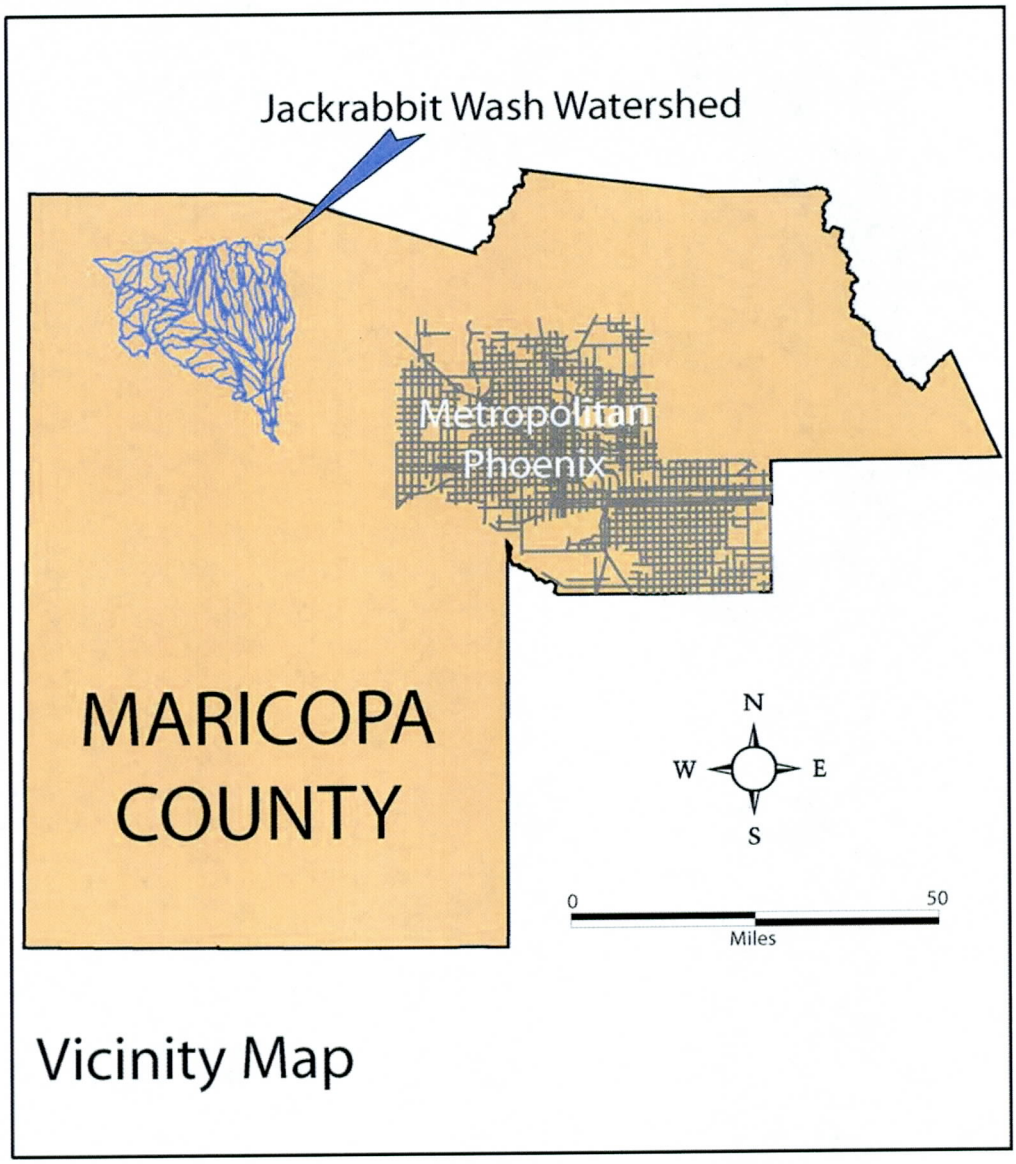

Figure 1. Vicinity map of the study area: Jackrabbit Wash watershed

During the installation of a new stream gage on Jackrabbit Wash near Vulture Mine Road on November 1, 2000, FCDMC personnel discovered evidence of very large, recent flood. Subsequently, the FCDMC and USGS conducted slope-area surveys which resulted in the following peak discharge estimates:

- FCDMC = 32,400 cfs at Vulture Mine Rd.
- USGS = 27,000 cfs at USGS gage (09516800) downstream of Wickenburg Rd.

The location of the indirect sites are shown in Figure 2.

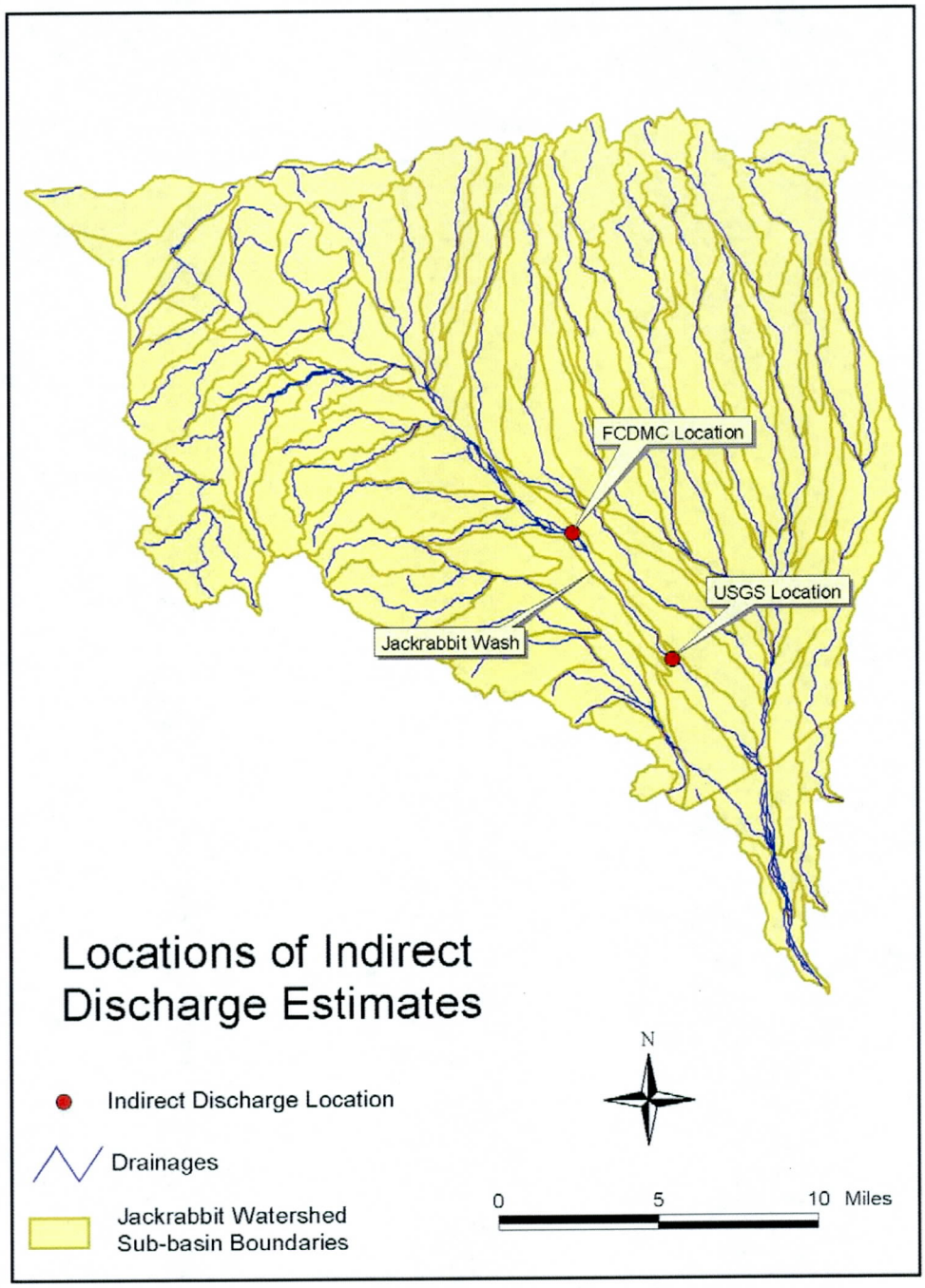

Figure 2. Locations of indirect discharge estimates

The JEF team was asked to investigate the characteristics of the October 2000 flood on Jackrabbit Wash in more detail than the FCDMC and USGS initial studies. In particular, the team was to:

- Examine weather radar and precipitation gage data describing the storm rainfall.
- Conduct additional indirect estimates of peak discharge at other locations in the watershed.
- Identify areas of surface change using Landsat satellite data to identify the flood inundation limits.
- Compare mapped inundation areas with geomorphic maps and Flood Insurance Study delineations.
- Provide a geologic and historical context for the extent, magnitude, frequency, and source area of the flood.

2. Storm Rainfall Reconstruction

NEXRAD radar data and ALERT precipitation gage data were examined to more clearly define the time(s) at which flood producing rainfall occurred in October 2000. The first discovery was that two separate large rainfall events occurred in October 2000 which could have been responsible for the significant flooding on Jackrabbit Wash. The first period of rainfall was between about 1200 October 21 to 1200 October 22. A second period of significant rainfall occurred between about 0400 to 1600 on October 27, 2000.

2.1 Depths

Rainfall depths for both October 2000 storms were reconstructed from National Weather Service (NWS) NEXRAD radar and FCDMC ALERT precipitation gage data. Data were collected for the end of October 2000 to identify the location and quantity of rainfall in the watershed.

2.1.1 Radar

NEXRAD images from the October 2000 storms were requested from the National Climatic Data Center (NCDC) archives, but the NCDC reported that the data for the dates of interest were missing from the archives. Therefore, similar data were collected from the local National Weather Service (NWS) office. The Phoenix NWS office was able to recover a limited number of images from their database which were of interest to this project. The most valuable images were radar estimates of total storm precipitation depths for the area. Color printouts provided to JEF by the NWS were scanned and fitted into their approximate geographic position over the watershed (Figure 3 and Figure 4). Spatial correlation of Jackrabbit Wash itself on the radar image and in the GIS database in the upper watershed shows reasonable correspondence.

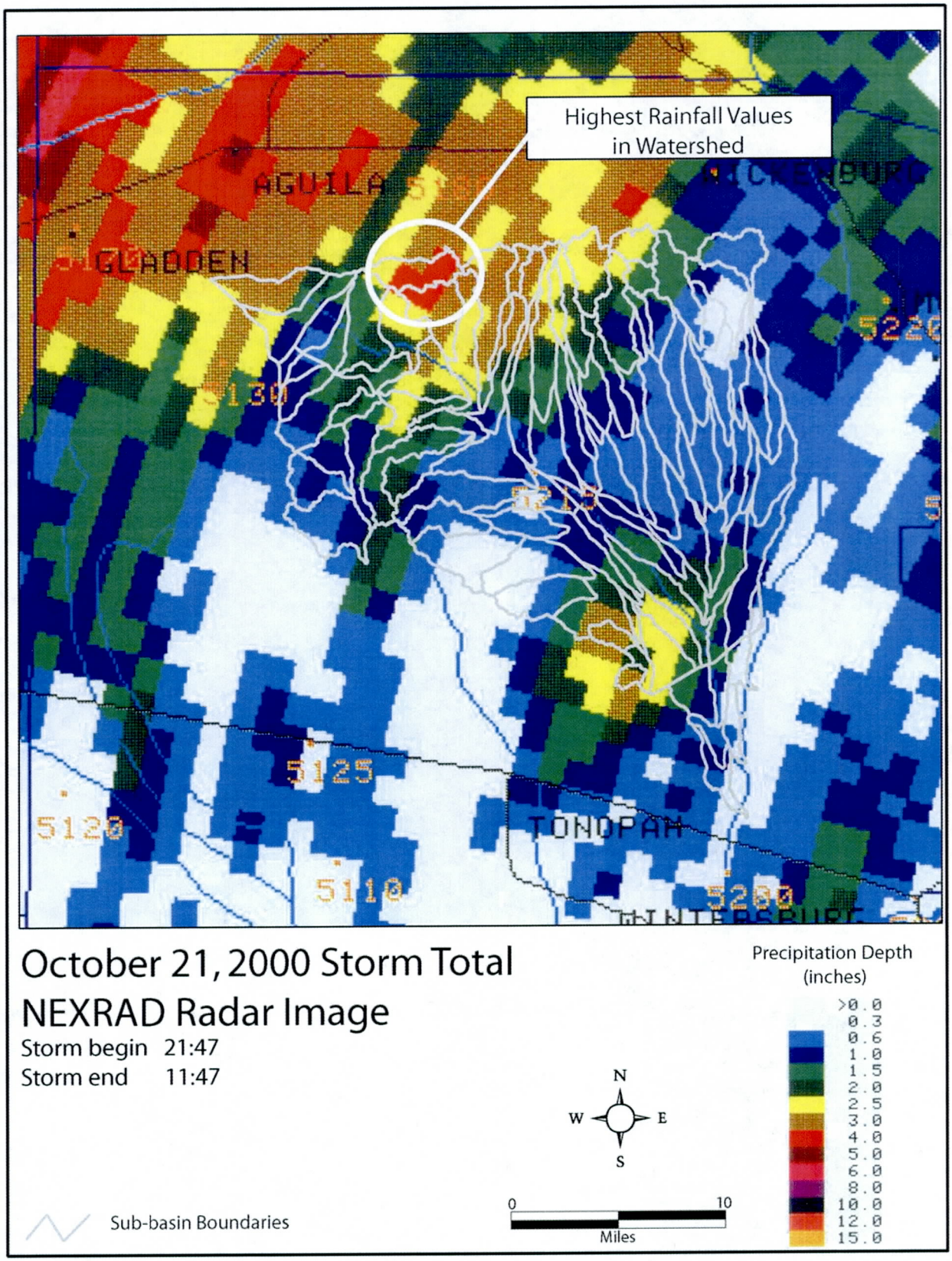

Figure 3. October 21, 2000 NEXRAD image showing the area of highest rainfall

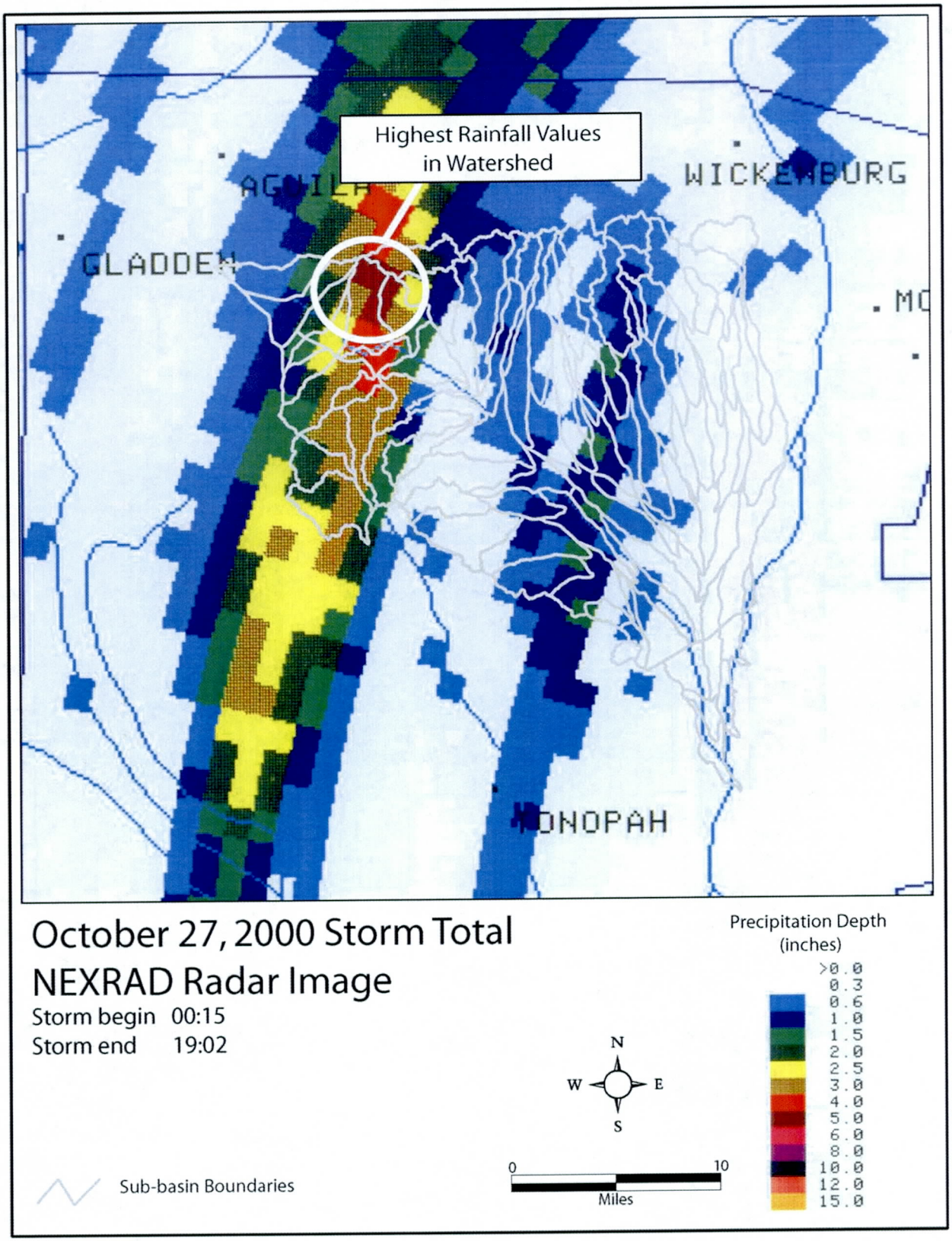

Figure 4. October 27, 2000 NEXRAD image showing the area of highest rainfall

2.1.2 ALERT gages

The FCDMC also operates a large network of precipitation gages in Maricopa County. Figure 5 shows the location of rain gages near Jackrabbit Wash. Unfortunately, the coverage within the watershed is not as dense as other areas of Maricopa County, with only two gages in the watershed and seven near the perimeter.

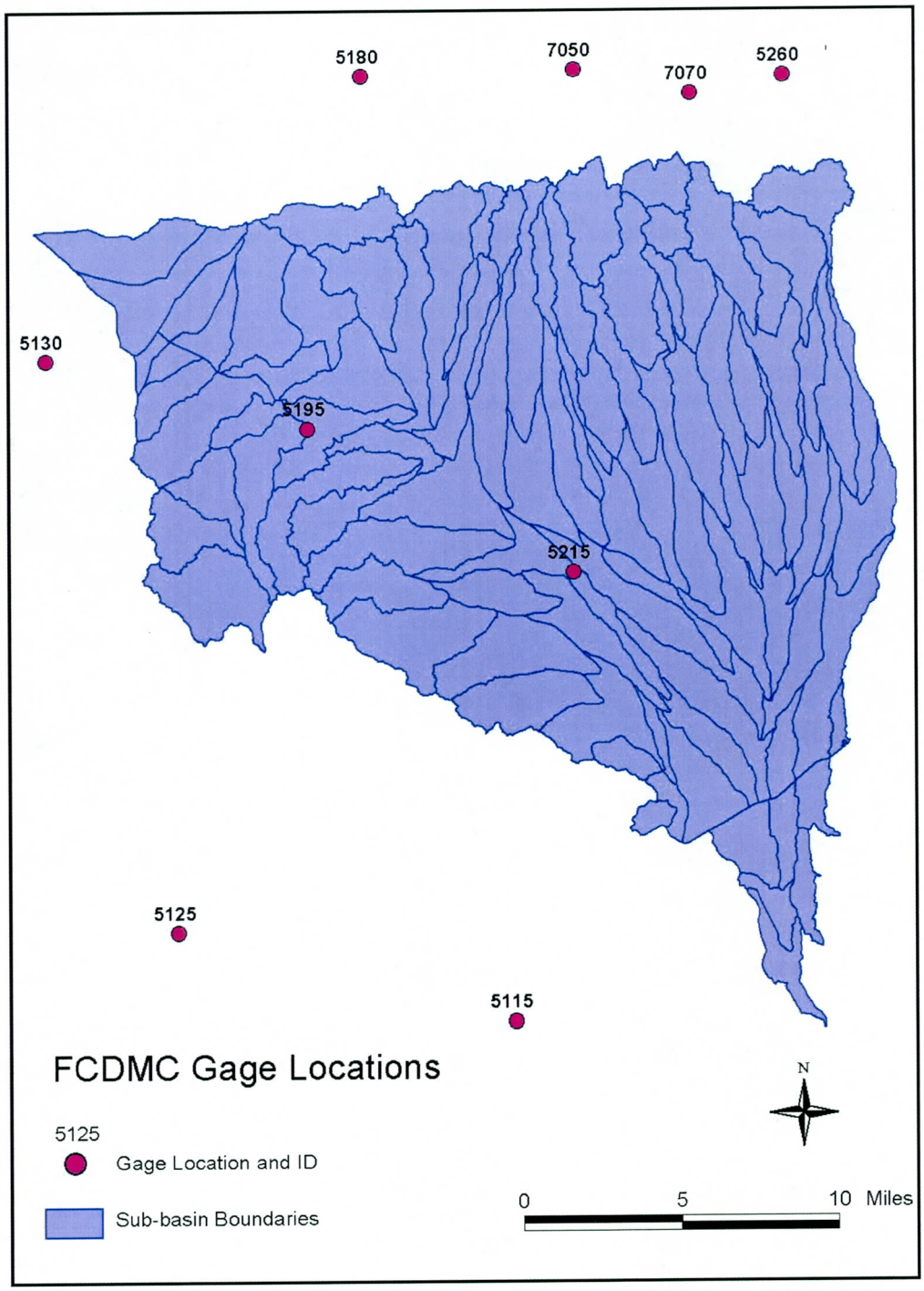

Figure 5. FCDMC rain gage locations near the Jackrabbit Wash watershed

Table 1 summarizes the October 2000 storm precipitation depth totals for the FCDMC rain gages shown in Figure 5.

Table 1. Total cumulative rainfall for October 21 and 27 storms

FCDMC Rain Gage ID	October 21 Storm Total (inches)	October 27 Storm Total (inches)
5115	0.56	0.80
5125	0.80	1.67
5130	2.79	0.72
5180	2.52	2.58
5195	Not Installed[1]	Not Installed
5215	0.52	0.60
5260	1.32	0.96
7050	2.28	1.24
7070	3.86	1.20

2.2 Area

A comparison of the depth-area reduction factors from the October 27 storm and the synthetic FCDMC 6-hour storm was conducted and is discussed in Section 2.2.1. Analysis of rain gage depth-duration data showed the October 21 storm, although greater in overall rainfall depth, was much longer in duration than the 27th storm, which was characterized by a shorter duration but higher intensity than the 21st storm (discussed in Section 2.3). This indicates the peak discharge related to the high water mark along Jackrabbit Wash was more likely associated with the October 27 event. Therefore, only the aerial reduction data from the October 27 storm is discussed below.

2.2.1 Depth-Area Relationships

Figure 6 shows the isopluvial plots from the NEXRAD map for the October 27 storm. Areas calculated from these plots were used to compute the depth-area relationship for this storm. The rain gage temporal distribution indicates the duration of the October 21 and 27 storms were about twelve hours and three hours respectively. The depth-area reduction curves for these durations were derived from HYDRO-40 (Zehr and Myers, 1984). Figure 7 is a comparison of depth-area reduction factors for the October 27 storm, HYDRO-40 3-hour and 12-hour, and the FCDMC synthetic 6-hour design storm. The results show the reduction factors for the October 27 storm are significantly less than the synthetic values for the same area, indicating the most intense area of rainfall was spatially smaller than the FCDMC synthetic 6-hour storm. Figure 7 also shows that the October 27th storm had a similar spatial decay pattern to the HYDRO-40 3-hour storm.

[1] Gage 5195 was installed on November 1, 2000

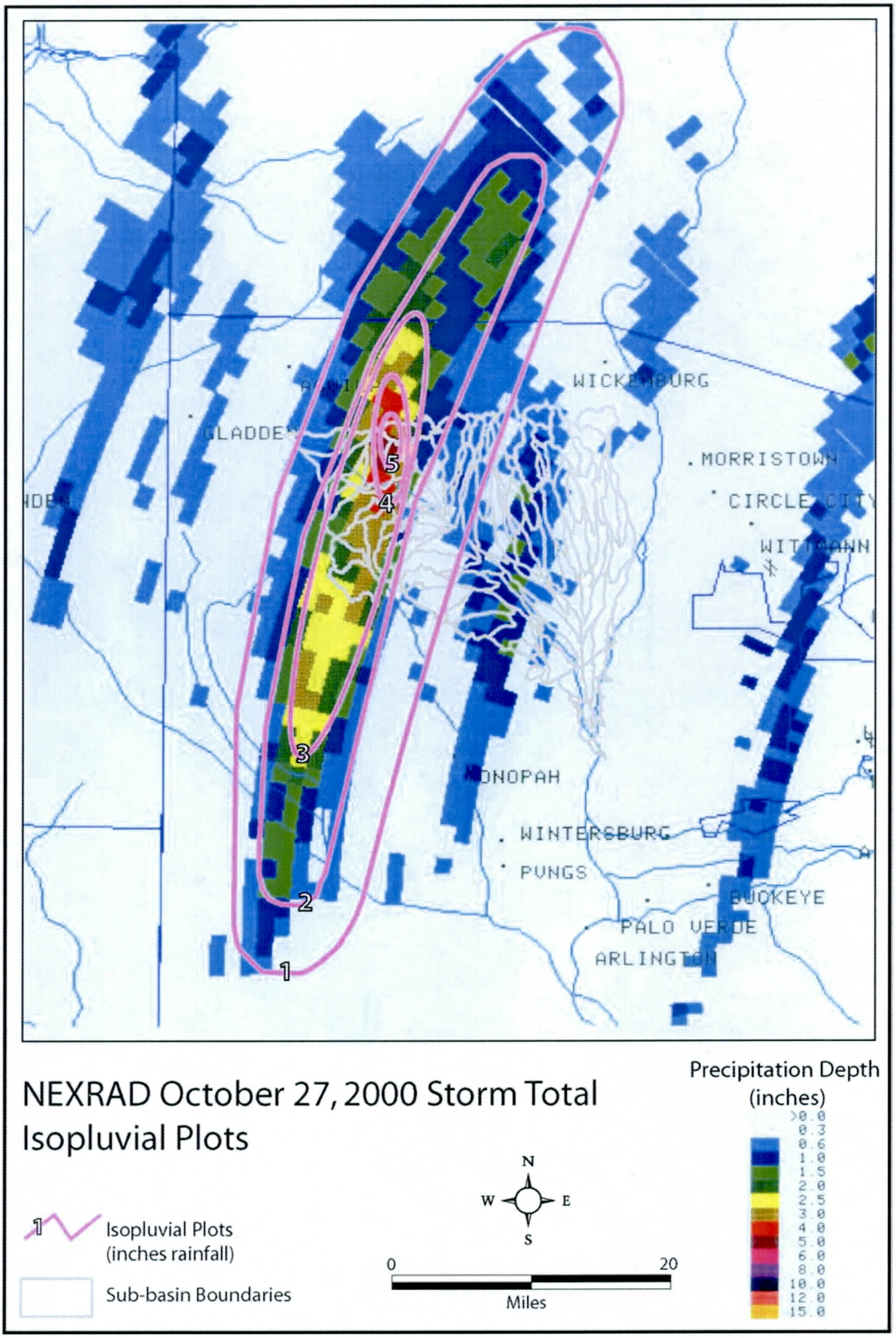

Figure 6. Isopluvial plots for the October 27 NEXRAD storm map

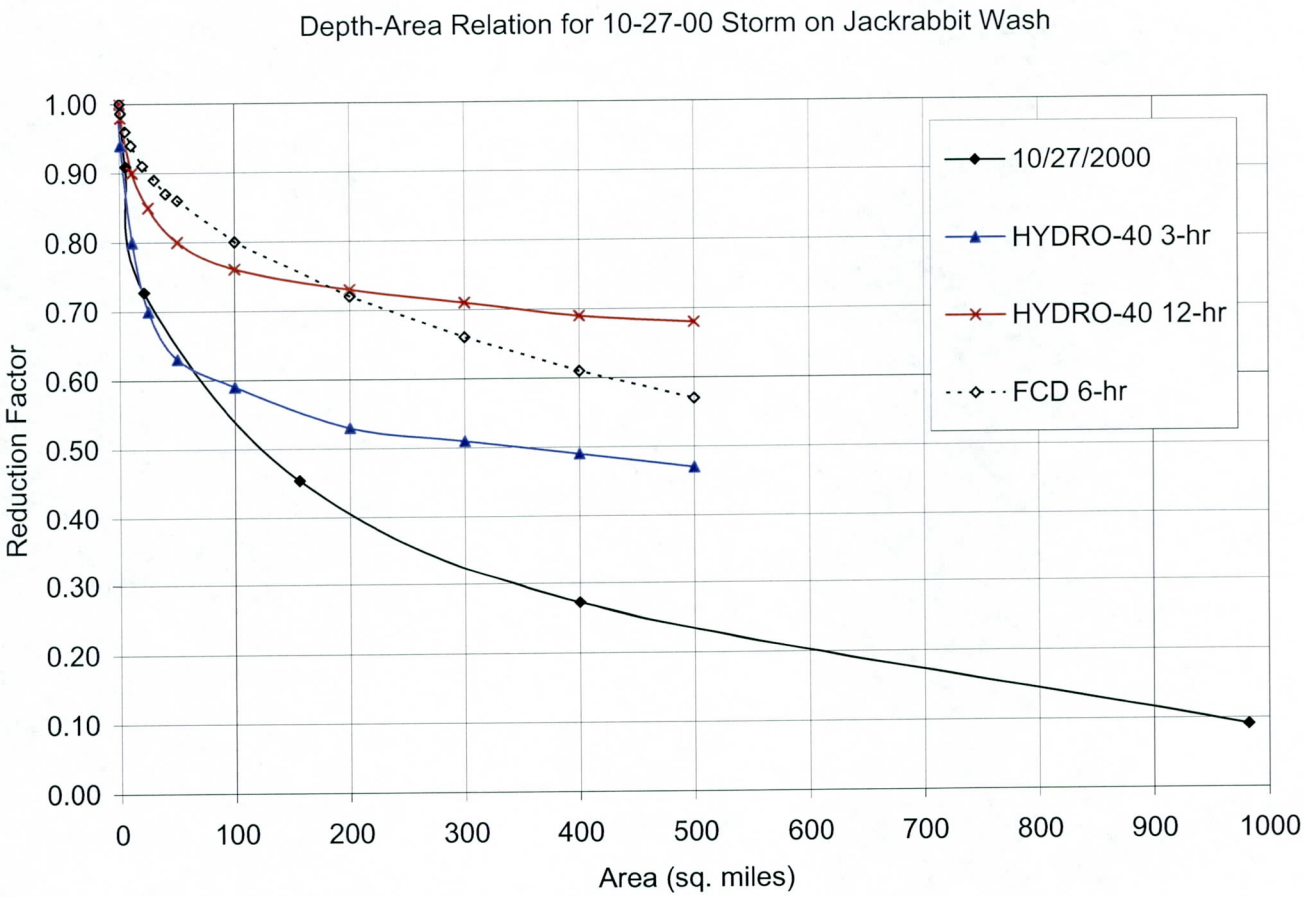

Figure 7. Comparison of FCDMC 6-hr Depth-Area Reduction Factors and Depth-Area Relation for 10-27-00 Storm

Rainfall data from both the October 2000 storm events were incorporated into the original Flood Insurance Study (FIS) 100-year HEC-1 models (Section 3.2.1). Figure 8 shows the rainfall depth versus drainage area relationships from the reconstructed HEC-1 models compared with the original FIS model data and the October 27 NEXRAD isopluvial data. The October 21 and October 27 plots represent average precipitation depth over sub-watersheds contributing to specific geographic locations in the Jackrabbit Wash watershed. Note that the aerially reduced rainfall depths for the October 21 storm are all much less than the 24-hour synthetic values from the FIS HEC-1 model and the 12-hour values estimated from NOAA Atlas II (Miller, et al., 1973). Comparison of the 27th storm, however, shows that the average rainfall depth for an area of approximately 80 mi^2 within Jackrabbit Wash is equal to the FIS HEC-1 6-hour storm depths. In addition, the plot shows that for an area of approximately 150 mi^2 (the approximate drainage area at the FCDMC gage location – location 3 in Figure 8), the isopluvial depths are equal to the FIS 6-hour model value. This indicates the 27th storm could be considered approximately a 100-year rainfall for drainage areas of approximately 80 mi^2 in Jackrabbit Wash. However, note that the storm itself had at least one point rainfall value which exceeded the 500-year probability but was not centered on the Jackrabbit Wash watershed upstream of the FCDMC gage (Figure 6).

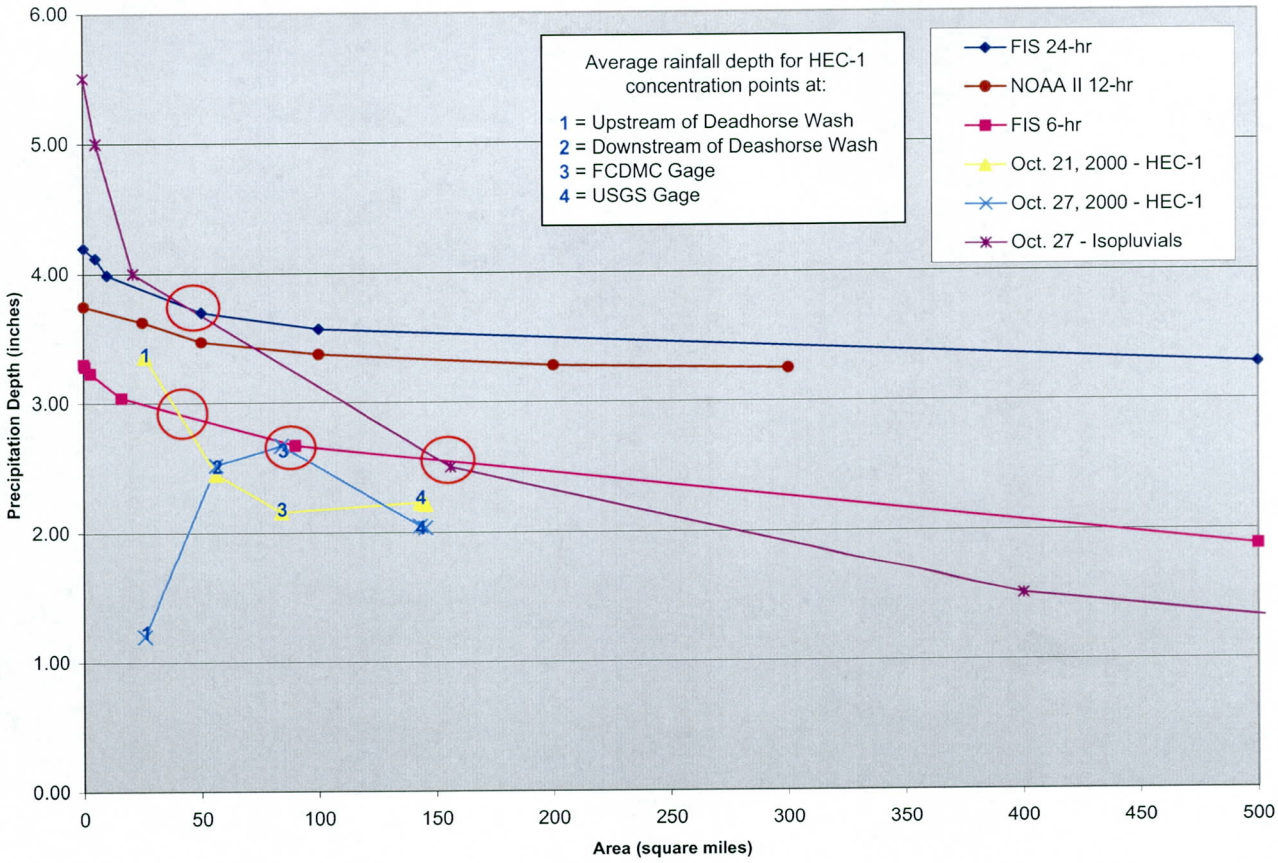

Figure 8. Comparison of Rainfall Depth vs. Drainage Area for FIS models, reconstructed HEC-1 models, and Isopluvials interpreted from NEXRAD. The red circles highlight the comparison points discussed.

2.3 Temporal Distributions

In order to model the storms in HEC-1, temporal distributions of the rainfall needed to be estimated. Unfortunately, the hourly or more detailed NEXRAD data were not available from the National Climatic Data Center (NCDC) or the local NWS office. Therefore, the temporal distributions were derived from ALERT rain gages.

2.3.1 Oct. 21-22, 2000

ALERT rain gages in the vicinity of Jackrabbit Wash showed significant rainfall accumulations between about 1200 on October 21 to 1200 on October 22. Figure 9 shows the cumulative rainfall at a number of FCDMC ALERT gages in and around the Jackrabbit Wash watershed. Based on this plot, the temporal distribution for FCDMC gage 7070 was selected as representative of the intense rainfall pattern for the 21st-22nd storm for use in the HEC-1 modeling. Although gage 7070 is located outside the Jackrabbit Wash watershed (see Figure 5), the temporal distribution of rainfall recorded at this gage is assumed to have been similar to the very intense rainfall that fell within the watershed. Note the similarity of the storm total precipitation in the vicinity of gage 7070 to the maximum precipitation within the Jackrabbit Wash watershed.

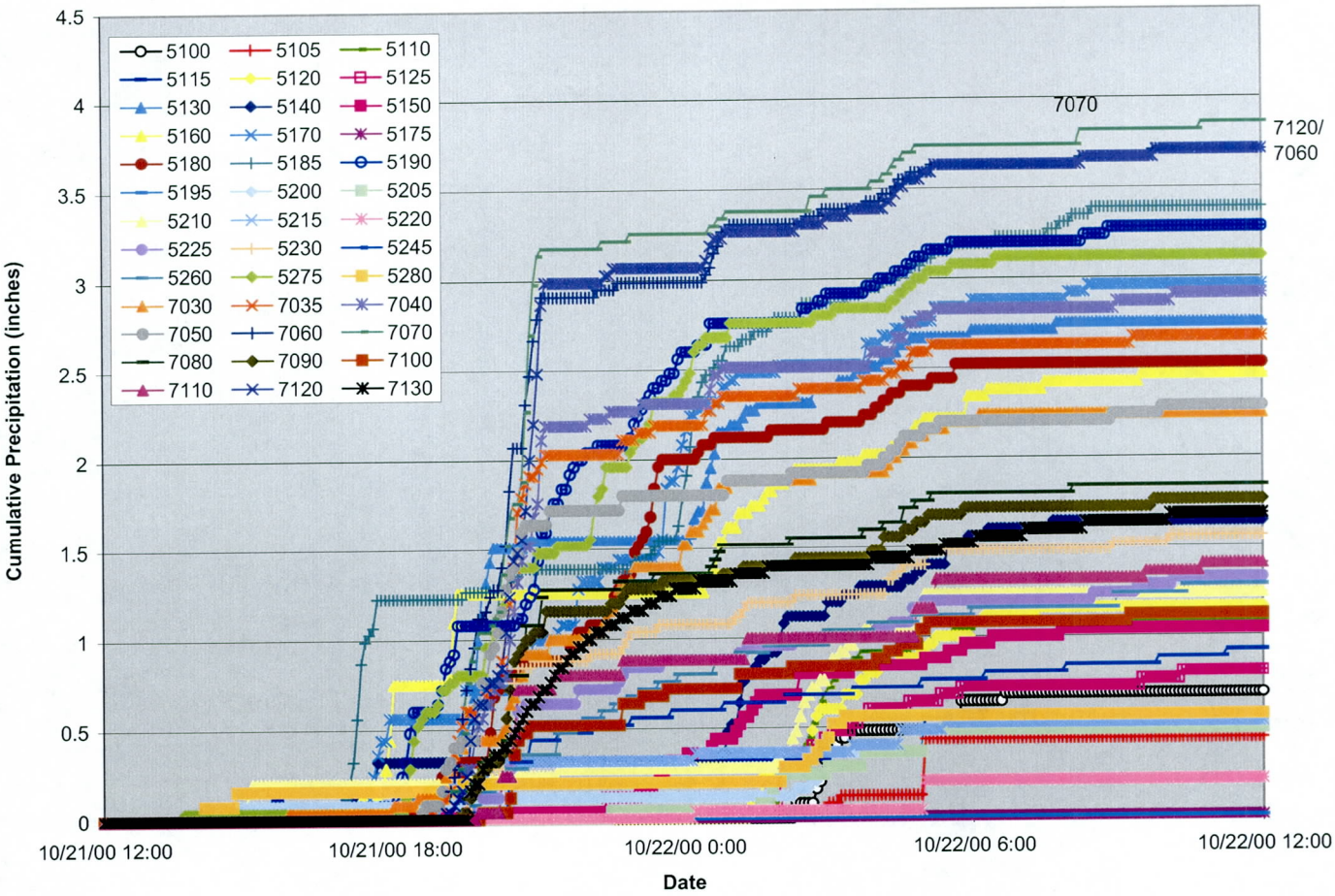

Figure 9. Cumulative rainfall for FCDMC ALERT stations near Jackrabbit Wash watershed, Oct. 21-22, 2000

2.3.2 Oct. 27, 2000

ALERT rain gages in the vicinity of Jackrabbit Wash also recorded significant rainfall accumulations on October 27. Figure 10 shows the cumulative rainfall at surrounding FCDMC ALERT gages on October 27, 2000. The results of this plot indicate rain gage 5180 to be the most appropriate for the HEC-1 modeling based on similar rationale used to select gage 7070 for the 21st storm.

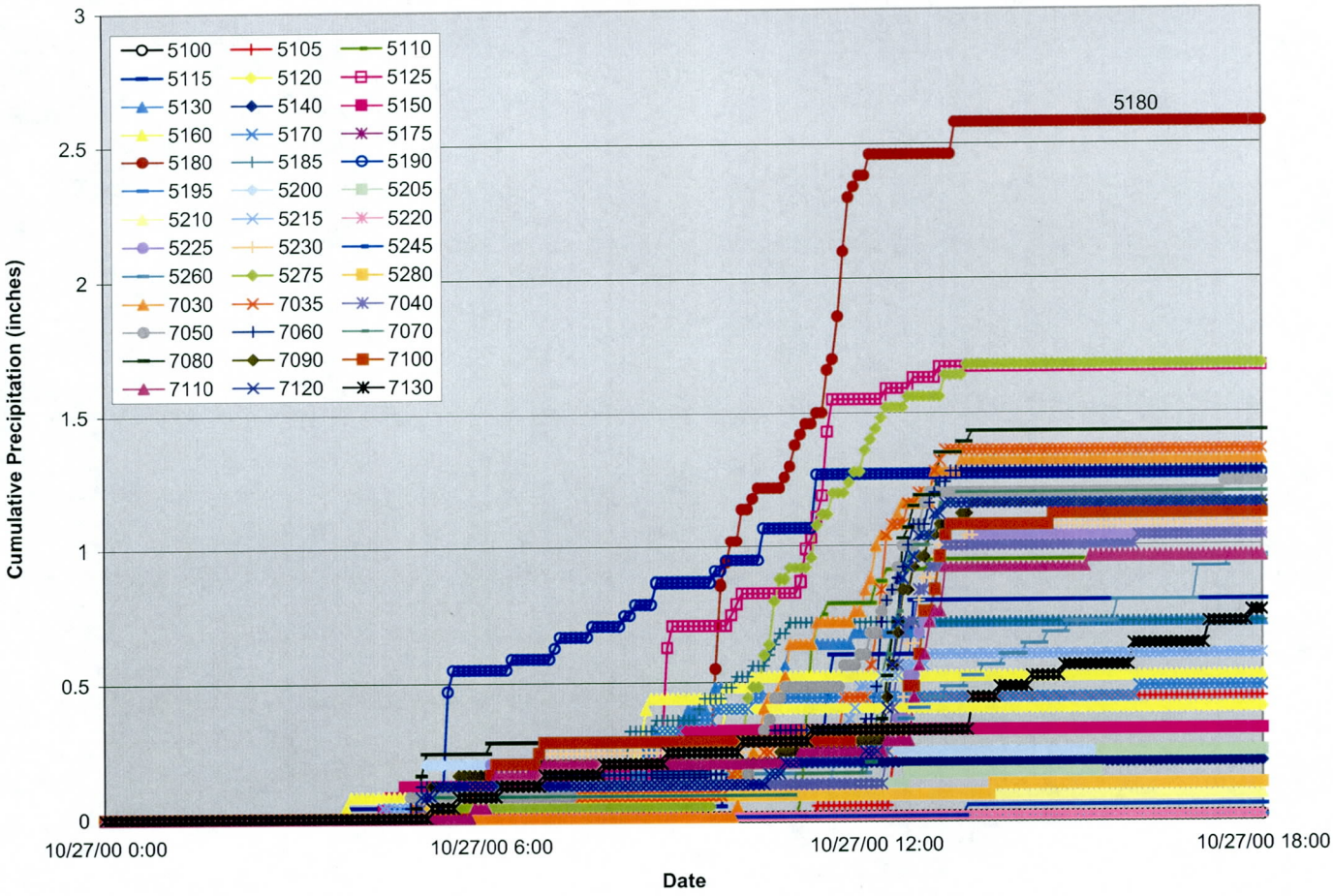

Figure 10. Cumulative rainfall for FCDMC ALERT stations near Jackrabbit Wash watershed, Oct. 27, 2000

2.3.3 Comparison to "100-year storm"

Temporal distributions from both the October 2000 storms were compared with synthetic SCS rainfall distributions as shown in Figure 11. The October 21 storm closely matched the SCS type IIA distribution while the October 27 storm plot indicates a shorter duration but a more intense overall rainfall, similar to the FCDMC 6-hour Pattern 1 synthetic storm.

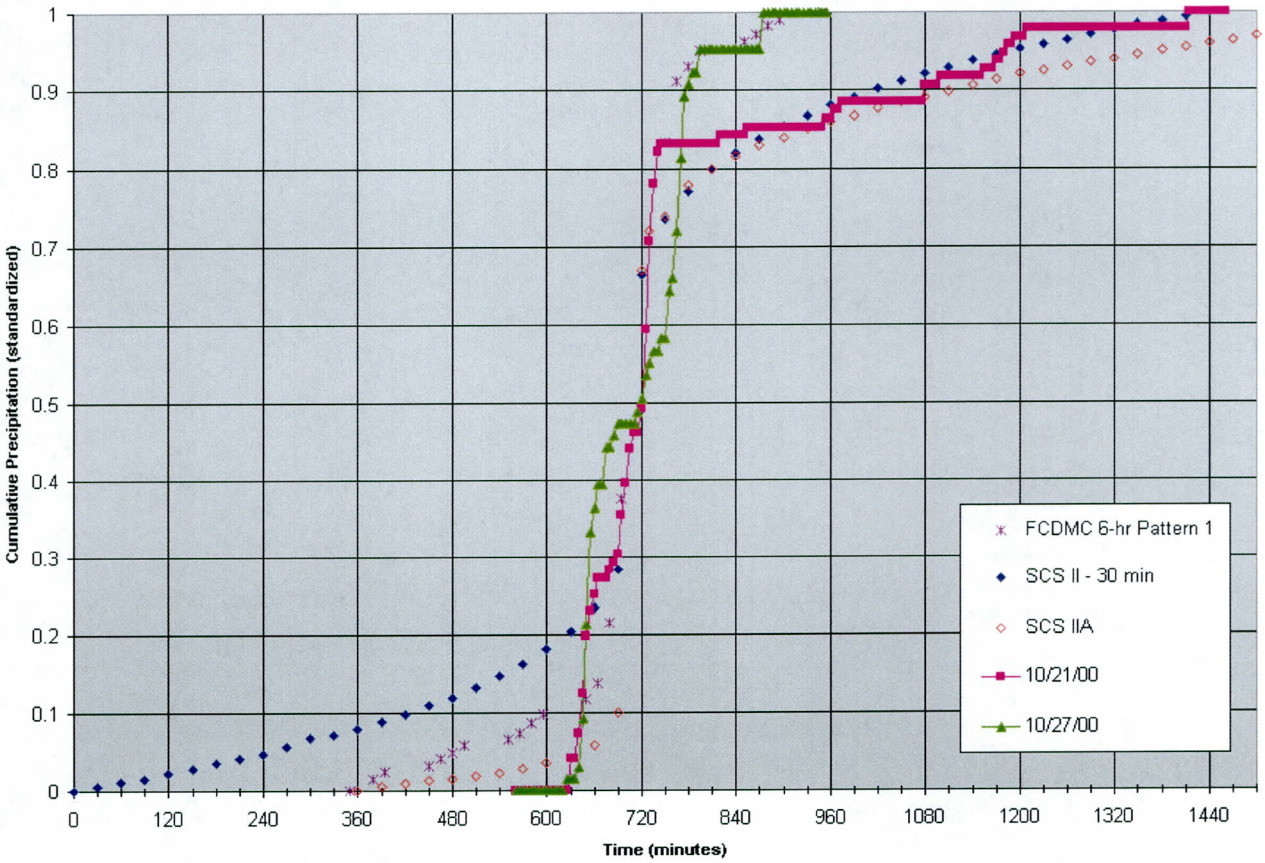

Figure 11. Normalized comparison of temporal distributions

2.4 Statistical Analyses

A statistical analysis was preformed to determine a probability estimate for the October 2000 storms. As previously described, both radar and rain gage data indicated two large storm events within a period of five days. Each storm was analyzed separately to determine its recurrence interval. Figure 3 and Figure 9 show the areas of greatest point rainfall for each storm within the watershed. Point rainfall from both rain gage and radar data were analyzed and are summarized in Table 2 and Table 3. Only one rain gage (#5215) was located directly within the Jackrabbit Wash watershed in October 2000. As shown in Table 1 and Figure 4, the bulk of intense rainfall on the 27th fell west of that single rain gage. NEXRAD data were also analyzed for each sub-basin within the study area. A weighted average rainfall was estimated for concentration points of interest within the watershed (Table 4). The basin average value was multiplied by the inverse of the depth-area reduction factors from HYDRO-40 to estimate an equivalent point rainfall. This value was used in conjunction with Table 6 to determine the return period for each location. The results are summarized in Table 5. The October 27 storm duration in Table 5 shows both 3- and 6-hour values. This was done to illustrate the sensitivity of the return period estimate to the duration. The return period column for 10/27 in Table 5 shows the significantly varying results between the 3- and 6-hour analyses. Return periods were calculated from a rainfall probability distribution created using the PREFRE program as described in the Drainage Design Manual (FCDMC, 1995) and depth-frequency maps from NOAA Atlas II (Miller et al., 1973). This distribution matrix is shown in Table 6.

Table 2. Maximum point rainfall from FCDMC rain gage data

Storm	FCDMC Gage ID	Maximum Point Rainfall (inches)	Storm Duration (hours)	Return Period (years)
October 21	7070	3.85	12	140
October 27	5180	2.60	3	43

Table 3. Maximum point rainfall from NEXRAD radar data

Storm	Maximum Point Rainfall (inches)	Storm Duration (hours)[2]	Return Period (years)
October 21	4.5	14	≈ 220
October 27	5.5	19	> 500

Table 4. Weighted average sub-basin rainfall

Location	Drainage Area (mi^2)	10/21 Average Rainfall (in)	10/27 Average Rainfall (in)
USGS Gage	145	2.22	2.03
FCDMC Gage	143	2.23	2.05
Downstream of Dead Horse Wash	84	2.16	2.67
Upstream of Dead Horse Wash	56	2.45	2.52

Table 5. Equivalent point rainfall and estimated return period for rain gage storm duration

Location	Drainage Area (mi^2)	Equivalent Point Rainfall (in)		10/21 Storm Duration (hours)	10/27 Storm Duration (hours)	10/21 Estimated Return Period (years)	10/27 Estimated Return Period (years)
		10/21	10/27				
USGS Gage	145	3.0	3.6	12	3/6	29	450 / 170
FCDMC Gage	143	3.0	3.6	12	3/6	29	450 / 170
Downstream of Dead Horse Wash	84	2.8	4.5	12	3/6	21	> 500 / > 500
Upstream of Dead Horse Wash	56	3.1	4.0	12	3/6	35	> 500 / 370
				Average Return Period =		29	> 500 / 300

[2] NEXRAD duration for a regional storm, not specific for Jackrabbit Wash. Rain gage duration most accurately represents duration for Jackrabbit Wash.

Table 6. Depth-duration frequency matrix for Jackrabbit Wash

Return Period							Duration
2-year	5-year	10-year	25-year	50-year	100-year	500-year	(minutes)
0.37	0.46	0.53	0.62	0.69	0.76	0.92	5
0.56	0.70	0.80	0.94	1.06	1.17	1.42	10
0.68	0.87	1.01	1.20	1.35	1.50	1.84	15
0.9	1.17	1.36	1.62	1.83	2.03	2.50	30
1.1	1.45	1.68	2.02	2.28	2.54	3.13	60
1.18	1.58	1.85	2.23	2.52	2.81	3.49	120
1.24	1.67	1.96	2.37	2.69	3.00	3.72	180
1.35	1.84	2.18	2.64	2.99	3.35	4.17	360
1.45	2.02	2.40	2.93	3.34	3.75	4.69	720
1.55	2.20	2.63	3.23	3.69	4.15	5.21	1440

2.4.1 Results

Statistical analyses of maximum point rainfall from both rain gage and radar data resulted in varying results for the return periods of the October 2000 storms. It was determined that the true storm durations were most accurately represented by the temporal distributions of rain gage data. These distributions suggested durations of twelve hours and three hours for the 21st and 27th storms, respectively. Weighted average rainfall for each sub-basin within the Jackrabbit Wash watershed was estimated from radar data from both storm events. This data provided the most comprehensive coverage of rainfall throughout the watershed, and combined with the durations derived from the rain gage data, was determined to most accurately represent each storm.

The results indicate the October 21 storm was approximately a 30-year event and the 27th storm was greater than a 500-year event for a 3-hour duration and about 300-year event for a 6-hour duration. While average total rainfall depth between the two storms did not vary significantly, the return period estimates were dramatically different. These results indicate that storm duration is an extremely sensitive parameter in the statistical analysis. In addition, the depth-area ratios from HYDRO-40 result in conservative return period estimates (Zehr & Myers, 1984). The following excerpt derived from that report explains the assumptions in the depth-area ratio calculations:

> *"....It was felt that the limited amount of data and the large amount of scatter precluded quantifying the variation (of areal reduction) with return period....use of the mean quantities is equivalent to determining the depth-area ratios for the 2.54-yr return period. Use of a mean curve for all return periods will lead to conservative estimates for all return periods greater than 2.54-yr. The difference at the 2-yr return period is small, and considering the degree of uncertainty associated with the entire analysis, can be considered negligible."*

Therefore, based on our analysis we concluded that the October 21 event was approximately a 30-year event and the October 27 event was greater than a 500-year event.

3. Storm Runoff Reconstruction

3.1 Stream Gage Data

The FCDMC stream gage on Jackrabbit Wash near Vulture Mine Road (# 5218) was not yet installed at the time of the October flood. However, an indirect discharge estimate of 32,400 cfs was made using the slope-area method in December 2000 by FCDMC staff.

The USGS crest stage gage (#09516800) located downstream of Wickenburg Road was destroyed by the October 2000 flood. The USGS also conducted a slope-area survey near their station and estimated the discharge at 27,000 cfs.

The USGS continuous stream gage station, Hassayampa River near Arlington (#09517000), showed flood runoff on both October 22nd and 27th. The unofficial peak discharge recorded on the morning of the 22nd was about 4,600 cfs. Unfortunately, the gage silted in during the October 27 flood. The USGS slope-area estimate of the peak discharge at #09517000 on the 27th was 22,200 cfs.

3.2 HEC-1 model reconstructions

A rainfall-runoff model using HEC-1 was developed by Burgess & Niple in 1991 as part of the Flood Insurance Study for Jackrabbit Wash. The model was developed using the old Hydrologic Design Manual for Maricopa County. As such some of the methodologies vary somewhat from those in the effective Drainage Design Manual for Maricopa County, Volume I, Hydrology which was most recently revised in 1995. The largest difference germane to the Jackrabbit Wash area was the use of arithmetic averaging of XKSAT values for calculation of map unit and sub-basin loss parameters and the use of 4.6 in/hr for sand. The current investigation did not recompute loss parameters for the watershed based on currently adopted methods which utilize logarithmic averaging and do not consider textural infiltration rates greater than 1.2 in/hr. It is likely that the older method will overestimate infiltration rates in some areas and underestimate them in others compared to the current method. However, the extent of the impact of these differences is uncertain.

3.2.1 Modifications to FIS model

Modifications to the FIS HEC-1 models (Burgess & Niple, 1991) were made to incorporate precipitation data from the October 2000 storms. Alternate antecedent moisture conditions (DTHETA) were modeled for each storm in an attempt to generate discharges that matched the indirect estimates. Models were designed for "dry" and "normal" conditions, with a third "wet" condition for the October 27 storm. These conditions and associated DTHETA values were used as described in the Drainage Design Manual Volume I, Table 4.2 (FCDMC, 1995).

In addition to DTHETA changes, a 5.04 mi^2 area was added to the HEC-1 model. This area located along the northwest boundary of the Jackrabbit Wash watershed was added based on examination of aerial photographs, field observations, and survey data by JEF for the Approximate Flood Delineation Study (JEF, in progress) (Figure 12). A flow split location was identified at the outlet of this basin with approximately 85% of the discharge entering Jackrabbit Wash; a value not previously accounted for in the original FIS HEC-1 models.

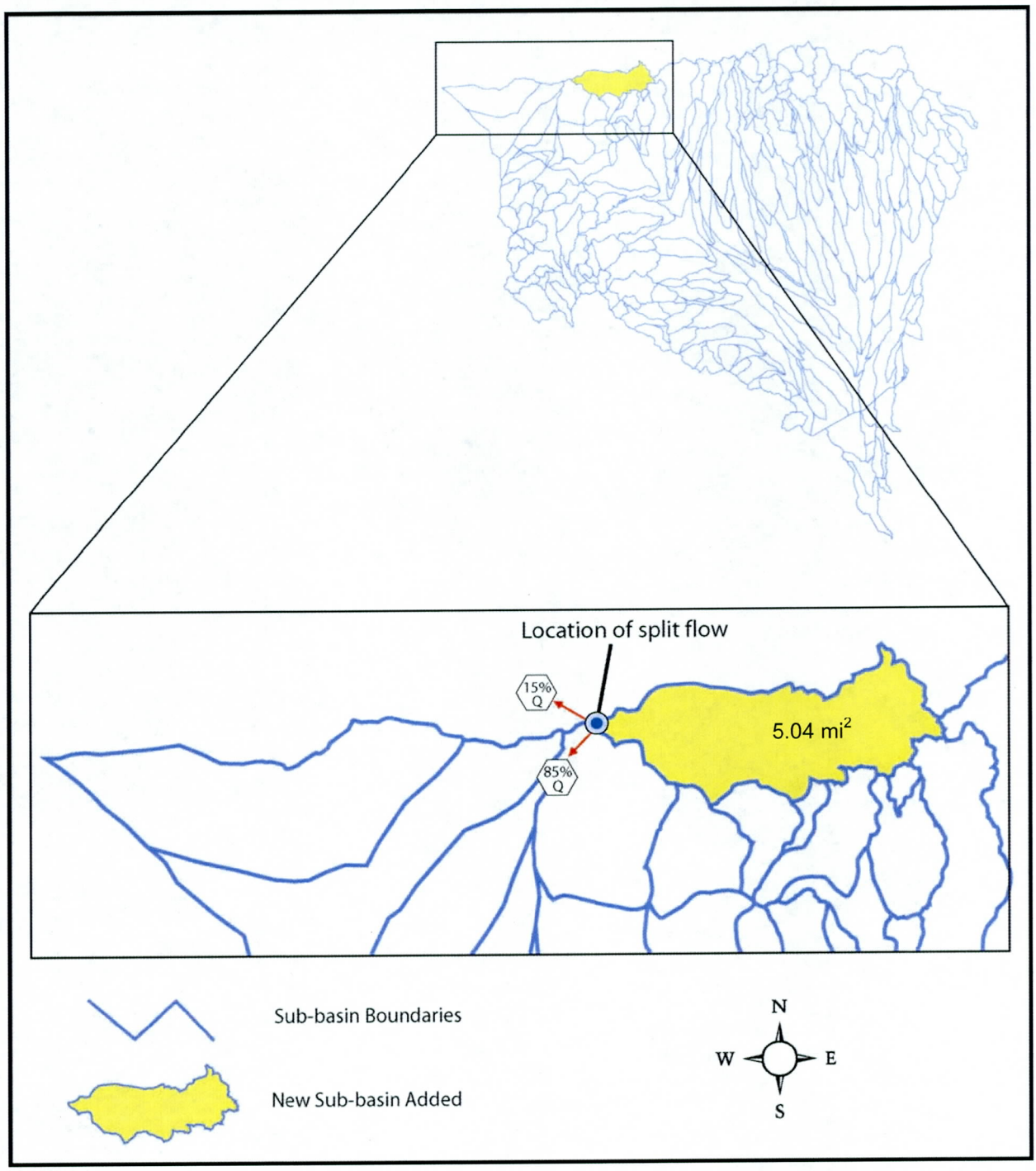

Figure 12. New sub-basin and split flow location

Portions of the FIS HEC-1 model downstream of Vulture Mine Road were removed to simplify the analysis, since the radar data showed that most of the rain fell in the upstream watershed. Moreover, the modeled area coincides with the drainage area that contributes runoff to the FCDMC and USGS gaging stations. The modified HEC-1 models are included on the attached CD with this report in Appendix E.

3.2.2 October 21-22 Storm

3.2.2.1 Dry

The antecedent moisture (DTHETA) condition was modeled as "dry" as defined in the Drainage Design Manual, Volume I, Table 4.2. It was determined that the "dry" antecedent model most likely represented actual field conditions prior to the October 21 storm based on rainfall data from the previous 30 days (Figure 13).

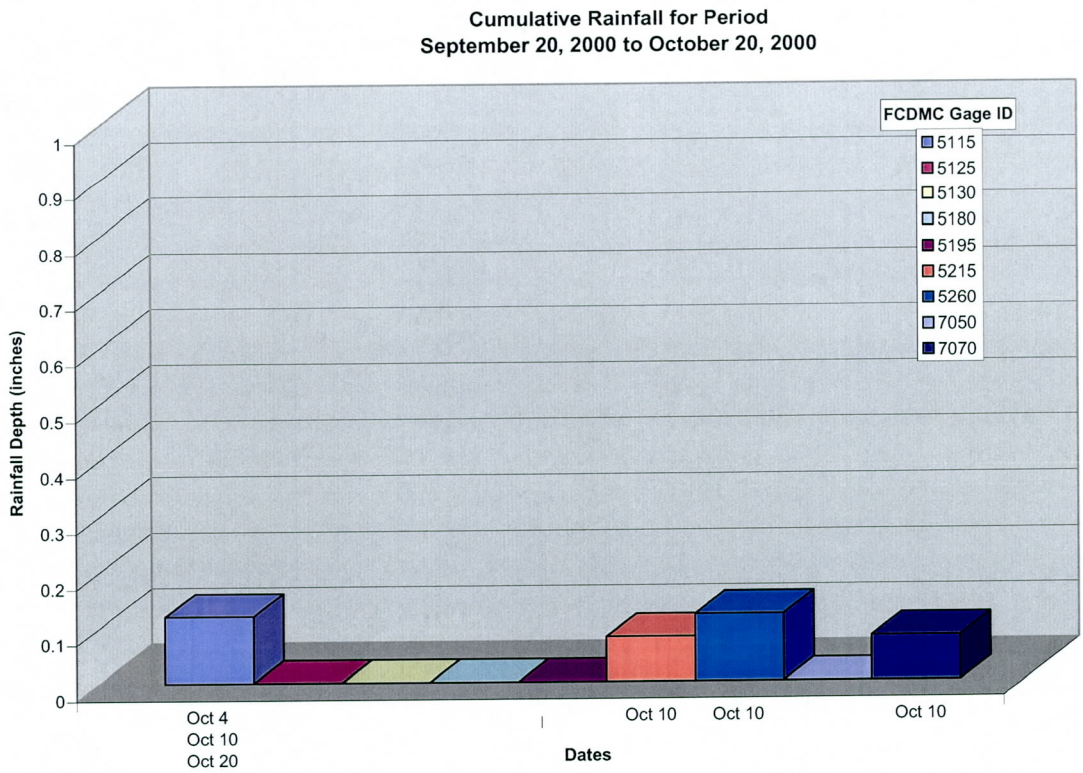

Figure 13. 30-day prior cumulative rainfall for FCDMC gages shown in Figure 5

Two models were developed using the dry condition: 1) accounting for channel transmission losses (HEC-1 RL records) and 2) discounting transmission losses. Table 7 compares the two dry model results with the FIS discharges and indirect estimates of the October 2000 flood(s). Table 7 shows that both HEC-1 models (with and without transmission losses) significantly underestimate the FCDMC indirect peak discharge estimate of 32,400 cfs and the USGS estimate of 27,000 cfs. This strongly indicates the October 2000 flood was not generated by the 21st storm under "dry" antecedent moisture conditions. The differences between the two new HEC-1 models are small for concentration points C8 through C21, and are much larger for C33 and C34. This is attributed to the significantly different reach lengths in the models (example: C8 to C10 length = 3,379 ft, C33 to C34 length = 28,195 ft). Another major difference is seen at the Dead Horse Wash confluence (C18) where the model results are significantly less than both the indirect and FIS 100-year estimates. This is caused by a combination of high XKSAT values from the original FIS models and relatively shallow rain depth in the HEC-1 models for the 21st

storm. This may be one area where the arithmetic averaging of XKSAT values might inadequately represent the "true" watershed response.

Table 7. "Dry" condition HEC-1 comparison for October 21-22 storm

JEF Indirect Reach/Cross-Section[3]	Drainage Area (mi^2)	HEC-1 KK ID	JEF Indirect Discharge for 10/27 (cfs)	HEC-1 Peak Q[4] (no losses) (cfs)	HEC-1 Peak Q[5] (losses accounted) (cfs)	FIS 100-yr Discharge (cfs)
Upper Jackrabbit (cross-section 1)	36	C8	7,600	7,900	7,700	11,400
Upper Jackrabbit below Oracho Ranch Rd. (cross-section 1)	43	C10	4,300	7,800	7,700	13,500
Dead Horse Wash (cross-section 1)	23	C18	9,300	430	400	7,700
Wildcat Well Area (cross-section 2)	107	C21	17,770	15,800	15,500	21,100
FCDMC Gage (cross-section 1)	143	C33	26,100	16,100	15,200	21,100
USGS Gage	145	C34	-	14,800	13,400	20,000

Note: FCDMC published indirect discharge estimate at the FCDMC Gage = 32,400 cfs
USGS indirect discharge at the USGS gage = 27,000 cfs

[3] See Appendix A for reach and cross-section locations
[4] Model: 102100dt.dat
[5] Model: 102100d.dat

3.2.2.2 Normal

For this model the DTHETA condition was modeled as "normal" as defined in the Drainage Design Manual, Volume I, Table 4.2. Table 8 compares discharge estimates from the "normal" condition HEC-1. This table indicates the same result as Table 7, the October 2000 flood was not generated by the 21st storm under "normal" antecedent moisture conditions.

Table 8. "Normal" condition HEC-1 comparison for the October 21 storm

JEF Indirect Reach/Cross-Section	Drainage Area (mi^2)	HEC-1 KK ID	JEF Indirect Discharge for 10/27 (cfs)	HEC-1 Peak Q[6] (cfs)	FIS 100-yr Discharge (cfs)
Upper Jackrabbit (cross-section 1)	36	C8	7,600	8,300	11,400
Upper Jackrabbit below Oracho Ranch Rd. (cross-section 1)	43	C10	4,300	8,300	13,500
Dead Horse Wash (cross-section 1)	23	C18	9,300	650	7,700
Wildcat Well Area (cross-section 2)	107	C21	17,770	17,100	21,100
FCDMC Gage (cross-section 1)	143	C33	26,100	17,000	21,100
USGS Gage	145	C34	-	15,200	20,000

Note: FCDMC published indirect discharge estimate at the FCDMC Gage = 32,400 cfs
USGS indirect discharge at the USGS gage = 27,000 cfs

[6] Model: 102100n.dat

3.2.3 October 27 Storm

3.2.3.1 Dry (FIS)

The antecedent moisture (DTHETA) condition was modeled as "dry" as defined in the Drainage Design Manual, Volume I, Table 4.2. Table 9 compares discharges for this modeled condition. Again, the discharge estimated from the new HEC-1 model is far below either the FCDMC or USGS indirect estimates.

Table 9. "Dry" condition HEC-1 comparison for the October 27, 2000 storm

JEF Indirect Reach/Cross-Section	Drainage Area (mi^2)	HEC-1 KK ID	JEF Indirect Discharge for 10/27 (cfs)	HEC-1 Peak Q[7] (cfs)	FIS 100-yr Discharge (cfs)
Upper Jackrabbit (cross-section 1)	36	C8	7,600	8,700	11,400
Upper Jackrabbit below Oracho Ranch Rd. (cross-section 1)	43	C10	4,300	9,000	13,500
Dead Horse Wash (cross-section 1)	23	C18	9,300	4,400	7,700
Wildcat Well Area (cross-section 2)	107	C21	17,770	14,600	21,100
FCDMC Gage (cross-section 1)	143	C33	26,100	14,500	21,100
USGS Gage	145	C34	-	13,600	20,000

Note: FCDMC published indirect discharge estimate at the FCDMC Gage = 32,400 cfs
USGS indirect discharge at the USGS gage = 27,000 cfs

3.2.3.2 Normal

This DTHETA condition was modeled as "normal" as defined in the Drainage Design Manual, Volume I, Table 4.2. It was initially determined that the "normal" condition most closely matched actual field conditions prior to the beginning of the October 27 storm, therefore two models were generated to compare the affect of transmission losses as was done for the October 21 "dry" condition, in an attempt to match the indirect discharge estimate at the FCDMC gage. Results are summarized below in Table 10. The peak discharge generated by the new HEC-1 model discounting losses was approximately 9,000 cfs lower than the indirect estimate, indicating a more saturated antecedent moisture conditions than "normal" as modeled in HEC-1 may have existed prior to the October 27 storm.

[7] Model 102700d.dat

Table 10. Comparison of "normal" condition HEC-1 for the October 27, 2000 storm

JEF Indirect Reach/Cross-Section	Drainage Area (mi^2)	HEC-1 KK ID	JEF Indirect Discharge for 10/27 (cfs)	HEC-1 Peak Q[8] (no losses) (cfs)	HEC-1 Peak Q[9] (losses accounted) (cfs)	FIS 100-yr Discharge (cfs)
Upper Jackrabbit (cross-section 1)	36	C8	7,600	9,100	9,000	11,400
Upper Jackrabbit below Oracho Ranch Rd. (cross-section 1)	43	C10	4,300	9,700	9,600	13,500
Dead Horse Wash (cross-section 1)	23	C18	9,300	5,100	4,900	7,700
Wildcat Well Area (cross-section 2)	107	C21	17,770	16,600	15,900	21,100
FCDMC Gage (cross-section 1)	143	C33	26,100	17,100	16,000	21,100
USGS Gage	145	C34	-	16,700	15,000	20,000

Note: FCDMC published indirect discharge estimate at the FCDMC Gage = 32,400 cfs
USGS indirect discharge at the USGS gage = 27,000 cfs

3.2.3.3 Wet

The final antecedent moisture condition (DTHETA) was modeled as "wet" as defined in the Drainage Design Manual, Volume I, Table 4.2. This was done to examine the effect of saturated soils due to the previous precipitation from the 21st storm. Two "wet" models were generated (discounting and accounting for transmission losses) for the purpose of generating discharges high enough to match the indirects. Results are summarized in Table 11. The new HEC-1 discharge estimate accounting channel losses generated a discharge estimate at the USGS gage that very closely matched the USGS indirect estimate of 27,000 cfs. The 29,000 cfs estimate resulting from the new HEC-1 model discounting losses falls between the FCDMC published estimate of 32,400 cfs and the 27,000 cfs USGS estimate. These results potentially indicate the Jackrabbit Wash watershed was still saturated from the October 21 storm at the time the October 27 storm occurred. The SCS AMC criteria shown in Table 13 show that this could have been the case.

[8] Model 102700nt.dat
[9] Model 102700n.dat

Table 11. Comparison of "wet" condition HEC-1 models for the October 27, 2000 storm

JEF Indirect Reach/Cross-Section	Drainage Area (mi^2)	HEC-1 KK ID	JEF Indirect Discharge for 10/27 (cfs)	HEC-1 Peak Q[10] (no losses) (cfs)	HEC-1 Peak Q[11] (losses accounted) (cfs)	FIS 100-yr Discharge (cfs)
Upper Jackrabbit (cross-section 1)	36	C8	7,600	12,600	12,600	11,400
Upper Jackrabbit below Oracho Ranch Rd. (cross-section 1)	43	C10	4,300	14,000	13,900	13,500
Dead Horse Wash (cross-section 1)	23	C18	9,300	8,500	8,200	7,700
Wildcat Well Area (cross-section 2)	107	C21	17,770	27,300	26,600	21,100
FCDMC Gage (cross-section 1)	143	C33	26,100	29,400	27,900	21,100
USGS Gage	145	C34	-	29,000	27,000	20,000

Note: FCDMC published indirect discharge estimate at the FCDMC Gage = 32,400 cfs
USGS indirect discharge at the USGS gage = 27,000 cfs

3.2.3.4 SCS IIA Distribution

The similarity in the SCS IIA distribution with the October 21, 2000 storm (Figure 11) created an interest in inputing the rainfall distribution into the FIS HEC-1 model.[12] The resulting discharges from this model were remarkably similar to the FCDMC published estimates at the FCDMC gage location (Table 12).

Table 12. Results for the SCS IIA distribution in the FIS HEC-1 model

JEF Indirect Reach/Cross-Section	Drainage Area (mi^2)	HEC-1 KK ID	JEF Indirect Discharge for 10/27 (cfs)	SCS IIA Model Peak Q[13] (cfs)	FIS 100-year Discharge (cfs)
Upper Jackrabbit (cross-section 1)	36	C8	7,600	17,000	11,400
Upper Jackrabbit below Oracho Ranch Rd. (cross-section 1)	43	C10	4,300	20,200	13,500
Dead Horse Wash (cross-section 1)	23	C18	9,300	12,100	7,700
Wildcat Well Area (cross-section 2)	107	C21	17,770	32,600	21,100
FCDMC Gage (cross-section 1)	143	C33	26,100	32,900	21,100
USGS Gage	145	C34	-	31,400	20,000

Note: FCDMC published indirect discharge estimate at the FCDMC Gage = 32,400 cfs
USGS indirect discharge at the USGS gage = 27,000 cfs

[10] Model 102700st.dat
[11] Model 102700s.dat
[12] Model org2a.dat
[13] Model org2a.dat

The discharge estimate with the SCS IIA distribution was 32,900 cfs while the FCDMC indirect estimate was 32,400 cfs. Although the similarity may be coincidental, the result indicates that the SCS IIA distribution may be the an appropriate storm distribution for predictive modeling of severe rainfall near Jackrabbit Wash. A more detailed and thorough investigation is required to confirm or dispute the appropriate application of the SCS IIA distribution to extreme flood hydrology in Maricopa County.

3.2.4 Summary

The three HEC-1 models for the October 21 storm underestimate discharge values compared to the indirect peak discharge estimates by the FCDMC and USGS. The results strongly indicate that the flood associated with the observed high water marks was not generated by the October 21 storm and is consistent with the statistical evaluation of the storm (discussed in Section 2.4). The HEC-1 evaluations for the October 27 storm also underestimate the discharge at the FCDMC gage site. However, results from the "wet" condition HEC-1 model assuming no transmission losses most closely matched the FCDMC indirect estimate at the FCDMC gage while the "wet" model with transmission losses matched the USGS indirect estimate. The SCS National Engineering Handbook (NEH, 1983) section on antecedent moisture conditions described three conditions (I, II, III) which are a function of the amount of rainfall in the previous 5 days (Table 13). These three conditions can be compared to the "dry", "normal", and "wet" conditions described above.

Table 13. NEH seasonal rainfall limits for antecedent moisture conditions

AMC GROUP	Total 5-day Antecedent Rainfall	
	Dormant Season (inches rain)	Growing Season (inches rain)
I	< 0.5	< 1.4
II	0.5 to 1.1	1.4 to 2.1
III	> 1.1	> 2.1

The 27th storm occurred between 5 and 6 days after the 21st storm and therefore could fall under either the AMC group I or III categories. The "wet" condition HEC-1 data for the 27th storm indicates the group III category is the most appropriate. Based on the indirect discharge estimates, the "wet" condition models reproduce the 27th storm most closely. However, the likelihood of a true saturated condition after 5 days seems unlikely. Discrepancies in discharge estimates may be attributed to HEC-1 assumptions, primarily the static nature of the rainfall distribution. Additional sources of error include those in the indirect estimates.

3.3 Indirect Discharge Estimates

3.3.1 Physiographic Description

One of the tasks undertaken was to determine the proportionate upper-watershed runoff source for the October 2000 storm. This was accomplished by both quantitative and qualitative hydrologic analysis. Factors considered included slope, area, hydraulic conductivity, drainage density, and percent impervious area. An analysis was conducted for the watershed upstream of Wildcat Well where the largest volume of rain occurred as well as the largest discharges. This upper-watershed area was subdivided into three sub-basins (A, B, C) with similar areas (Figure 14).

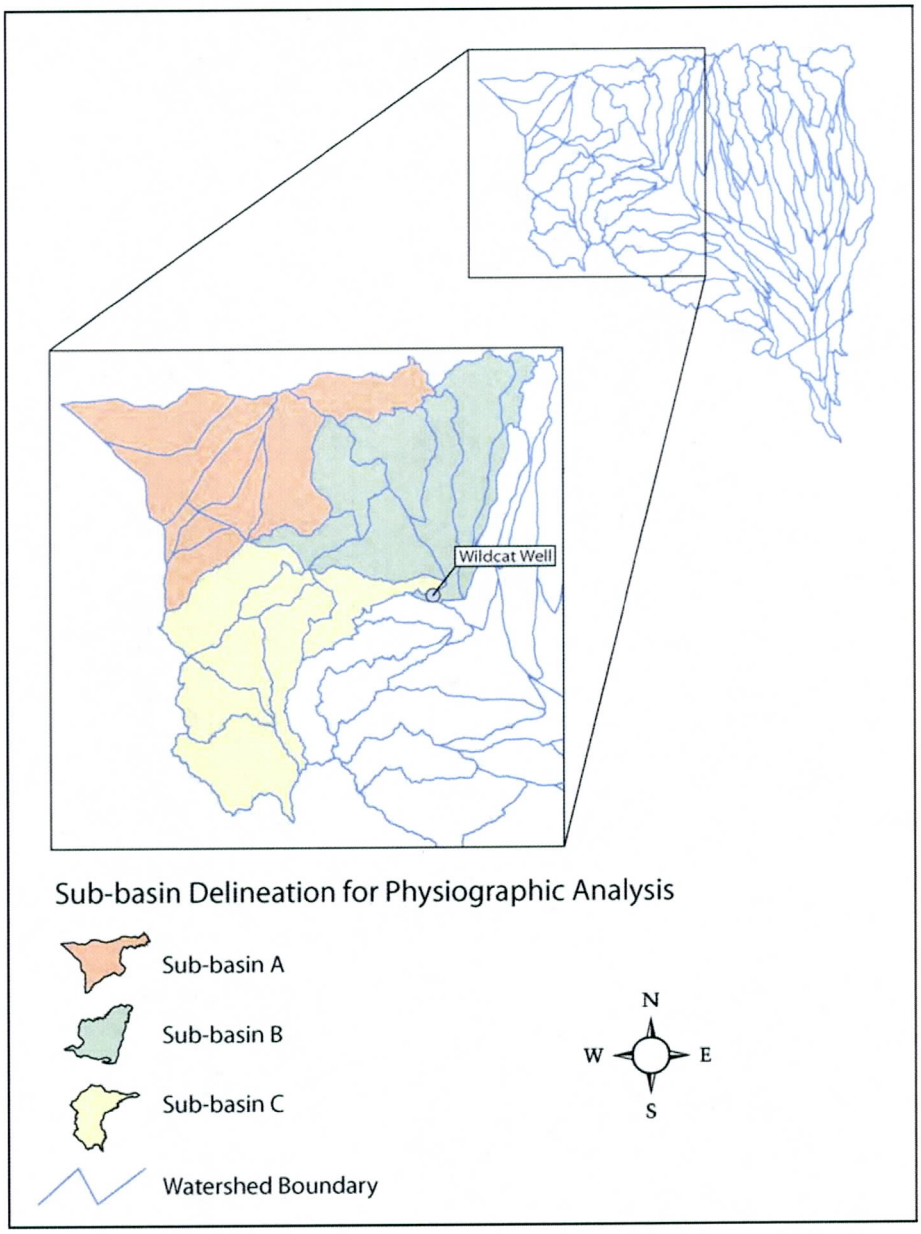

Figure 14. Physiographic sub-basin delineation

3.3.1.1 Hydrologic Characteristic Descriptions

Slope

Estimates of mean slope were made for each sub-basin outlined in Figure 14. Watersheds with steep slopes often generate higher peak discharges than equivalent basins with lower slopes. Sub-basin slopes were measured by calculating the weighted slope of each individual watershed within a sub-basin. These weighted slope values were summed up to calculate the average slope for the entire sub-basin. The results are summarized in Table 14 below. Results show that sub-basins B and C are nearly twice as steep and sub-basin A.

Soils

Soil data was analyzed to determine the relative hydraulic conductivity (XKSAT) for each sub-basin. Hydraulic conductivity is a measure of infiltration rate. Watersheds with high XKSAT values generate less runoff than watersheds with high XSKAT values. The XKSAT value for each soil unit within sub-basins A, B, and C was multiplied by the fraction of total area of that unit, producing an arithmetic weighted value comparable to the approach used in the original FIS. The weighted values were summed to compute a total weighted average for the entire sub-basin. Figure 15 illustrates the geographic distribution of XKSAT values. Sub-basin A is composed largely of soils with a value less than 0.1 in/hr. Therefore, sub-basin A should produce the highest amount of runoff assuming equal precipitation on all three sub-basins. However, multiple stock-tank detention ponds are present in sub-basin A (Figure 16), which can significantly attenuate the peak discharge through the sub-basin. Numeric results for the XKSAT analysis are summarized in Table 14.

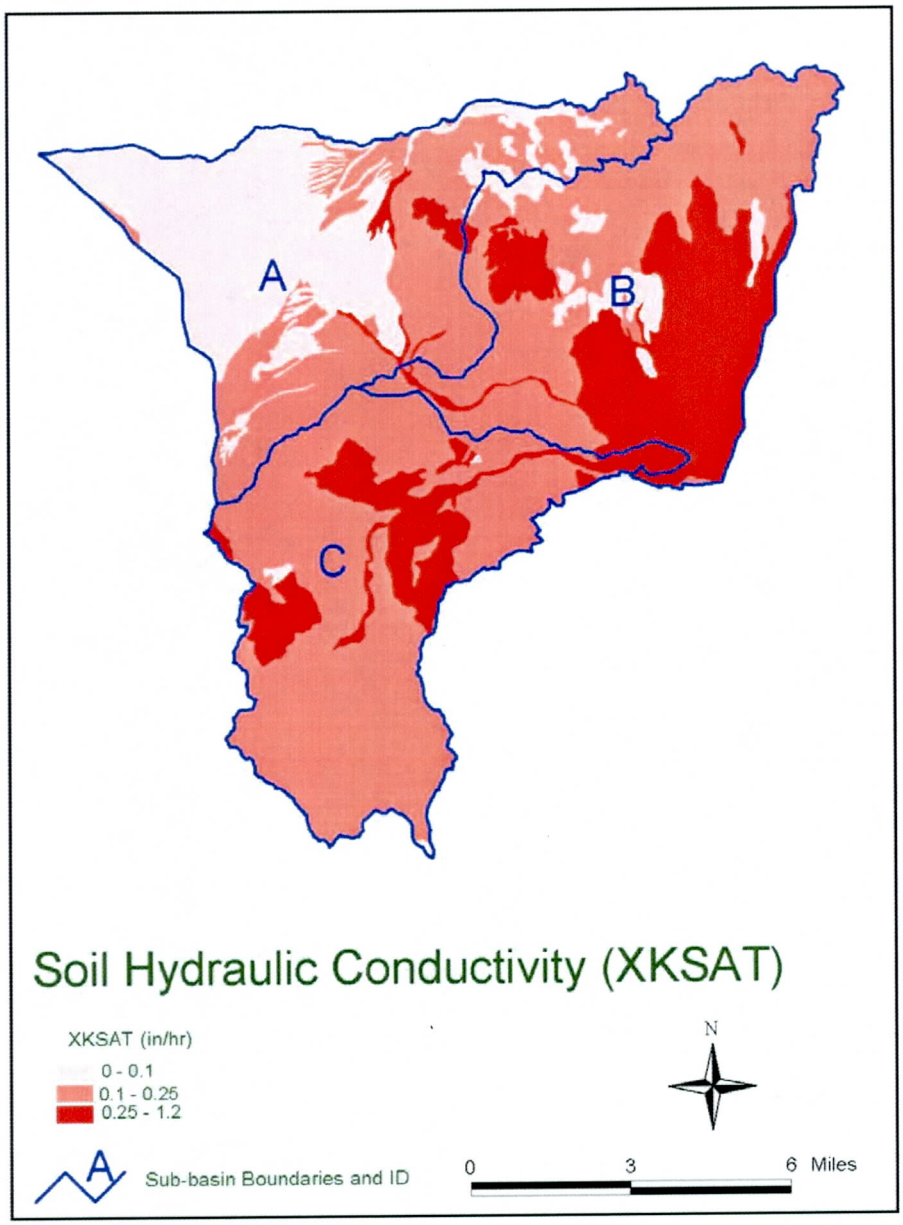

Figure 15. Soil hydraulic conductivity for sub-basins A, B, and C

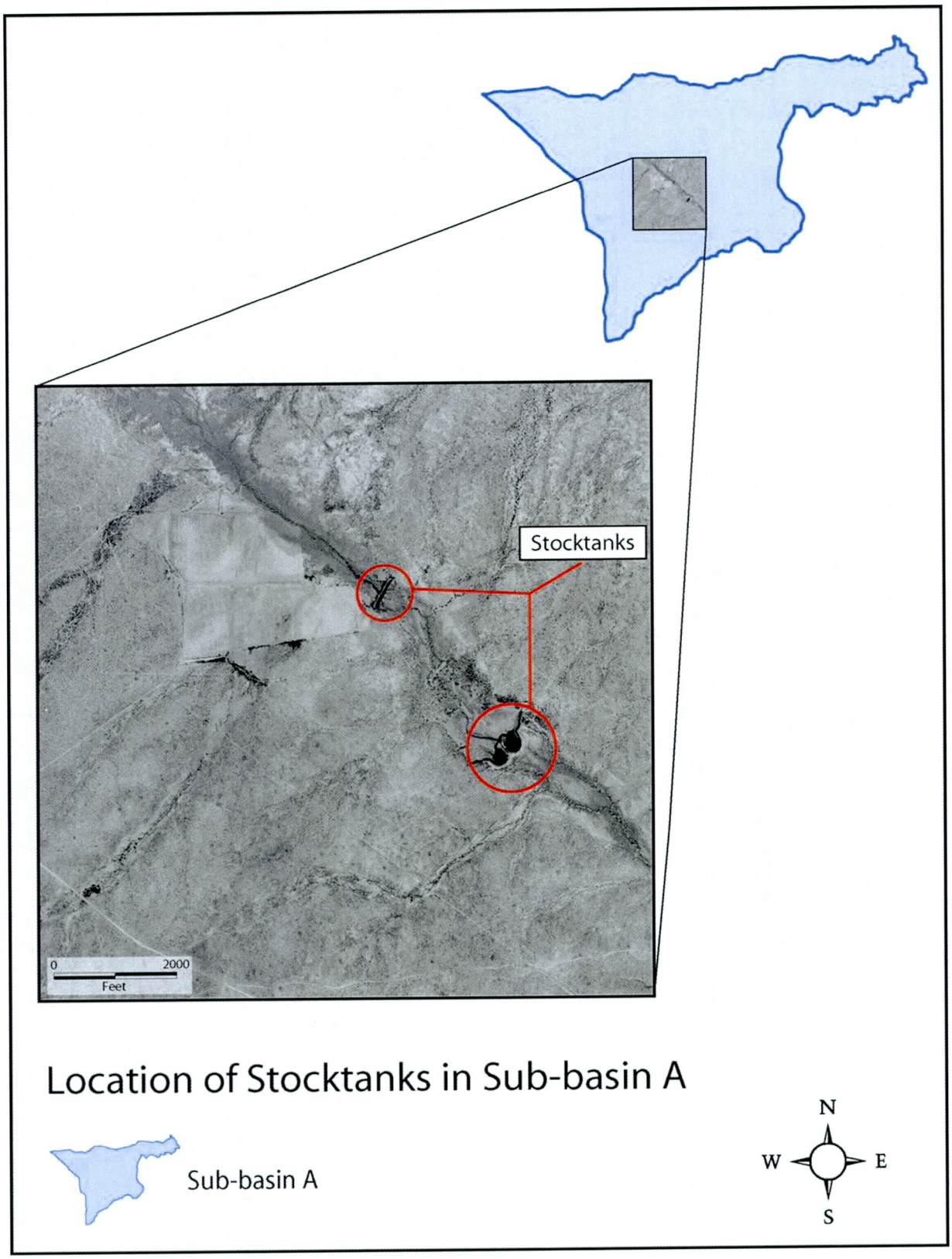

Figure 16. Location of stock tanks within sub-basin A

Percent Rock Outcrop

Impervious areas were estimated by using the percent bedrock outcrop information from the SCS soil data. Figure 17 shows sub-basin B contains the highest percent of bedrock (impervious area). Watersheds with high percent rock outcrop generate higher discharges than watersheds with low percent outcrop (all other factors being equal).

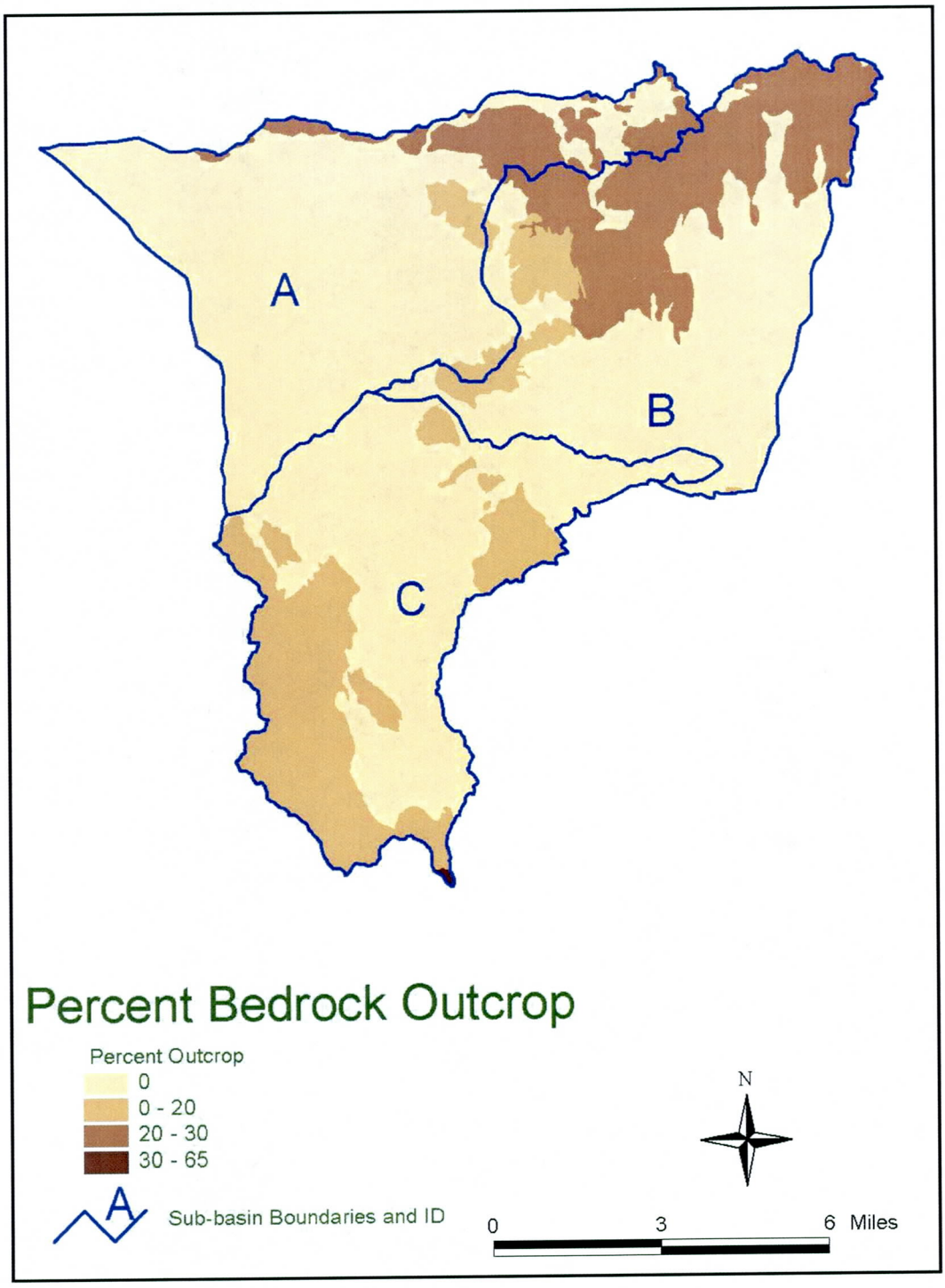

Figure 17. Distribution of percent bedrock outcrop for sub-basins A, B, and C

Drainage Density

Watershed drainage density can directly affect peak discharges from storm events. Areas characterized by dense drainage networks collect and channelize flow quickly, resulting in "flashy" hydrographs and high peak discharges. Low density drainage networks generally allow more overland flow resulting in more attenuated hydrographs and lower peak discharges. Drainages for sub-basins A, B, and C are shown in Figure 18. Results from drainage density analysis of Jackrabbit Wash are summarized in Table 14. Drainage density was evaluated by examination of the number of drainages present in each sub-basin. Sub-basin C has the highest drainage density of the three sub-basins considered.

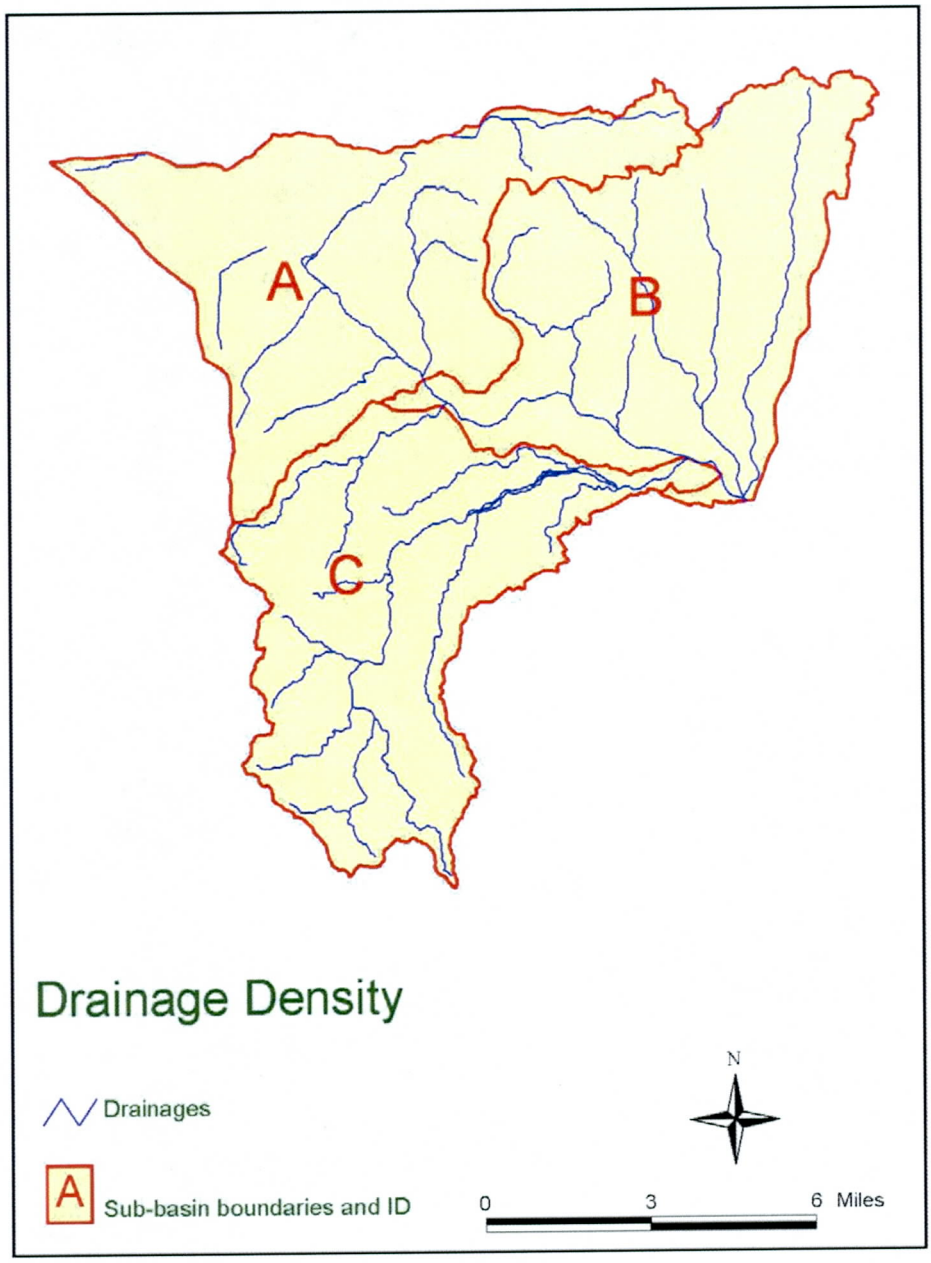

Figure 18. Sub-basin drainage densities

Table 14. Summary of the hydrologic characteristics analyzed

Sub-Basin	Area (mi^2)	Mean Slope (ft/ft)	Area Weighted XKSAT (in/hr)	Area Weighted Percent Outcrop	Drainage Density
A	35	0.003	0.11	3.4	Lowest
B	36	0.007	0.28	10.2	Moderate
C	34	0.008	0.25	7.6	Highest

3.3.1.2 Summary

Analyzing physiographic characteristics individually can be useful in describing the hydrologic characteristics for an individual drainage basin; however, when comparing two or more basins, the characteristics must be viewed wholly as a system. Table 15 is the interpreted results from the hydrologic characteristics.

Table 15. Individual results of physiographic analysis in comparison with indirect estimates

	Estimated Peak Discharge Ranking (from Table 14) 1 = highest estimated discharge 2 = intermediate estimated discharge 3 = lowest estimated discharge					
Sub-Basin	Area	Mean Slope	Weighted XKSAT	Weighted Percent Outcrop	Drainage Density	Indirect Estimates (cfs)
A	2	3	1	3	3	7,600
B	3	2	3	1	2	5,000[14]
C	1	1	2	2	1	9,300

As shown in Table 15 above, the indirect discharge estimates showed that sub-basin C produced the most runoff during the October 2000 storm events, and had the highest average rank of discharge producing characteristics. The physiographic characteristics suggest that this would be the expected result for similar rainfall over all three basins.

3.3.2 FCDMC Indirect Estimates

FCDMC personnel conducted a slope-area survey in December 2000. The purpose was twofold: one, to collect data to compute a rating curve for the new gaging station, and two, to estimate the peak discharge of the recent large flood(s).

The slope-area survey consisted of a 5,900 foot channel reach survey of high water marks along both banks of the channel downstream of the Vulture Mine Road crossing. Additionally, nine cross sections were surveyed. Manning's n-values of 0.028 to 0.045 were estimated. The FCDMC calculated an estimate of 32,400 cfs for the entire reach. The estimate is considered fair based on quality of high water marks, the length of channel surveyed, and the consistency of calculated results across the various subsections of the surveyed reach. Sub-reach estimates varied from 47,000 cfs to 24,600 cfs.

[14] Derived by summing discharges from cross-sections 3 and 4, Jackrabbit Wash near Wildcat Well reach.

3.3.3 USGS Indirect Estimates

The USGS also conducted a slope-area survey of the October flood(s). The surveyed reach is downstream of Wickenburg Road near the USGS crest-stage gage (#09516800). Results from the USGS survey indicate an estimate of 27,000 cfs. This estimate is considered "poor" according to the USGS criteria. The slope-area estimate was based on four cross sections. The poor rating was attributed at least in part to super-elevation along the right bank and the possibility of supercritical flow at one of the cross sections.

Additionally, the USGS estimated a peak discharge of 22,200 cfs at their Hassayampa River Arlington gage (#09517000). The hydrograph data at this continuous station were truncated by silting of the orifice line. The USGS estimates the peak occurred at about 1900 hours on 10/27/00.

3.3.4 JEF Indirect Estimates

JEF conducted indirect estimates at multiple locations throughout the Jackrabbit Wash watershed for the purpose of determining the tributary source of runoff for Jackrabbit Wash, and determining the viability of indirect estimates derived from digital terrain model (DTM) data.

3.3.4.1 Methods

2001 DTM data for the Jackrabbit Wash area were obtained from the Flood Control District of Maricopa County's orthophotography project. From this data, JEF generated a TIN model that was used to create 10 foot contour interval topography which was then used to generate 2 foot interpolated topography. Cross-sections were extracted from the 2 foot topographic map for indirect discharge estimates at various locations in the Jackrabbit Wash watershed (Figure 19).

Discharges were estimated by using FlowMaster 6.1 software. Manning's coefficients (n) were interpreted from 2001 orthophotos and field observations, and ranged from 0.035 to 0.060. High water marks were estimated from the orthophotos and field observations at each cross-section. The ratings assumed normal depth using bed slopes at each cross-section.

3.3.4.2 Results

Analysis of indirect estimates from DTM data resulted in reasonable discharge estimates. Two cross-sections from the JEF analysis (FCDMC gage site, cross-sections 1 and 3) were compared directly with geometric data from two cross sections from the FCDMC 2000 GPS survey data (Figure 20 and Figure 21). Table 16 summarizes the comparisons which were made where the JEF station locations were within 2 feet of the FCDMC stations.

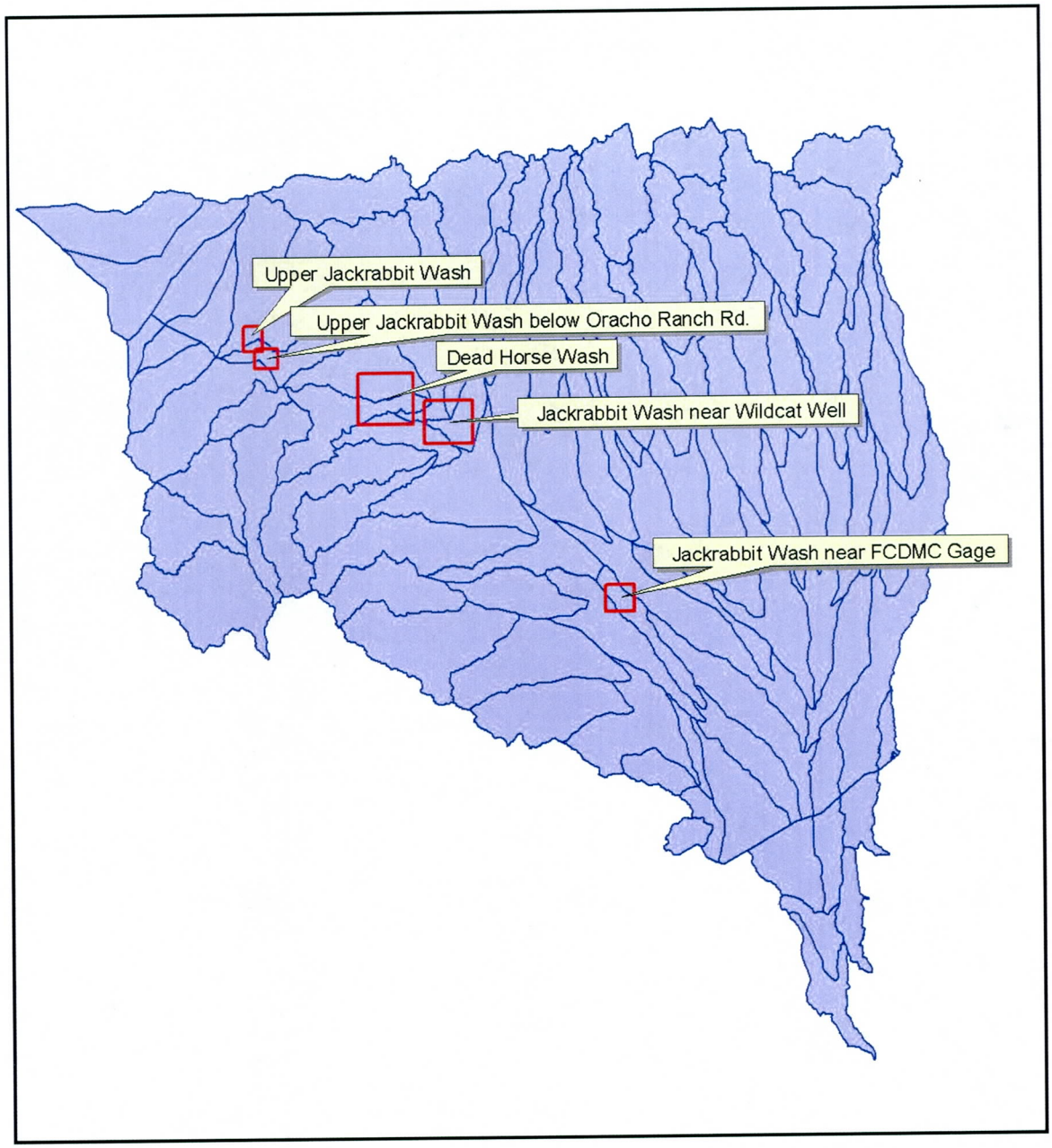

Watershed Map

Watershed Boundaries

Cross-Section Reach Locations

N
W E
S

0 3 6 Miles

Figure 19. Channel reach locations of JEF indirect discharge estimates

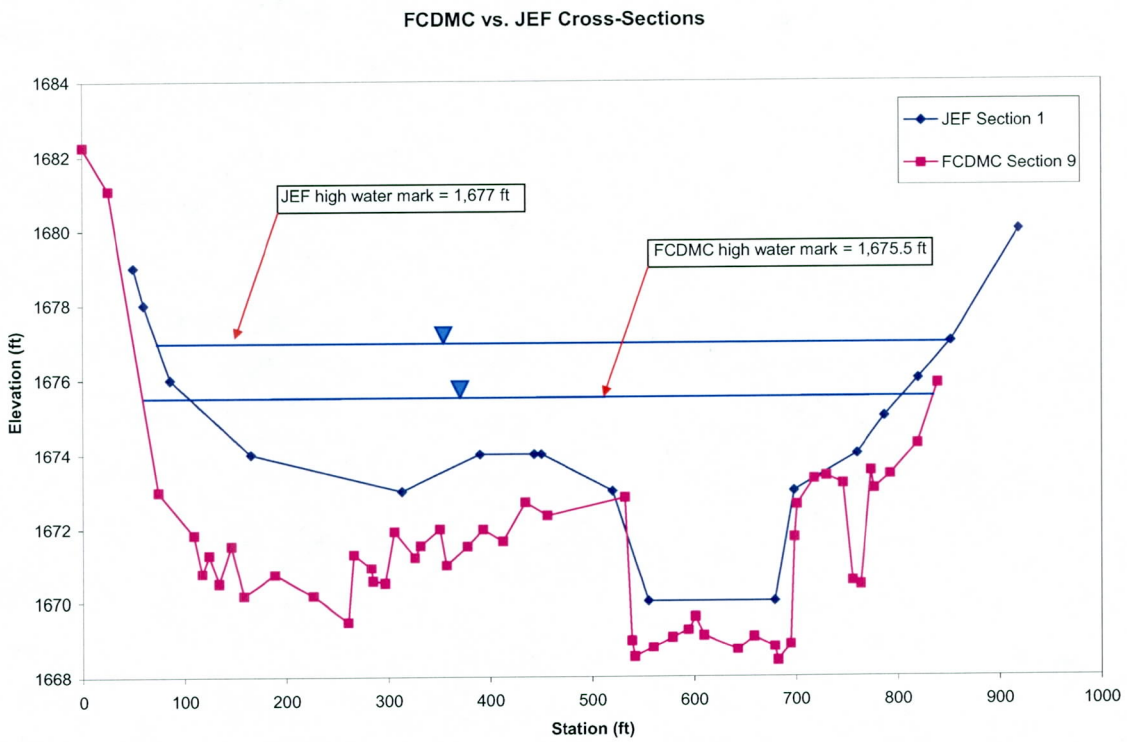

Figure 20. Plot comparison of JEF cross-section 1 with FCDMC cross-section 9

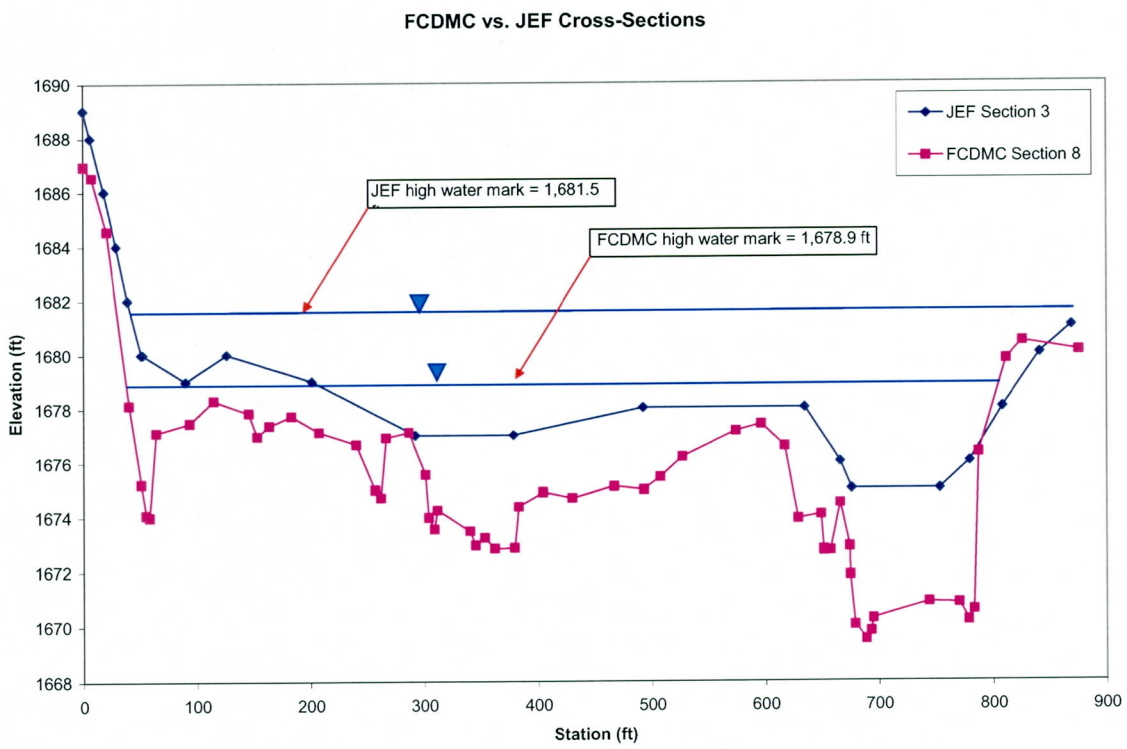

Figure 21. Plot comparison of JEF cross-section 3 with FCDMC cross-section 8

Table 16. Cross-section comparison of FCDMC and JEF indirect data

Data Source	Cross-Section ID	Station (ft)	Elevation (ft)	Elevation Difference (ft)
FCDMC	9	679	1669	1
JEF	1	679	1670	
FCDMC	9	698	1673	1
JEF	1	698	1672	
FCDMC	9	820	1676	2
JEF	1	819	1674	
FCDMC	8	6	1688	2
JEF	3	7	1687	
FCDMC	8	39	1682	4
JEF	3	40	1678	
FCDMC	8	51	1680	5
JEF	3	51	1675	
FCDMC	8	378	1677	4
JEF	3	379	1673	
FCDMC	8	492	1678	3
JEF	3	493	1675	
FCDMC	8	665	1676	2
JEF	3	665	1674	
FCDMC	8	675	1675	3
JEF	3	674	1672	

The mean elevation difference between the two data sets is 2.7 ft, within the potential error range for the 2 ft. interpolated topography. This difference is similar to the high water mark data comparison between the two data sets. Comparison of discharge estimates from the FCDMC and JEF data are summarized in Table 17.

Table 17. Comparison summary of FCDMC and JEF indirects

Data Source	Cross-Section	Discharge at Section (cfs)	Reach Average Discharge (cfs)
FCDMC	9	26,500	32,400[15]
JEF	1	26,100	
FCDMC	8	26,600	32,400
JEF	3	26,450	

When comparing individual cross-sections, the discharge estimates from the two data sets are very similar. Comparison of JEF cross-section 1 and FCDMC cross-section 9 differ by only 2 percent, while comparisons of cross-sections 3 and 8 vary by 7 percent. The results of this analysis show that indirect estimates derived from current DTM data in addition to analysis of aerial photography can provide reasonable results with relatively few hours invested. The results also show the importance of cross-section location selection for both methods.

[15] Published discharge estimate from cross-section 1-9; an approximately 6,000 ft. channel reach

3.4 Statistical Analysis

To place the October 2000 flood within the context of the 100-year recurrence interval it is important to examine both physical and statistical data. Table 18 is a comparison of indirect discharge estimates for Jackrabbit Wash with statistical information.

Table 18. Comparison of discharge estimates for Jackrabbit Wash *(statistical data is shaded)*

Data Source	Location	Recurrence Interval (years)	Discharge Estimate (cfs)
FCDMC Indirect (Oct 2000)	FCDMC Gage Site	-	32,400
FIS (HEC-1)	FCDMC Gage Site	100	21,100
FIS (HEC-1)	USGS Gage Site	100	20,000
USGS Regression Equation[16]	FCDMC Gage Site	100	37,300
USGS 1991 Published Value[17] (n=16)	USGS Gage Site	100	32,900
USGS Regression Equation	USGS Gage Site	100	37,500
USGS 1998 Published Value[18] (n=23)	USGS Gage Site	100	33,900
LP3 Distribution[19] pre Oct. 2000 (n=27)	UGSG Gage Site	100	39,100
LP3 Distribution post Oct. 2000 (FCD Peak for WY 2001) (n=28)	UGSG Gage Site	100	63,700
LP3 Distribution post Oct. 2000 (USGS Peak for WY 2001)	UGSG Gage Site	100	60,100

The data above show that the FCDMC indirect value is approximately 90% of the mean statistical estimate of the 100-year peak discharge when the 2000 peak discharge is excluded from the computation. The average standard error of the regression equation estimates is 39 percent (Thomas, et al., 1997). Note that the FIS discharges are lower than the minimum value suggested by the Region 12 equation standard error (i.e. 37,500 – 14,625 = 22,875 cfs).

The log-Pearson III analyses suggest that the FIS discharges would have been within the 95% confidence limits without the October 2000 peak included in the record (Figure 22). However, when included, the lower limit of the 95% confidence interval for the 0.01 probability flood is about 24,000 cfs using the FCDMC estimate of the peak (Figure 23). Using the USGS estimate of the peak discharge of 27,000 cfs, the lower limit of the 95% confidence interval is 22,800 cfs.

[16] Source: *Methods for Estimating Magnitude and Frequency of Floods in the Southwestern United States, USGS, 1997.* (Central Arizona Region 12). USGS Water Supply Paper 2433, Equation: $Q = 10^{(6.55-3.17AREA^{-0.11})}(ELEV/1000)^{-0.454}$

[17] Source: *Basin characteristics and streamflow statistics in Arizona as of 1989*, USGS, WRIR 91-4041

[18] Source: *Statistical Summaries of streamflow data and characteristics of drainage basins for selected streamflow-gaging stations in Arizona through Water Year 1996*, USGS Report 98-4225

[19] LP3 = Log Pearson Type III probability distribution. Estimated using HEC-WRC by JEF.

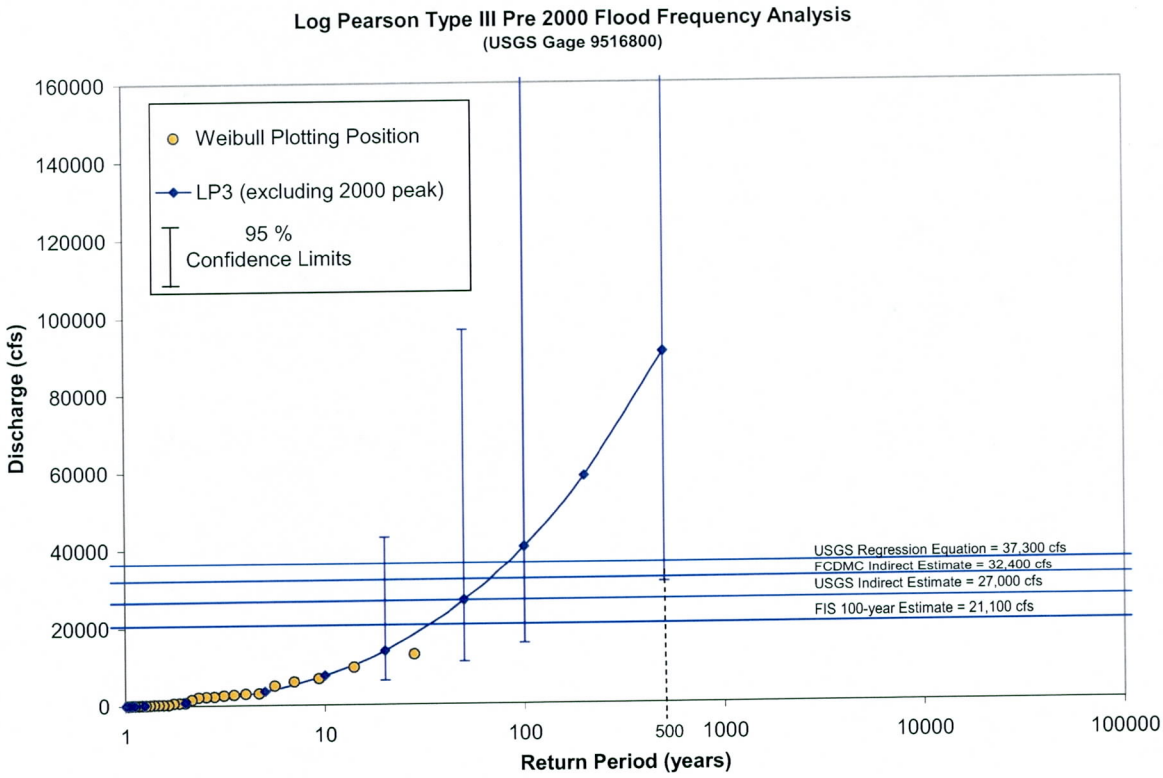

Figure 22. Flood frequency analysis for gage data through Water Year 2000.

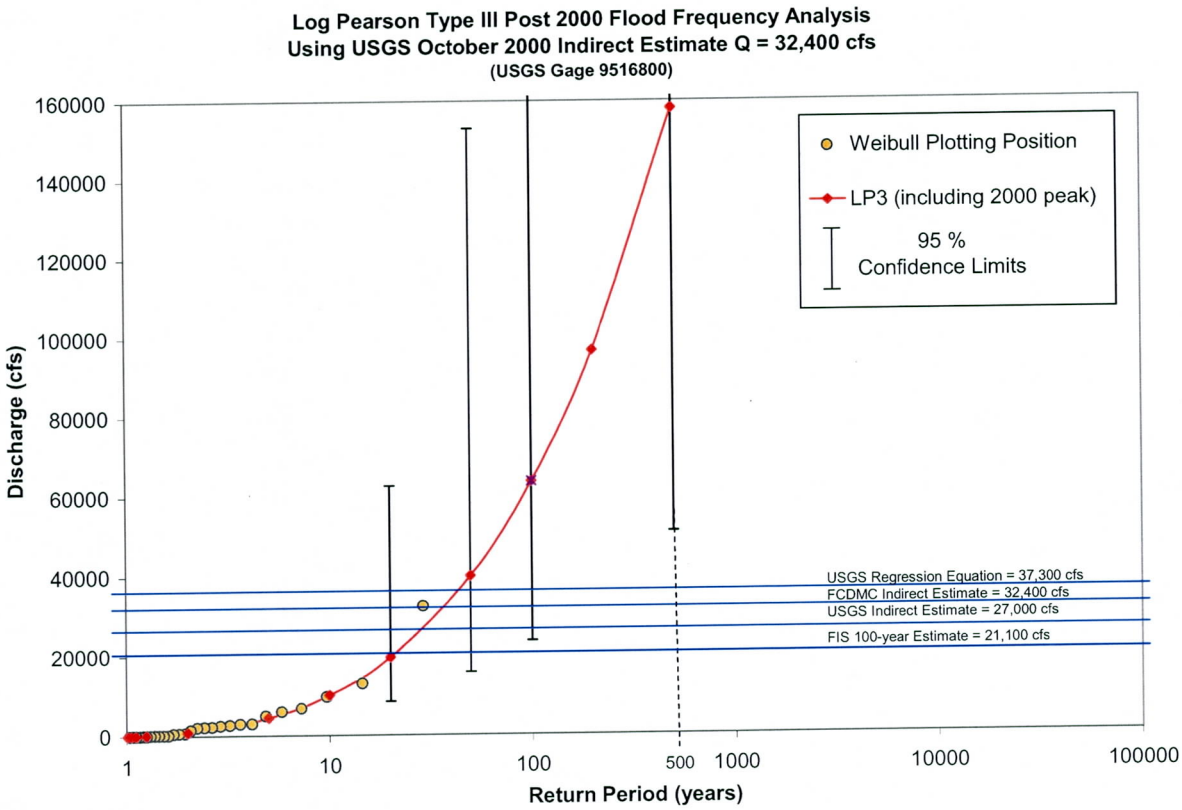

Figure 23. Flood frequency analysis for gage data through Water Year 2001

3.4.1 Non-Exceedence Analysis

A non-exceedence analysis is designed to determine a paleohydrologic bound for high magnitude, low frequency floods over a measured time interval (Levish et al., 1997). This method involves the study of geomorphic features adjacent to the fluvial system that are affected or altered only by large magnitude, low frequency floods. Relevant features may include abandoned flood plains, alluvial terraces, and alluvial fans and may range in age from hundreds to thousands of years. The result is an estimate of the maximum discharge during the minimum time interval since stabilization or abandonment of the surface representing the non-exceedence bound, and thus, is a conservative estimate for flood frequency (Levish et al., 1997).

A non-exceedence analysis was conduced for Jackrabbit Wash near the FCDMC gage site. Geologic mapping for this project by the AZGS (Section 5) resulted in the description of five geologic units (Figure 28). Two of these units were described as Ql (Late Pleistocene) and Qm (Middle Pleistocene). They represent non-exceedence bounds for flooding along Jackrabbit Wash. Cross-section data from the FCDMC December 2000 survey were used to determine the non-exceedence discharge estimate for the non-exceedence statistical model (Figure 24). A normal depth estimate of the maximum discharge that fits below the Ql surface at this section was 45,700 cfs.

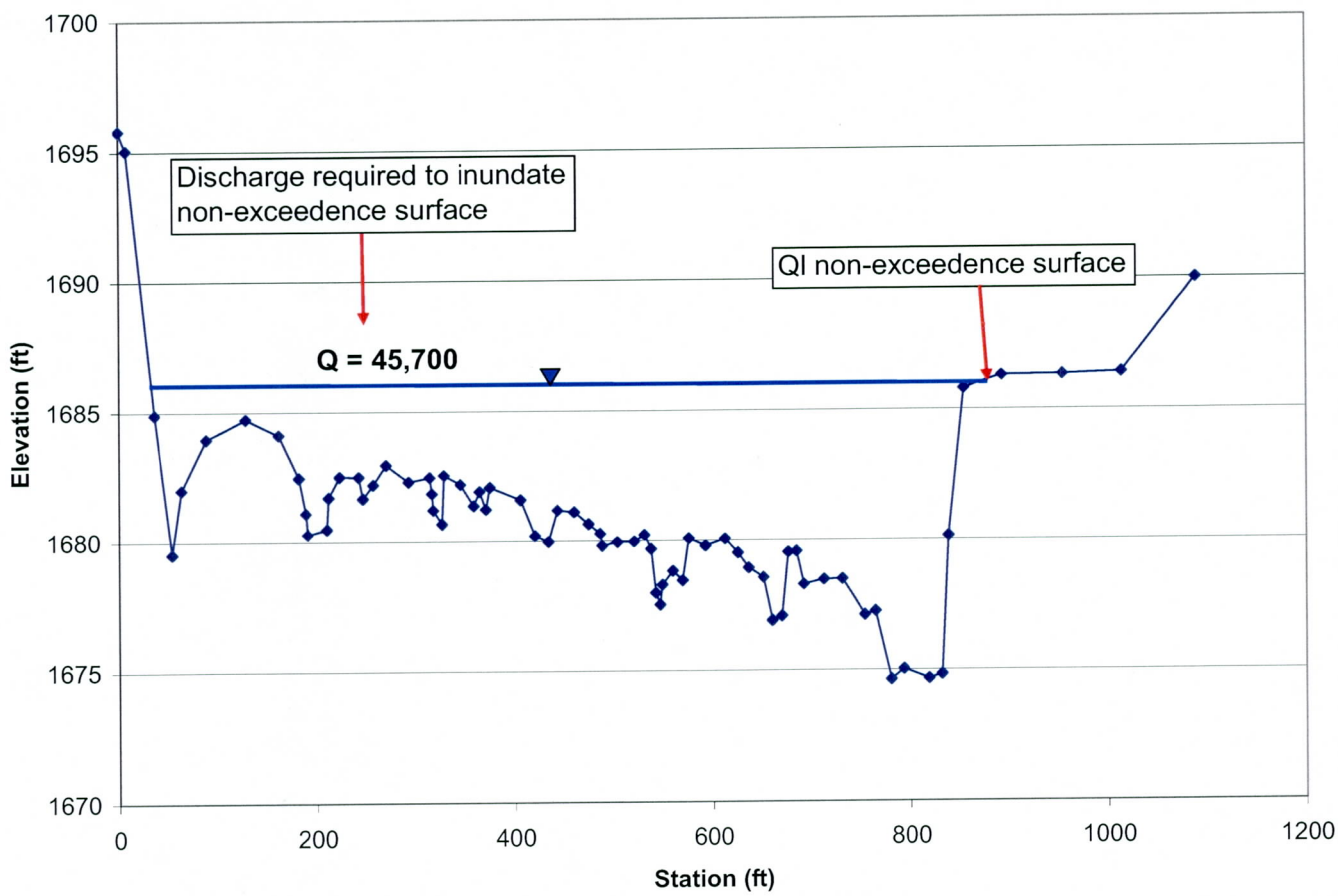

Figure 24. Cross-section 7 from FCDMC December 2000 survey showing Ql non-exceedence surface

The non-exceedence flood frequency analysis was done using the FLDFRQ3 1.1 (O'Connell, 1999) software program. The FLDFRQ3 program incorporates non-exceedence bound data and allows for numeric uncertainties. This information was combined with the gage data from USGS gage #9516800 through water year 2001. The FCDMC indirect discharge of 32,400 cfs for the October 2000 flood was used in the model for water year 2001. FLDFRQ3 uses a Bayesian methodology approach to solve the Maximum Likelihood Estimation (MLE) as described by Stedinger and Cohn (1986). The Bayesian approach uses an integration grid to determine consistent frequency functions at various probabilities (O'Connell, 1999). In summary, FLDFRQ3 combines the annual gage peak discharge data and non-exceedence information (including the non-exceedence discharge, estimated age of non-exceedence surface, and numeric degree of uncertainty with each) into the probability distribution. Input and output sheets from the model are attached in Appendix D. The age of unit Ql was estimated at 10,000 years before present, a conservative estimate for the unit. The AZGS mapped the age of the Ql unit as 10,000 to 100,000 years before present (Section 5). The input data used in the FLDFRQ3 model included the non-exceedence discharge estimate of 45,700 cfs, a 10,000 year age estimate for the Ql surface, and high uncertainty value for each. Table 19 is a summary of the FLDFRQ3 analysis results. Figure 25 is a plot of the FLDFRQ3 results.

Table 19. FLDFRQ3 results for non-exceedence analysis

Frequency Estimates	
Return Period	Discharge
(years)	(cfs)
5	4,200
10	7,000
50	14,400
100	17,700
500	25,000
800	27,000 (USGS indirect)
3,100	32,400 (FCDMC indirect)

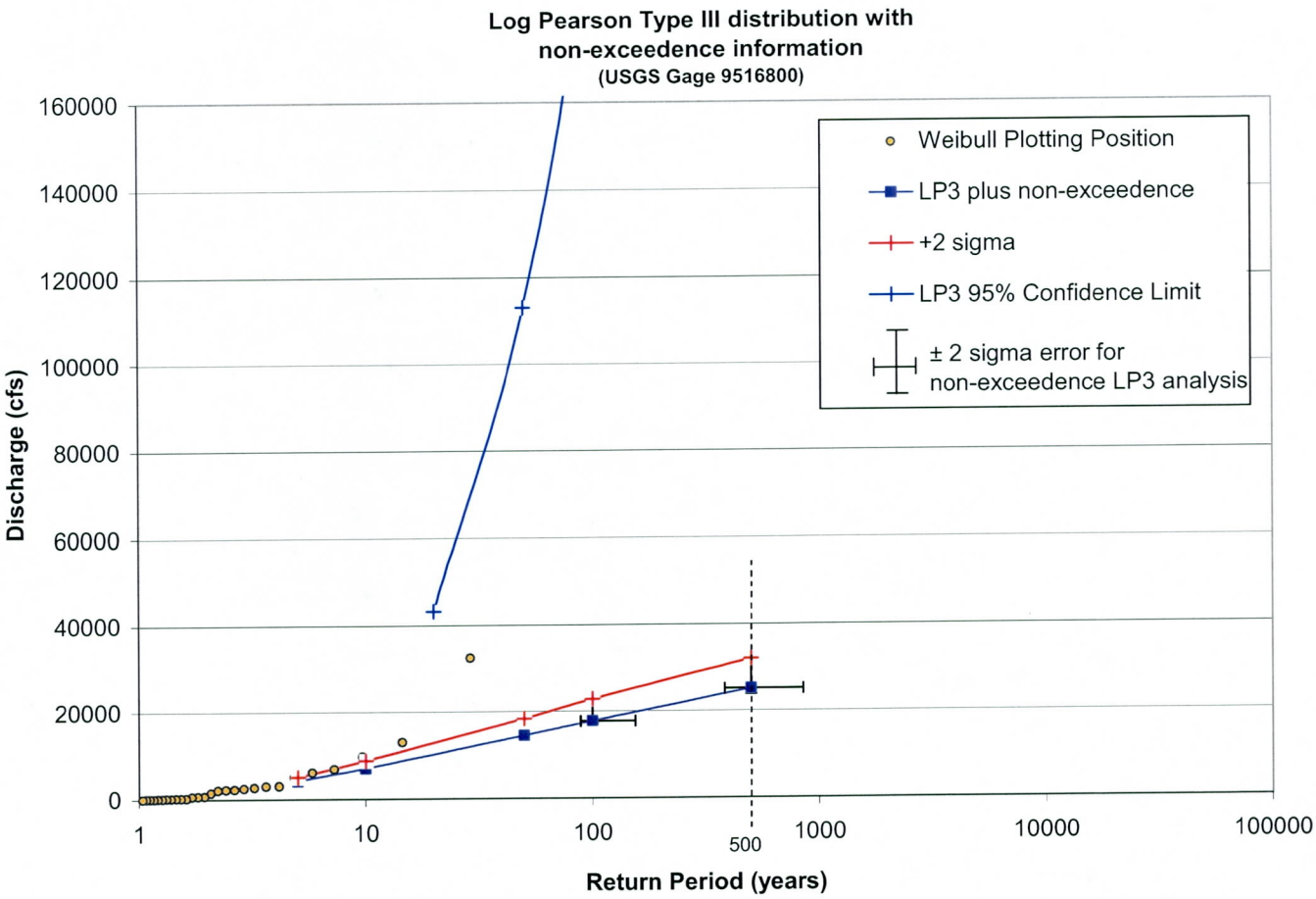

Figure 25. Probability distribution plot from FLDFRQ3 analysis including non-exceedence information

Figure 25 shows the that degree of uncertainty in the probability distribution is dramatically reduced by the inclusion of the non-exceedence data as shown by the +2 sigma and 95% confidence plots. Thus, the frequency curve may be more reliably extended beyond the measured data.

Results of the non-exceedence analysis indicate the October 2000 flood was an unprecedented event. Figure 26 is a plot of both the U.S. and regional area versus discharge envelope curve (House, 1996) This figure shows that the October 2000 flood on Jackrabbit Wash is the largest observed event for a watershed of its size, further supporting the conclusion that the October 2000 flood on Jackrabbit Wash was a rare event that may have far exceeded the 100-year recurrence interval.

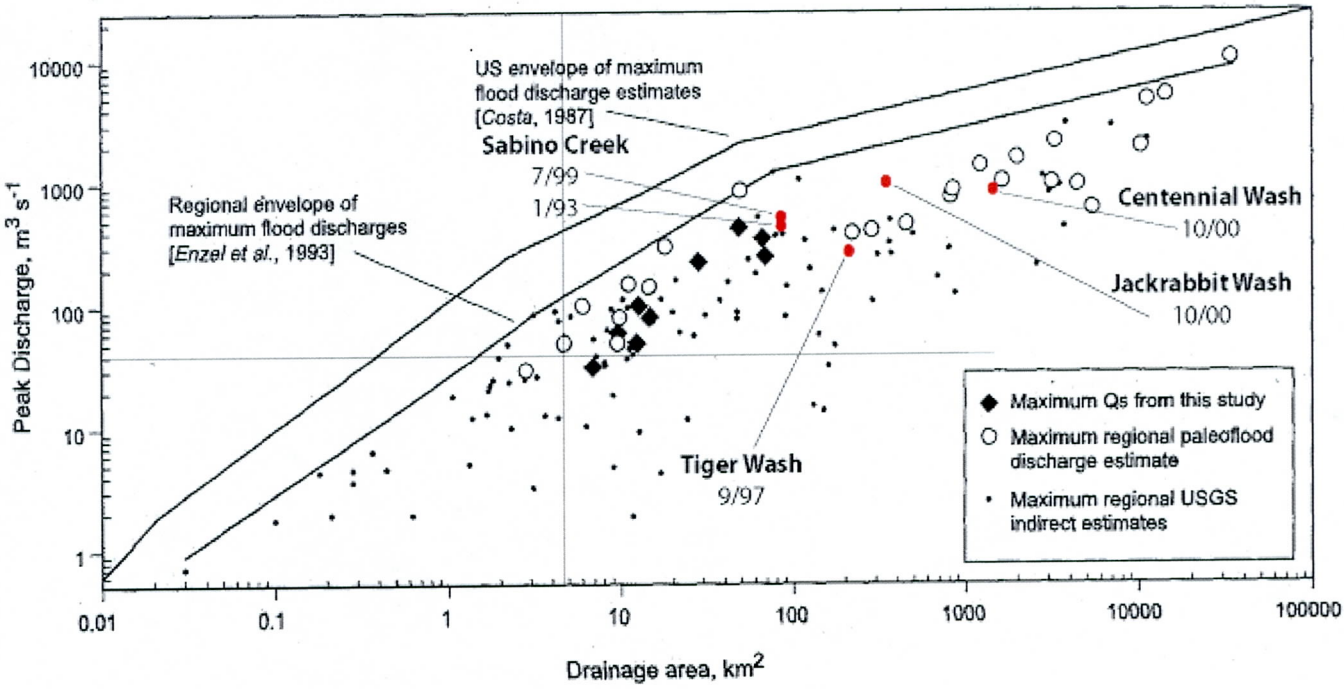

Figure 26. Peak discharge verses drainage area envelope curves for the U.S. and the lower Colorado River region (House and Baker, 2001)

3.4.2 Results

Pre-2000 frequency analyses of peak discharge values for Jackrabbit Wash indicate the October 2000 event was somewhat less than the 100-year flood. When including the FCDMC indirect discharge estimate (32,400 cfs) into the statistics, the results indicate the October 2000 flood was between a 20- and 50-year event. As described in Section 2.4, the statistical analyses for the October 2000 rainfall resulted in a return period of 30-year for the October 21 event and point rainfall in excess of the 500-year event for October 27. Non-exceedence information indicates there is no evidence that a flood greater than 45,700 cfs has occurred on Jackrabbit Wash in the past 10,000 years. This provides a "cap" for historic flooding and constrains the statistical analysis resulting in less uncertainty in return period estimates. Our conclusion is that a 30-year rainfall closely followed by a greater than 500-year rainfall caused an 800- to 3,000-year flood. In summary, the October 2000 flood had a peak discharge of about 32,400 cfs and was an 800- to 3,000-year event, while the FIS 100-year discharge estimate of 21,000 cfs is probably a 200- to 300-year event.

4. Landsat Based Flood Detection

Dr. Larry Mayer, adjunct professor of geosciences at the University of Arizona, has developed methodologies to detect landscape changes using Landsat ETM+ sensor data (Mayer and Pearthree, 2001). Changes in landscape due to flooding can be detected by analysis of the remote sensing data from before and after the event (Figure 27).

Figure 27. Jackrabbit Wash Landsat change image taken after the October 2000 flood

Dr. Mayer applied this technique to Jackrabbit Wash to detect the extent of surface changes from the October 2000 flood (Figure 27). The following is an abstract and summary from Dr. Mayer's report from this analysis. The entire report is attached in Appendix B.

Abstract
Landscape change detection using Landsat ETM+ sensor data and image processing methods based on band orthogonalization are used for initial mapping of flood inundation along Jackrabbit Wash, in Maricopa County. Results indicate that image processing of Landsat data, which has a nominal 30 meter pixel size spatial resolution, can provide a direct method to document flooding in remote areas of Arizona. This study analyzes a portion of two Landsat scenes covering part of Maricopa County, west of Phoenix, Arizona. The study finds that Jackrabbit Wash, in contrast to many of the adjacent streams, has a spectral signature that indicates there was detectable landscape modification associated with the October 2000 flood. The area of flooding is clearly indicated on the processed satellite image as a band of yellow. Field validation consisting of checking several reaches of Jackrabbit Wash.....corroborated the evidence from the satellite change image. Ubiquitous evidence for very significant flooding was found. The performance of the change detection on a regional basis appears strong. On the local basis, not every pixel which showed evidence for inundation in the field was highlighted as changed on the change image. A significant finding is that the flooding affected the upstream portions of Jackrabbit Wash and therefore must be related to storm precipitation in the headwaters area.

Conclusions
The methodology for making change images for detecting flooding discussed in this report is a single step procedure that requires little operator training. The methodology has been validated for alluvial fan flooding for Tiger Wash (Mayer and Pearthree, in press). The satellite change image.....clearly indicated that Jackrabbit Wash had undergone landscape change between.....November [of 1999 and 2000].....[The] change was indicated by the color yellow on the change image. Based on field checking in the area of Jackrabbit Wash near Vulture Mine Road, we find that wherever yellow occurs in a stream, significant flooding is indicated. Because we see change from the upper parts of Jackrabbit Wash all the way to its confluence with the Hassayampa River, we can infer that the flooding was localized, was produced by rainfall in the headwaters region, and escaped significant transmission loss, perhaps due to antecedent moisture conditions.

The procedure outlined in this report indicates that band orthogonalization is an effective method for finding areas of flood inundation in remote regions of Arizona, mapping the extent of known floods, and that much of the data are significant even at the resolution of individual 30 m pixels.

5. Geomorphic Analysis

The Arizona Geological Survey (AZGS) conducted field interpretation and mapping of the geomorphic surfaces adjacent to Jackrabbit Wash near the FCDMC gage site at Vulture Mine Road (Figure 28).

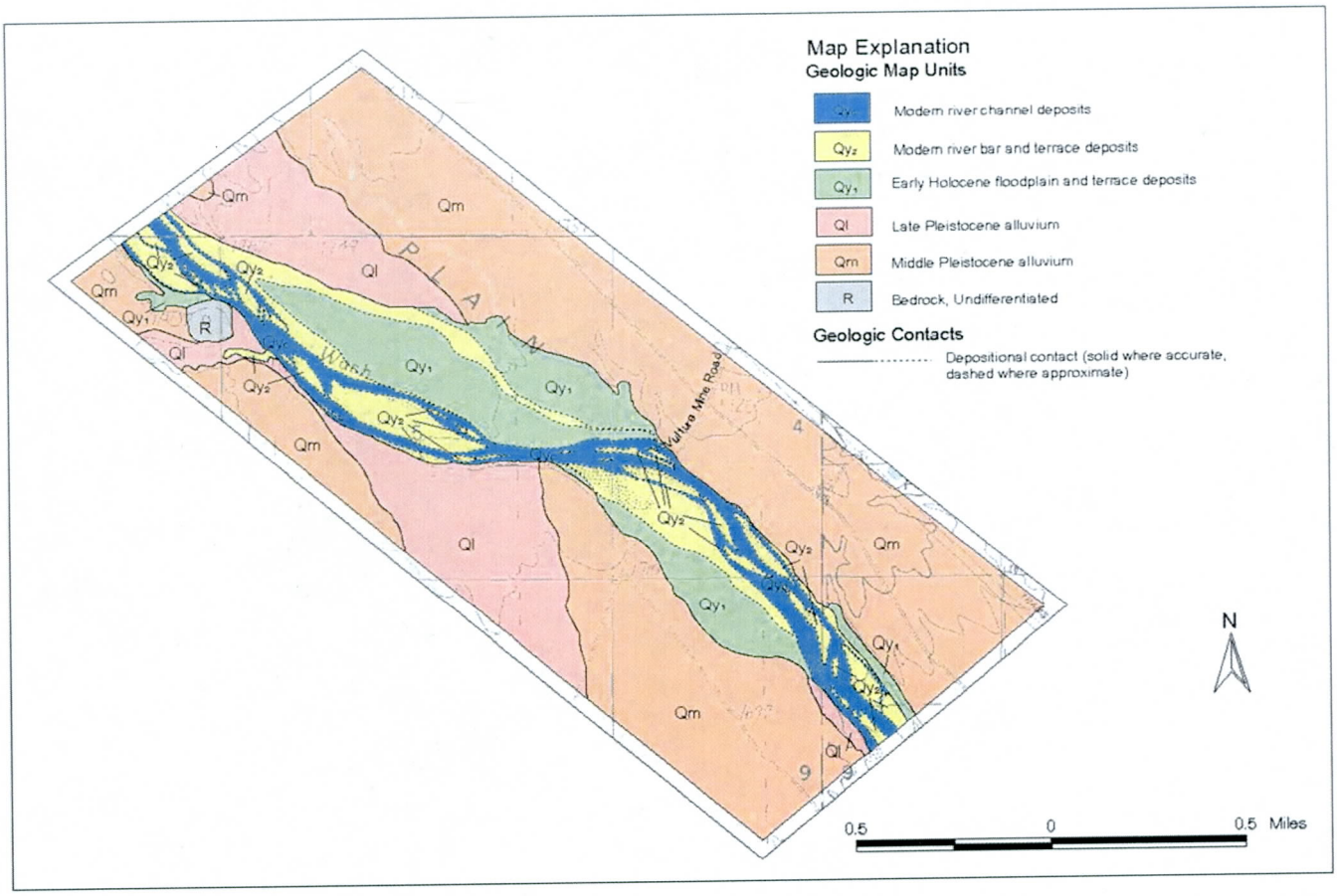

Figure 28. Surficial geologic map of Jackrabbit Wash at the Vulture Mine Road crossing

The purpose of the AZGS study was to compare field evidence from the October 2000 flood with the geologic record to determine the flood's historical context. The following are excerpts of the Introduction and Conclusions from the AZGS report. The complete AZGS report is attached in Appendix C.

INTRODUCTION

Mayer (2000) developed a new method to detect landscape change from flooding by quantitatively comparing two Landsat 7 satellite data scenes taken before and after a flooding event. Mayer and Pearthree (2002) first evaluated this method on Tiger Wash fan, a large distributary system in western Maricopa County. They found a strong correlation between the detected changes from remote-sensing data and extent of flood inundation from field mapping. This change detection methodology was applied to Jackrabbit Wash, which experienced a very large flood in October 2000. The goal of this study is to assess how well this method detects flood inundation and extent on a piedmont tributary system like Jackrabbit Wash. This report compares extent of flood inundation derived from the satellite change image with field data.

Geologic and geomorphic information can also provide invaluable information of flood hazards in piedmont areas (Field and Pearthree, 1992; Hjalmarson and Kemna, 1991; Pearthree and others, 1992; Field, 1994a and 1994b; Hjalmarson, 1994; Klawon and Pearthree, 2000). Mapping surficial geologic deposits based on surficial characteristics such as surface color, soil development, accumulation of calcium carbonate, development of desert varnish and desert pavement, drainage patterns and entrenchment, local topography, and vegetation provides

information about the age of the deposit and potential inundation from flooding. Analyzing evidence of flood extent and flow characteristics provides information about potential erosion hazards and channel changes (Klawon and Pearthree, 2000). Surficial geologic mapping and channel change analysis of Jackrabbit Wash was conducted at Vulture Mine Road crossing.

CONCLUSIONS

Geomorphologic investigations of Jackrabbit Wash following the large flood of October 2000 provide information on the extent and character of inundation in that flood, the usefulness of satellite change detection methods in delineating the extent of flood inundation, and the value of geologic and geomorphic information in delineating flood corridors. Reconnaissance field investigations were conducted at a number of sites along Jackrabbit Wash to evaluate the extent and character of inundation in the October 2000 flood. These observations were compared with the data derived from analysis of changes in satellite images from before and after the flood. The fit between the field observations and the extent of colors reflecting various kinds of changes was found to be very good, with the greatest uncertainties being in areas of very shallow inundation and less-than-perfect georectification of the satellite data. High-resolution, georectified aerial images provided by the FCDMC were used to improve the accuracy of the delineation of the extent of inundation along 25 miles of Jackrabbit Wash.

More detailed field investigations were conducted along a 2-mile-long reach of Jackrabbit Wash on either side of the Vulture Mine Road crossing. The extent and depth of inundation in the 2000 flood was mapped in detail, and inundation was subdivided into several depth categories ranging from very shallow flow up to deep channel flow. We found that colors on the satellite change image that are suggestive of change correlated very well with the overall extent of inundation, and various colors on the satellite change image correlated fairly well with different flow depths. We mapped the surficial geology of this reach using pre-flood aerial photos and field observations. The distribution of Holocene channel and terrace deposits along Jackrabbit Wash defines the areas that have been subject to substantial erosion or deposition over the past few thousand years. Higher Pleistocene terraces provide the topographic constraints for this geologic floodplain. We found that nearly all of the geologic floodplain along this part of Jackrabbit Wash was inundated in the 2000 flood, and locally the youngest Pleistocene terraces were subject to very shallow inundation. The extent of inundation in the 2000 flood attests to the relatively extreme nature of this flood. Comparison of the size of the peak discharge in the 2000 flood on Jackrabbit Wash with floods from drainages of similar size in the lower Colorado River region also indicates that it was an extreme event. Analysis of historical aerial photos of this reach documented changes in the extent of channels, bars and terraces over the past 50 years or so. Channel areas were most extensive in 1953 and in late 2000, which suggests that Jackrabbit Wash experienced a large flood sometime shortly before 1953. Extensive changes in channel position and associated bank erosion occurred at the expense of Holocene bars and terraces through the historical record, but no detectable erosion into banks formed by Pleistocene deposits occurred during that interval.

6. Flood Inundation Limits

6.1 Landsat vs. Aerial Photo Analysis

Jackrabbit Wash inundation limits for the October 2000 flood were created from the Landsat change images. The AZGS then refined these limits with the aid of the December 2000 orthographic aerial photographs. Some areas required relatively minor adjustments while other areas required greater adjustments. Figure 29 shows an example of an area where relatively little adjustment of the Landsat inundation limits were required. Figure 30 shows an area that required more adjustment. The overall inundation limits are shown in Plate 1 of Appendix C and are also provided as an ArcView shapefile on CD-ROM in Appendix E.

Potential sources for the reaches needing greater adjustments include the 30 m Landsat image resolution and image registration. Geo-referencing and registration errors between the aerial photographs and the satellite images can result in discrepancies in the flood limit delineation between the two data sets. Given the 30 meter pixel size and registration issues, the correspondence between field and Landsat data is considered quite good.

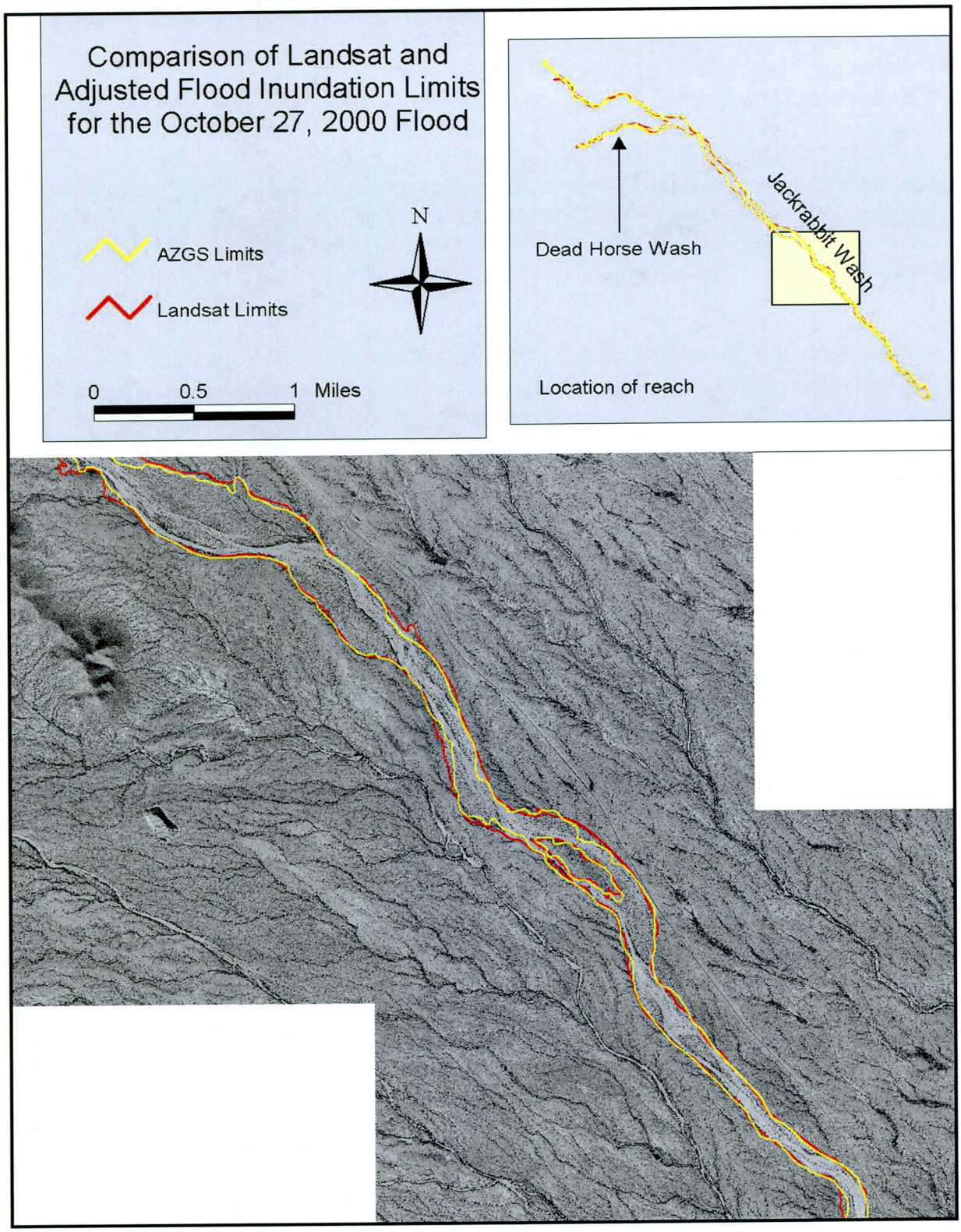

Figure 29. Area with minor adjustments to Landsat flood inundation limits

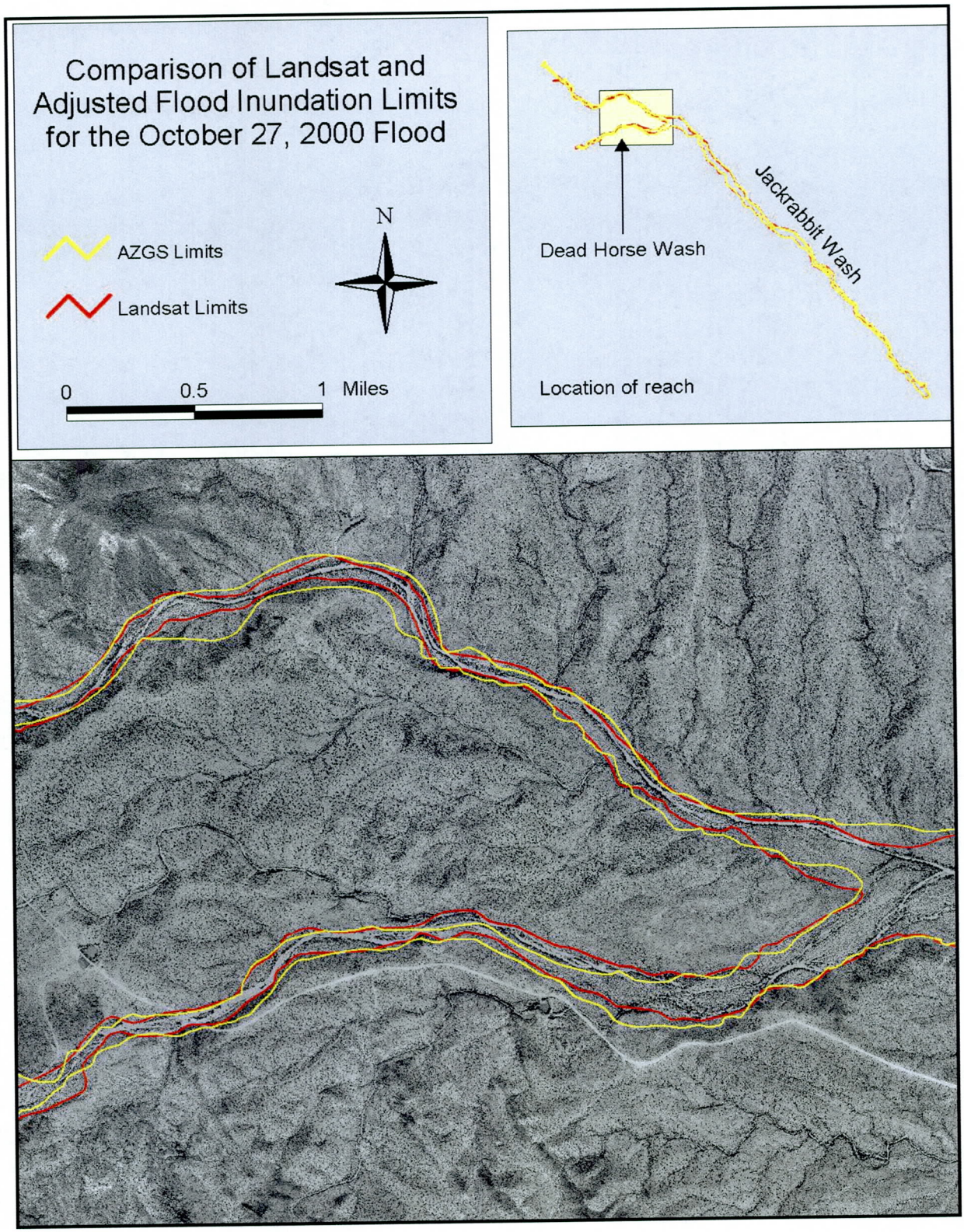

Figure 30. Area requiring greater adjustment to Landsat flood inundation limits

6.2 Aerial Photo vs. FIS 100-year Analysis

The AZGS adjusted planimetric limits of the areas inundated by the October 2000 floods corresponded reasonably close to the FIS 100-year floodplain. A few areas of obvious discrepancies between the planimetric limits of the October 2000 flood and the FIS 100-year floodplain were identified. Reaches in which the flood limits planimetrically exceeded the FIS limits may indicate changes in channel geometry caused by the flood. Figure 31 shows an example where both channel change and possible errors in the original floodplain delineation may have resulted in areas outside the FEMA floodplain being inundated. Additionally, inaccurate delineation in the original FIS analysis may account for discrepancies.

A few of the causes for the difference may include:

- Localized erosion of channel banks
- Lateral channel migration
- Channel aggradation or degradation
- Significant overbank flows

All of the areas where erosion occurred or the inundation limits of the October 2000 flood(s) extended outside the FIS 100-year floodplain are located within the geologic floodplain of Jackrabbit Wash. That is, inundation and erosion fro the October 2000 flood(s) was limited to Holocene surfaces associated with Jackrabbit Wash. Small areas of lateral erosion of Pleistocene surfaces are exceptions to this generalization. However, these areas could have been identified by a geomorphic based erosion hazard assessment.

Figure 32 shows the FCDMC surveyed high water marks in comparison with the flood inundation limits and the FIS limits. The high water marks very closely match the FIS 100-year floodplain's planimetric limit in this reach. This suggests that the water surface elevations are also similar. However, because of vertical datum differences between the 1991 FIS mapping and the 2000 GPS survey, the precise vertical comparison is beyond the scope of this project. Examination of the FIS work maps and the December 2000 survey data show differences between two and four feet between the FIS base flood elevations and the October 2000 flood high water marks. These differences could be due to datum differences, mapping accuracy, actual water surface differences or some combination of all of these. The latter is most likely the case.

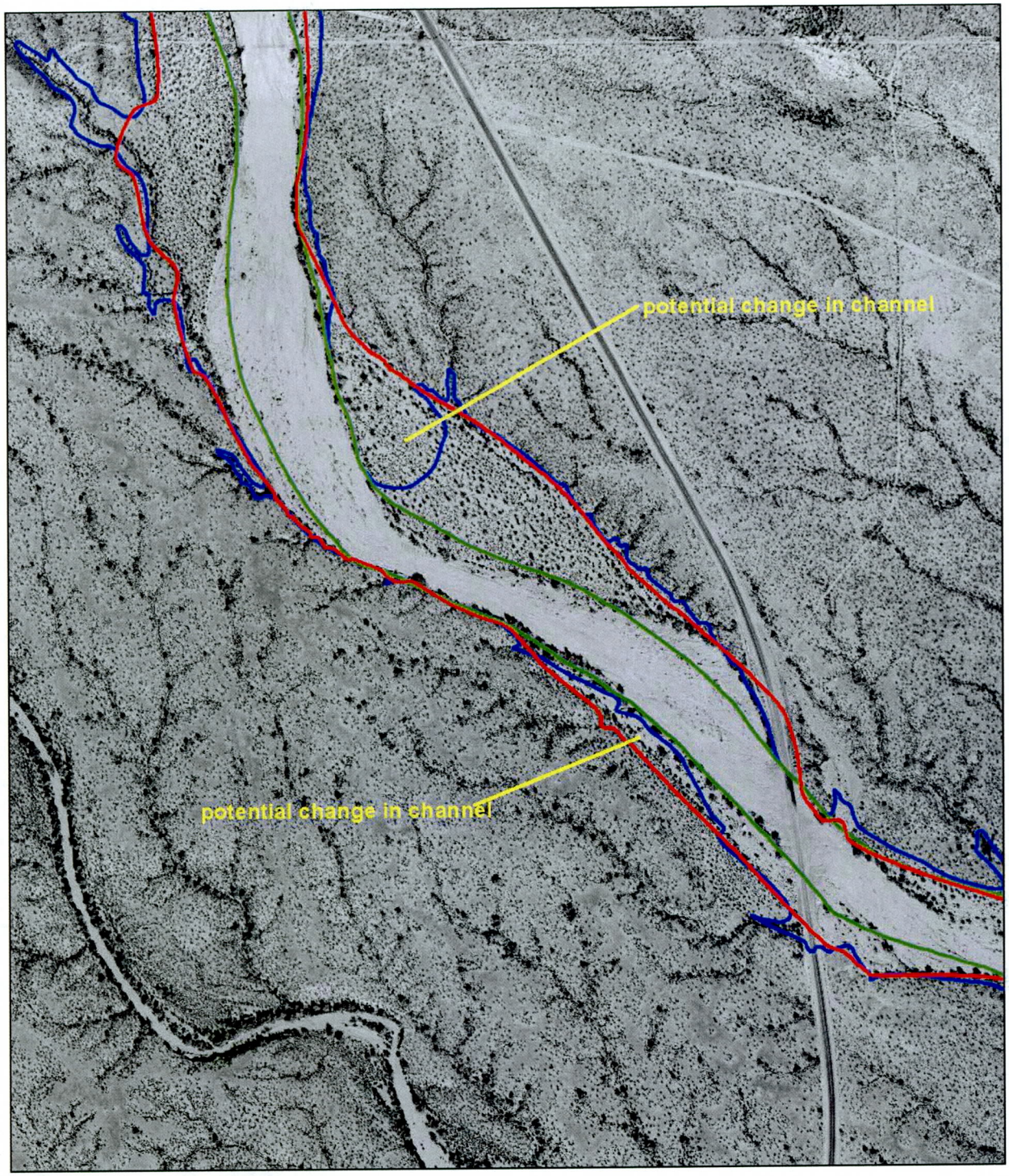

Flood Inundation vs. FIS Floodplain

AZGS Limits
FIS 100-year Floodplain
FIS 100-year Floodway

N

0 0.5 1 Miles

Figure 31. Example of flood inundation limits exceeding the FIS floodplain limits

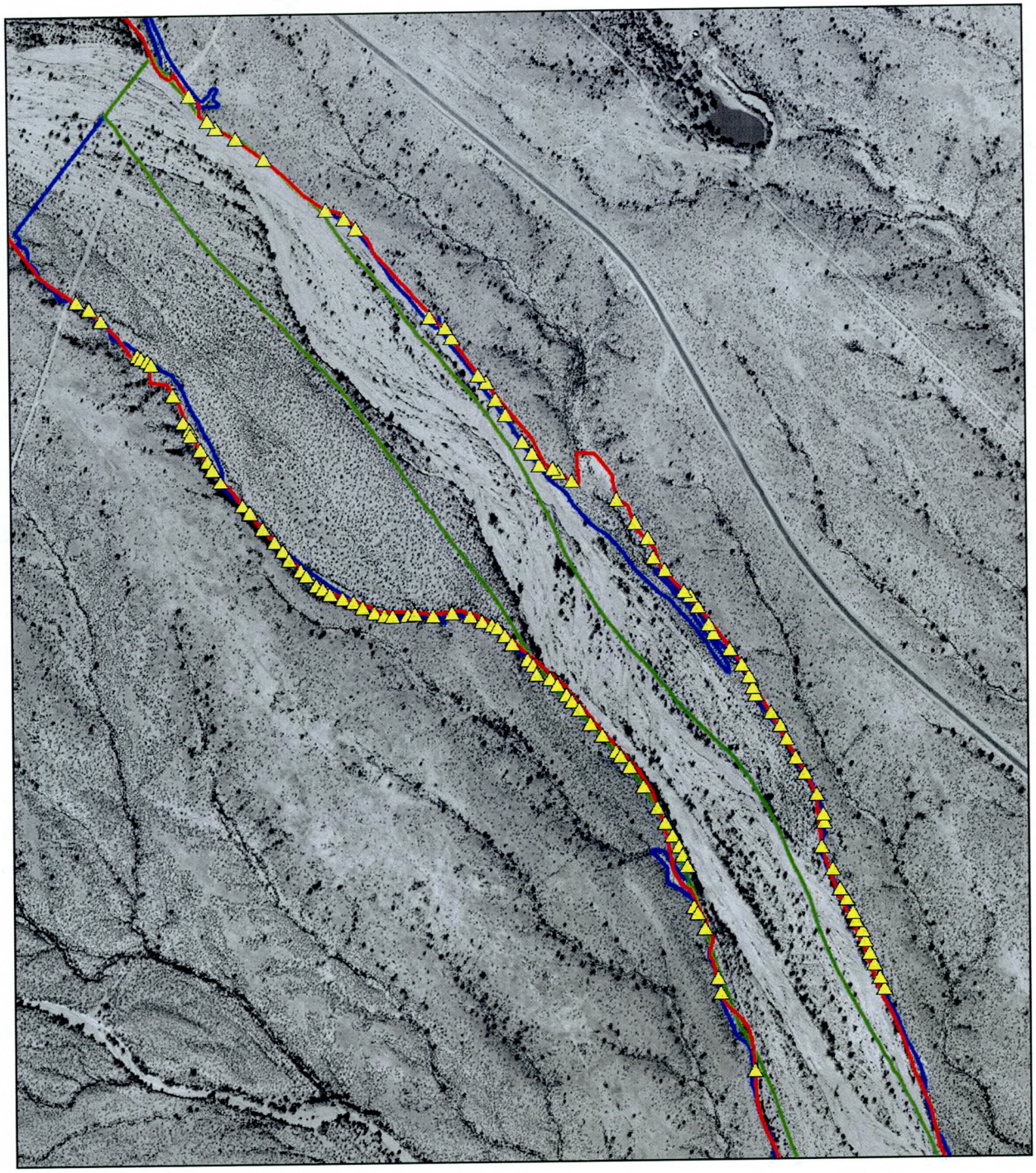

Flood Inundation Comparison

AZGS Limits
FIS 100-year Floodplain
FIS 100-year Floodway
FCDMC High Water Marks

N

0 0.5 1 Miles

Figure 32. FCDMC high water marks in comparison with FIS 100-year limits

7. Conclusions

The following important conclusions can be drawn from the data and analyses provided in this report and its appendices:

- Both of the storms that occurred in October 2000 had maximum point rainfall depths based on radar data that exceeded the statistical 100-year event in the Jackrabbit Wash watershed.
- Aerially averaged radar derived rainfall depths for these storms resulted return periods of approximately 30-years and >500-years for the October 21 and 27 storms respectively.
- Peak runoff generated by the October 27 storm was greater than the FIS defined 100-year peak discharge on Jackrabbit Wash between Vulture Mine and Wickenburg Roads, and from Dead Horse Wash.
- Two or more storms with relatively high recurrence intervals can produce runoff with a lower recurrence interval if the storms occur within a short period of one another.
- The return period for rainfall is not necessarily equal to the return period of the runoff produced by that rainfall. Moreover, the return period for either rainfall or runoff varies depending on where and how one looks at it.
- HEC-1 modeling of a saturated watershed produced peak discharge estimates comparable to indirect discharge estimates of the October 2000 flood.
- Indirect discharge estimates derived from digital terrain model data can quickly and cost-effectively produce reasonable results.
- Landsat satellite data can be useful in quickly interpreting flood inundation limits over large areas. Moreover, it may also be capable of identifying different types of flooding (i.e. shallow flooding versus deep channel flooding).
- Geomorphic investigations and interpretations can aid in placing a particular flood into the long-term historical context of the fluvial system in addition to providing detailed flood inundation limits and potential erosion hazard locations.
- Non-exceedence analysis indicates the recurrence interval for the October 2000 flood ranges between 800- and 3000-years for the reach between Vulture Mine and Wickenburg Roads.
- The geologic floodplain may be a suitable regulatory tool for definition of flood and erosion hazards without the statistical uncertainties associated with the 100-year floodplain.
- Assigning probability to a hydrometeorological event is imprecise.

8. References

Burgess & Niple, 1991, Jackrabbit Wash Floodplain Delineation Study, prepared for Flood Control District of Maricopa County.

FCDMC, 1995, Drainage Design Manual, Volume I, Hydrology.

House, P.K., and Baker, V.R., 2001, Paleohydrology of flash floods in small desert watersheds in western Arizona: Water Resour. Res., 37, 1825-1839.

JEF, *In Progress*, Approximate Zone A floodplain delineation study of watershed '00', FCDMC Contract No. 2000C019.

Levish, D.R., Ostenaa, D.A., and O'Connell, D.R.H., 1997, Paleoflood Hydrology and Dam Safety: Waterpower '97 Proceedings of the International Conference on Hydropower, August 5-8, K.J. Mahoney, ed., American Society of Civil Engineers, New York. p. 2205-2214.

Miller, et al., 1973, NOAA Atlas II, National Oceanic and Atmospheric Administration.

O'Connell, D.R.H., 1999, FLDFRQ3 User's Guide (Release 1.1), U.S. Bureau of Reclamation, Denver, CO, 19 p. ftp://ftp.seismo.usbr.gov/pub/outgoing/geomatic/src/fldfrq3/

Stedinger, J.R. and Cohn, T.A., 1986, Flood frequency analysis with historical and Paleoflood information: Water Resources Research, v. 22, pp. 785-793.

Thomas, B.E., and Hjalmarson, H.W., 1997, Methods for estimating magnitude and frequency of floods in the Southwestern United States, U.S. Geological Survey water-supply paper 2433, p. 57-60.

USDA, 1983 *revised*, National Engineering Handbook, Soil Conservation Service.

Zehr, R.M., and Myers, V.A., 1984, Depth-area ratios in the semi-arid Southwest United States, NOAA Technical Memorandum NWS HYDRO-40, National Oceanic and Atmospheric Administration, Office of Hydrology, Silver Spring, MD., 45 p.

APPENDIX A

Indirect Discharge Estimates

Indirect Discharge Estimates

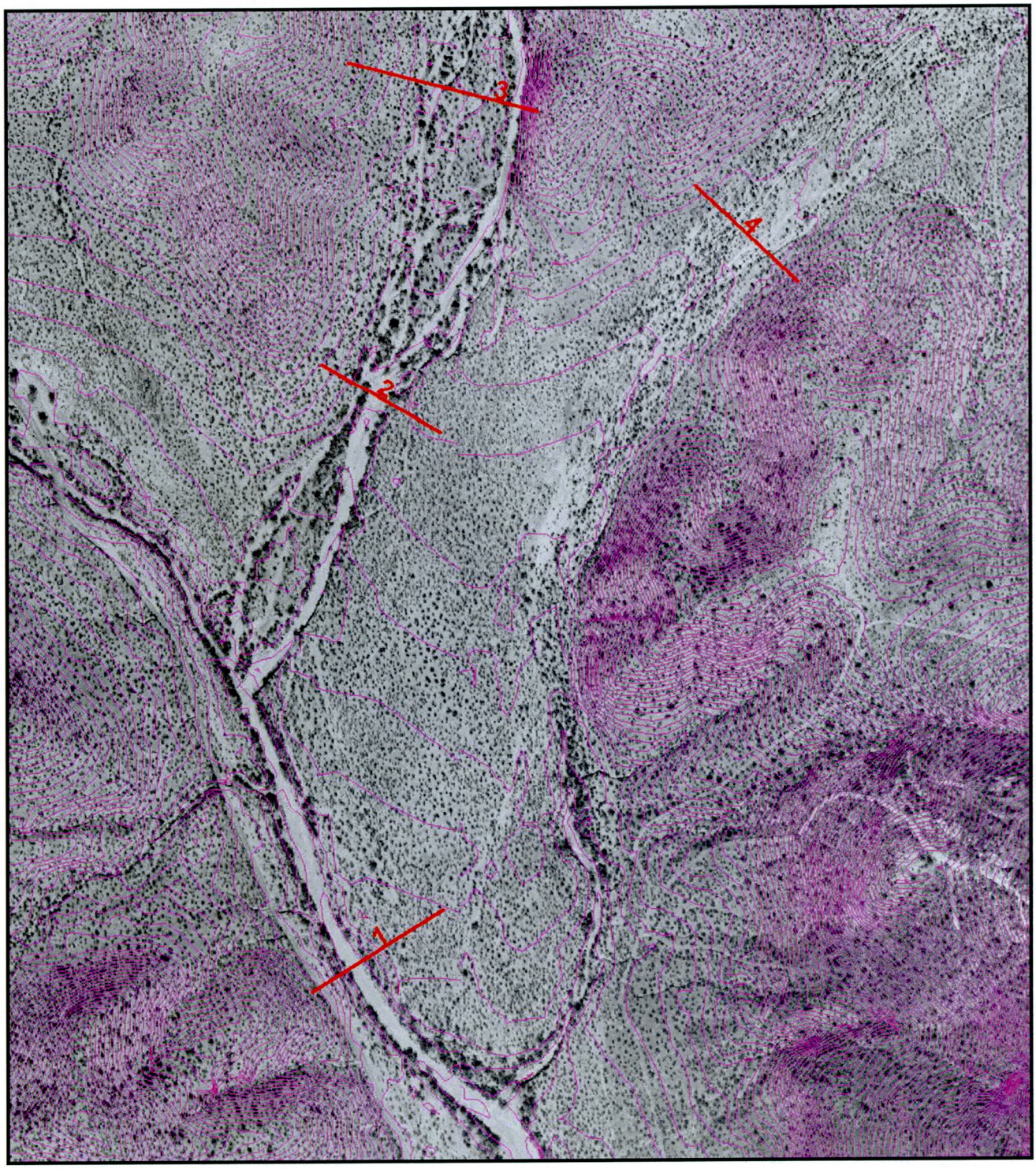

Upper Jackrabbit Wash

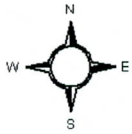

1 Cross-Section Location and ID

0 300 600 Feet

Contour Interval = 2 ft.

Indirect Discharge Estimates

Project Description	
Worksheet	100
Flow Element	Irregular Channel
Method	Manning's Formula
Solve For	Discharge

Section Data		
Mannings Coefficient	0.040	
Slope	0.006000	ft/ft
Water Surface Elevation	2,160.00	ft
Elevation Range	2,159.00 to 2,170.00	
Discharge	747.78	cfs

Upper Jackrabbit Wash Cross-Section 4

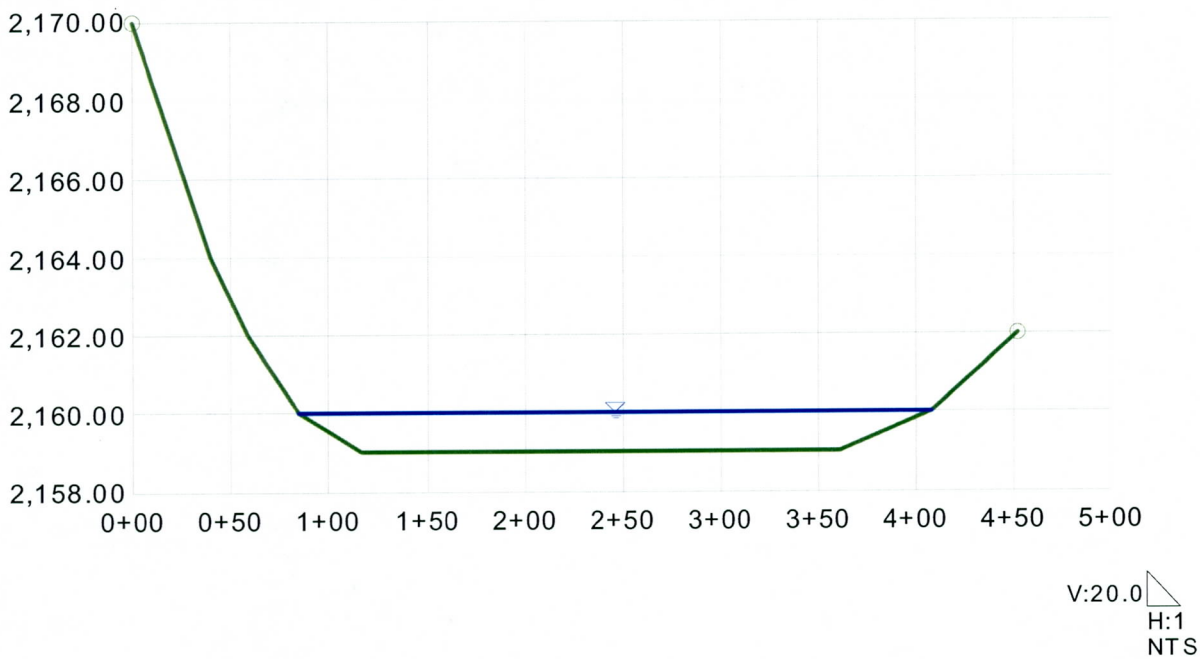

Max Depth (ft)	Flow Area (ft²)	Froude Number	Velocity (ft/s)	Top Width (ft)
1.00	283.5	0.50	2.64	323.00

© Haestad Methods, Inc. 37 Brookside Road Waterbury, CT 06708 USA (203) 755-1666

Indirect Discharge Estimates

Project Description	
Worksheet	200
Flow Element	Irregular Channel
Method	Manning's Formula
Solve For	Discharge

Section Data		
Mannings Coefficient	0.045	
Slope	0.007000	ft/ft
Water Surface Elevation	2,163.00	ft
Elevation Range	2,159.10 to 2,177.00	
Discharge	2,017.95	cfs

Upper Jackrabbit Wash Cross-Section 3

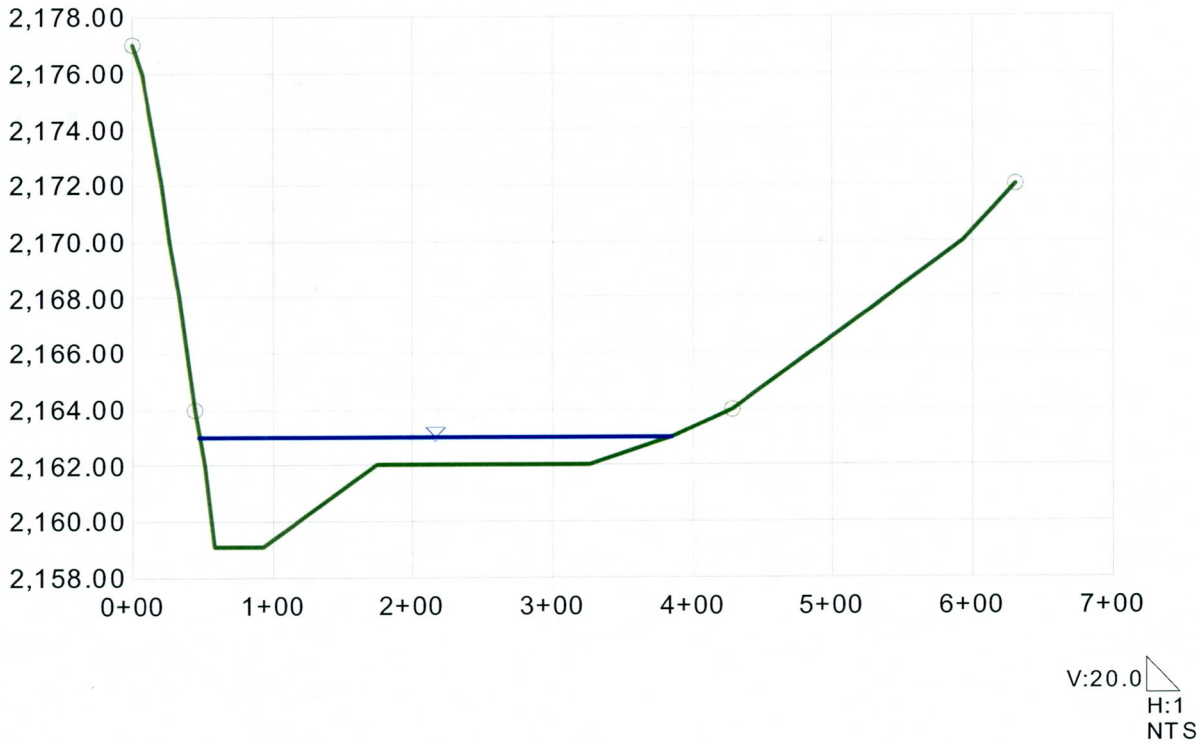

Max Depth (ft)	Flow Area (ft²)	Froude Number	Velocity (ft/s)	Top Width (ft)
3.90	536.5	0.53	3.76	337.00

© Haestad Methods, Inc. 37 Brookside Road Waterbury, CT 06708 USA (203) 755-1666

Indirect Discharge Estimates

Project Description	
Worksheet	100
Flow Element	Irregular Channel
Method	Manning's Formula
Solve For	Discharge

Section Data		
Mannings Coefficient	0.045	
Slope	0.007000	ft/ft
Water Surface Elevation	2,156.00	ft
Elevation Range	2,153.50 to 2,160.00	
Discharge	654.30	cfs

Upper Jackrabbit Wash Cross-Section 2

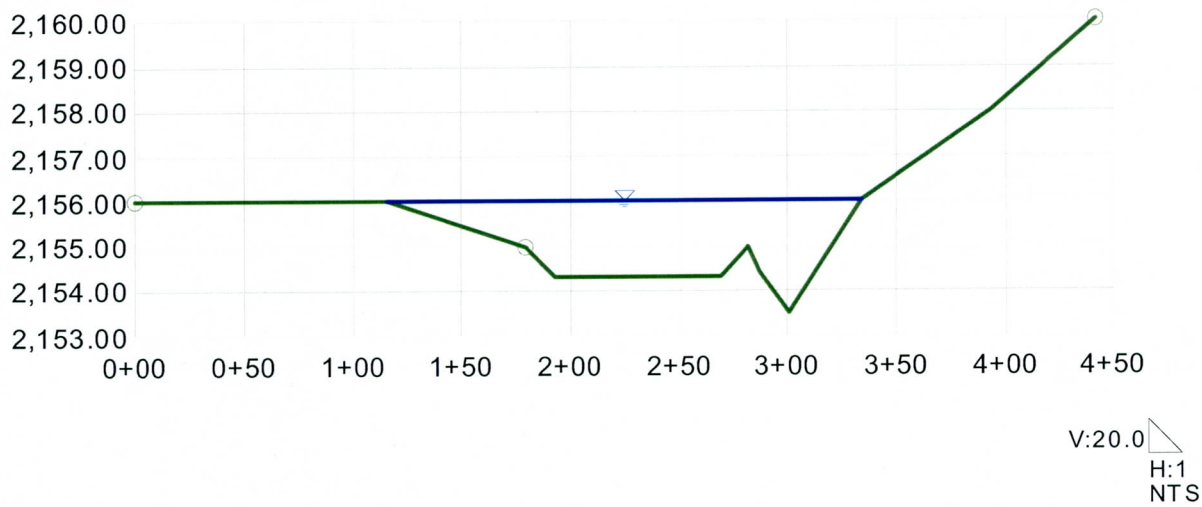

Max Depth (ft)	Flow Area (ft²)	Froude Number	Velocity (ft/s)	Top Width (ft)
2.50	273.6	0.47	2.39	334.00

JE Fuller Hydrology & Geomorphology, Inc.

Project Engineer: Ted Lehman

FlowMaster v6.1 [614k]
© Haestad Methods, Inc. 37 Brookside Road Waterbury, CT 06708 USA (203) 755-1666

Indirect Discharge Estimates

Project Description	
Worksheet	900
Flow Element	Irregular Channel
Method	Manning's Formula
Solve For	Discharge

Section Data	
Mannings Coefficient	0.045
Slope	0.004000 ft/ft
Water Surface Elevation	2,147.00 ft
Elevation Range	2,139.20 to 2,152.00
Discharge	7,648.02 cfs

Upper Jackrabbit Wash Cross-Section 1

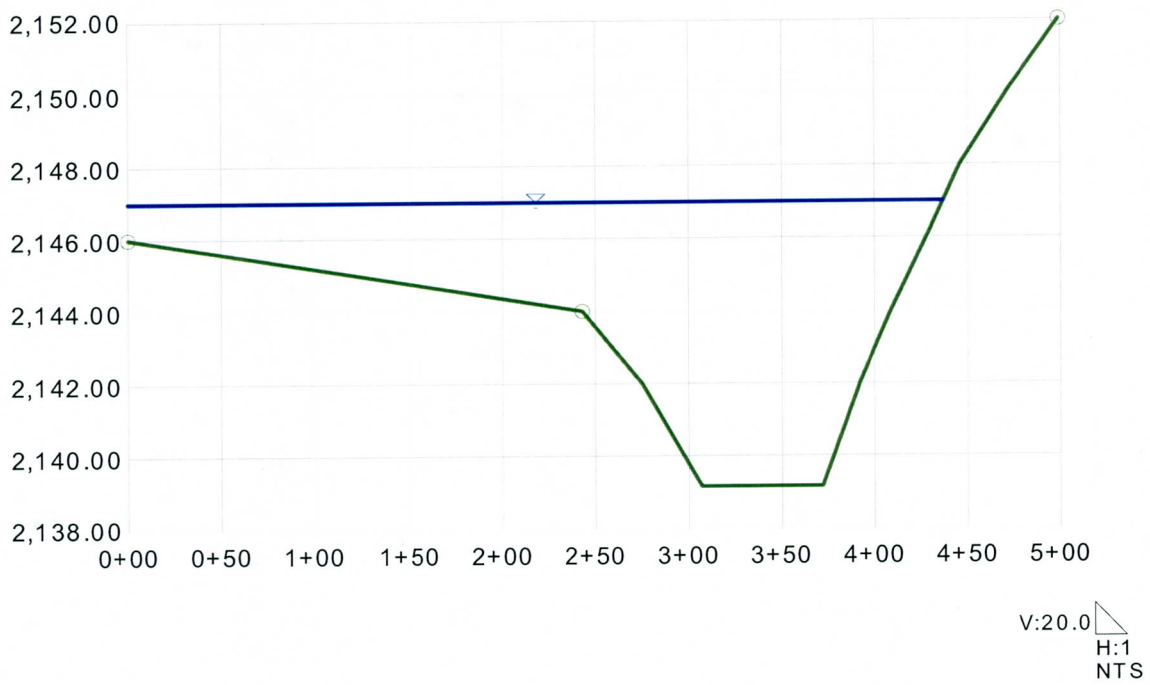

Max Depth (ft)	Flow Area (ft²)	Froude Number	Velocity (ft/s)	Top Width (ft)
7.80	1,562.8	0.46	4.89	437.00

© Haestad Methods, Inc. 37 Brookside Road Waterbury, CT 06708 USA (203) 755-1666

Indirect Discharge Estimates

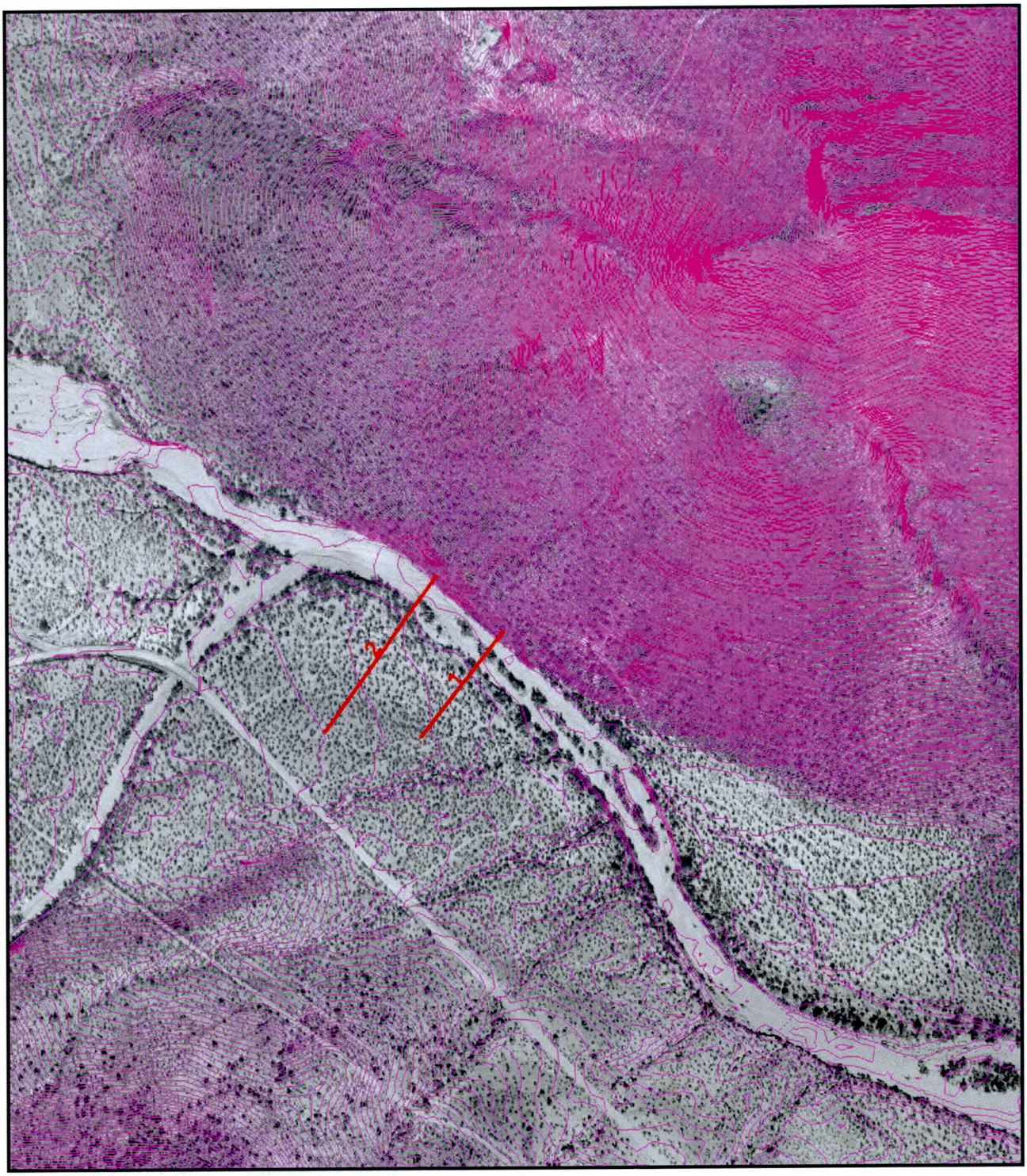

Upper Jackrabbit Wash below Oracho Ranch Road

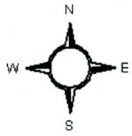

1 Cross-Section Location and ID

0 200 400 Feet

Contour Interval = 2 ft.

Indirect Discharge Estimates

Project Description	
Worksheet	800
Flow Element	Irregular Channel
Method	Manning's Formula
Solve For	Discharge

Section Data		
Mannings Coefficient	0.060	
Slope	0.006000	ft/ft
Water Surface Elevation	2,129.70	ft
Elevation Range	2,124.00 to 2,134.00	
Discharge	3,329.52	cfs

Upper Jackrabbit downstream of Oracho Ranch Rd. Cross-Section 2

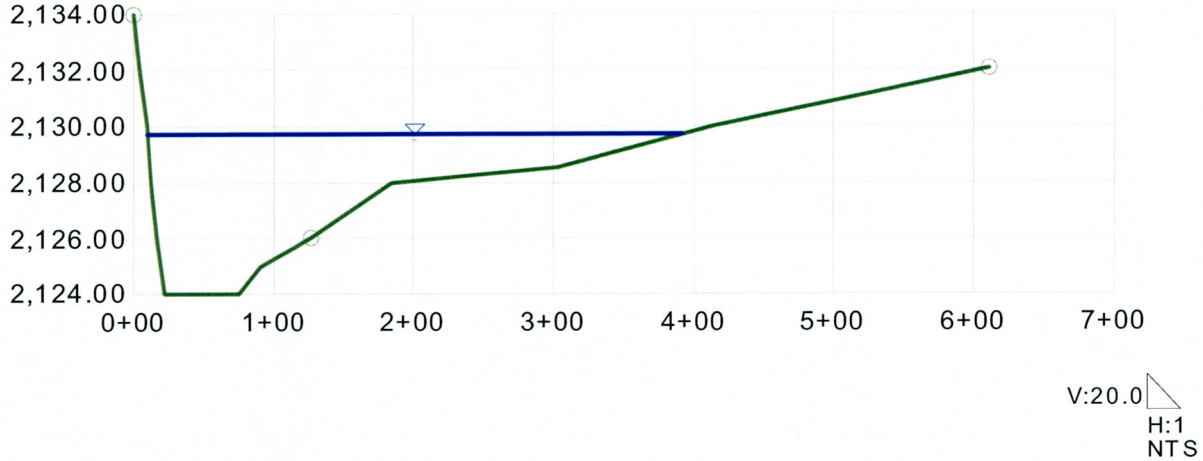

Max Depth (ft)	Flow Area (ft²)	Froude Number	Velocity (ft/s)	Top Width (ft)
5.70	952.9	0.39	3.49	383.00

© Haestad Methods, Inc. 37 Brookside Road Waterbury, CT 06708 USA (203) 755-1666

Indirect Discharge Estimates

Project Description	
Worksheet	700
Flow Element	Irregular Channel
Method	Manning's Formula
Solve For	Discharge

Section Data		
Mannings Coefficient	0.035	
Slope	0.006000	ft/ft
Water Surface Elevation	2,128.00	ft
Elevation Range	2,123.00 to 2,137.00	
Discharge	4,335.01	cfs

Upper Jackrabbit downstream of Oracho Ranch Rd. Cross-Section 1

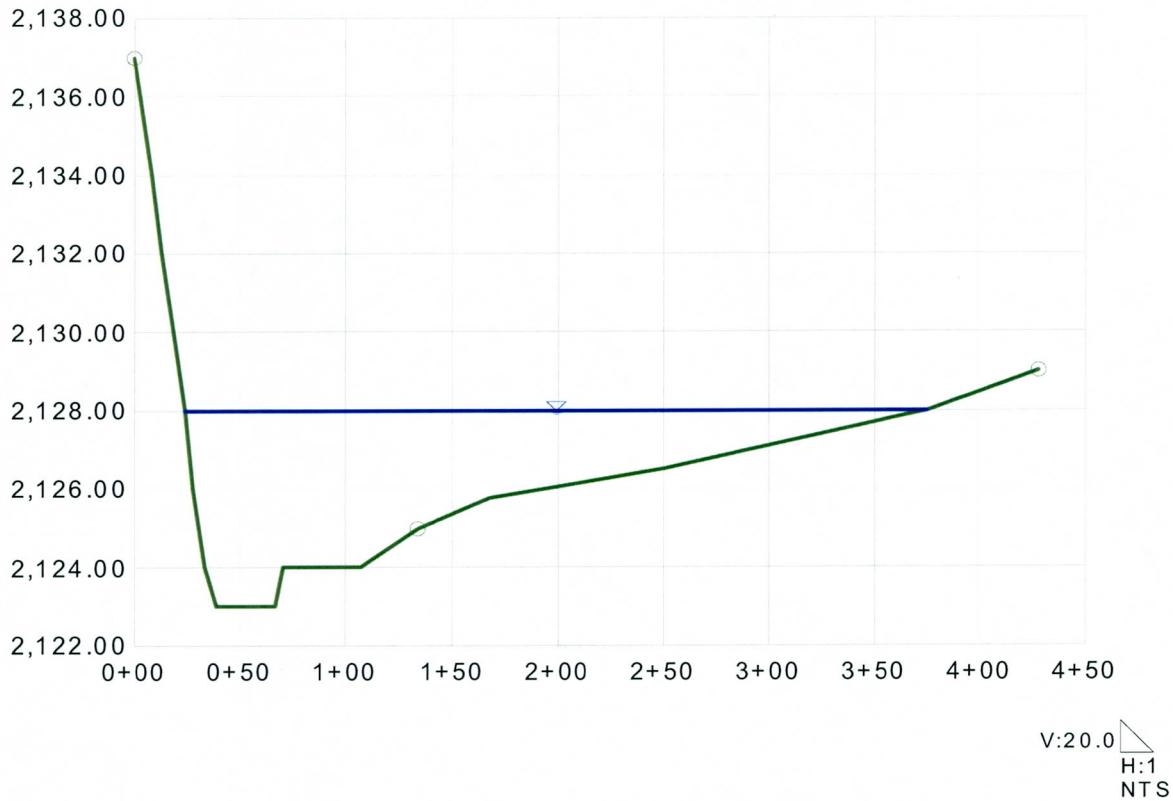

Max Depth (ft)	Flow Area (ft²)	Froude Number	Velocity (ft/s)	Top Width (ft)
5.00	778.2	0.66	5.57	351.00

© Haestad Methods, Inc. 37 Brookside Road Waterbury, CT 06708 USA (203) 755-1666

Indirect Discharge Estimates

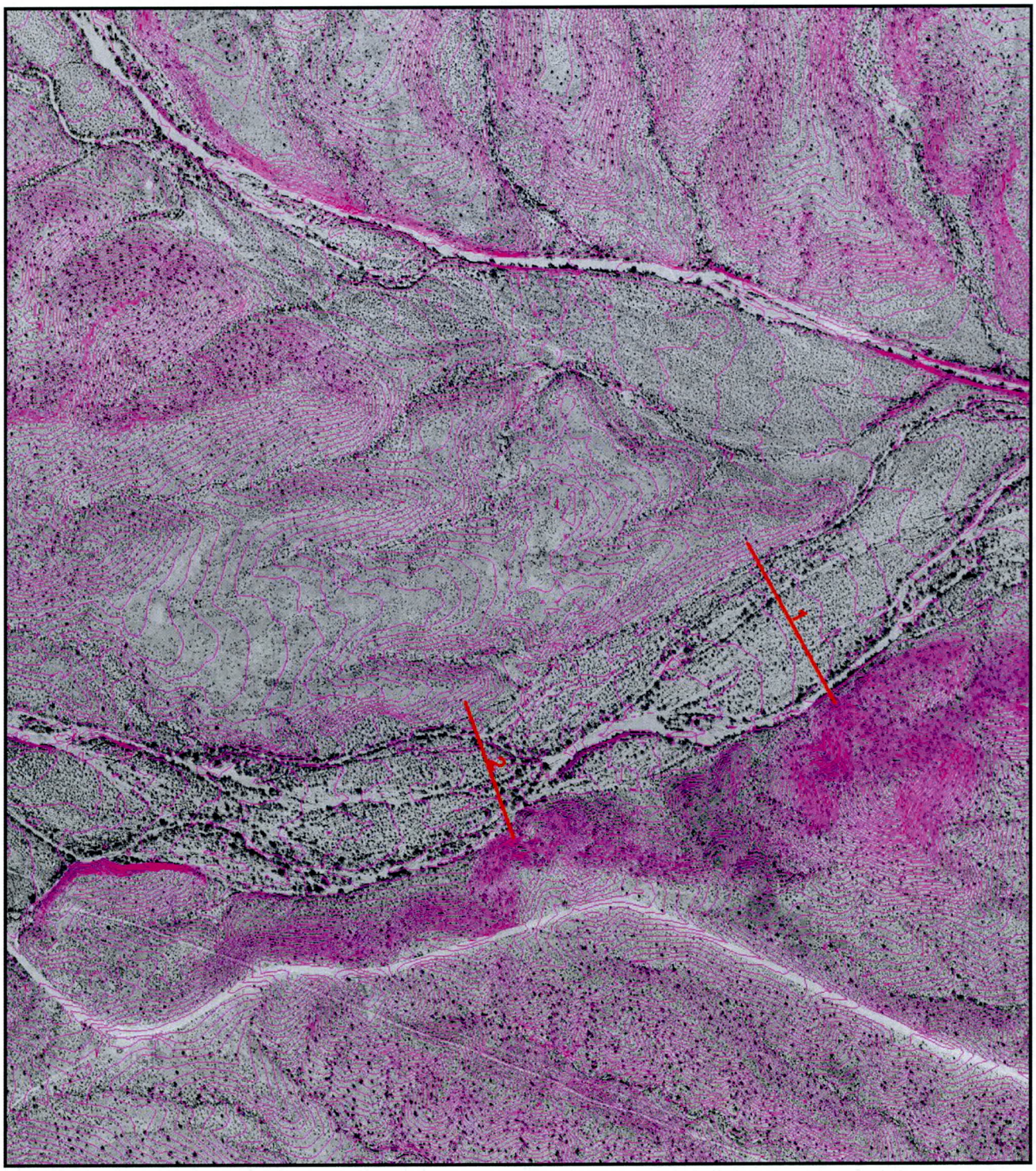

Dead Horse Wash

1 Cross-Section Location and ID

Contour Interval = 2 ft.

N
W E
S

0 400 800 Feet

Indirect Discharge Estimates

Project Description	
Worksheet	200
Flow Element	Irregular Channel
Method	Manning's Formula
Solve For	Discharge

Section Data		
Mannings Coefficient	0.050	
Slope	0.008000	ft/ft
Water Surface Elevation	2,021.00	ft
Elevation Range	2,017.00 to 2,028.00	
Discharge	9,322.09	cfs

Dead Horse Wash Section 2

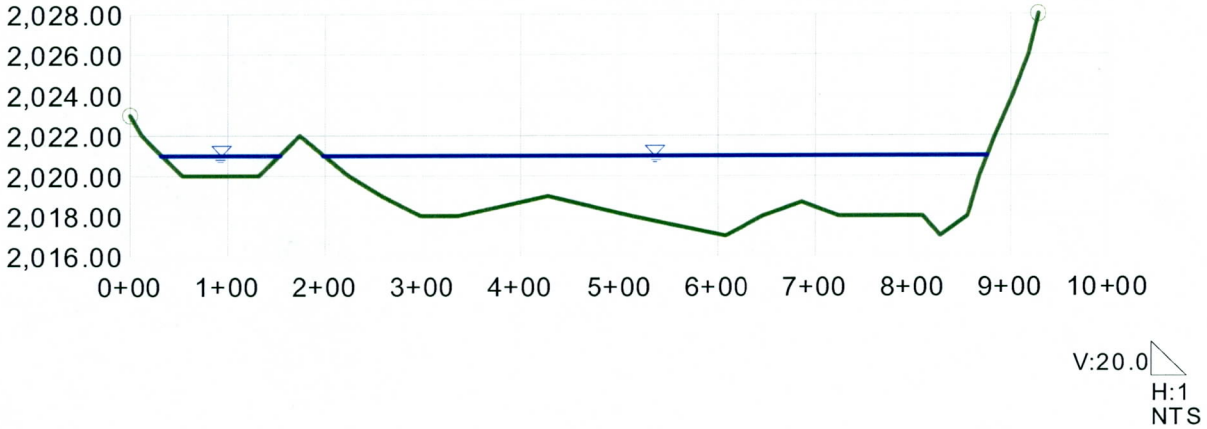

Max Depth (ft)	Flow Area (ft²)	Froude Number	Velocity (ft/s)	Top Width (ft)
4.00	1,938.8	0.54	4.81	796.50

© Haestad Methods, Inc. 37 Brookside Road Waterbury, CT 06708 USA (203) 755-1666

Indirect Discharge Estimates

Project Description	
Worksheet	100
Flow Element	Irregular Channel
Method	Manning's Formula
Solve For	Discharge

Section Data		
Mannings Coefficient	0.045	
Slope	0.007000	ft/ft
Water Surface Elevation	2,005.50	ft
Elevation Range	2,001.00 to 2,014.00	
Discharge	16,984.95	cfs

Dead Horse Wash Section 1

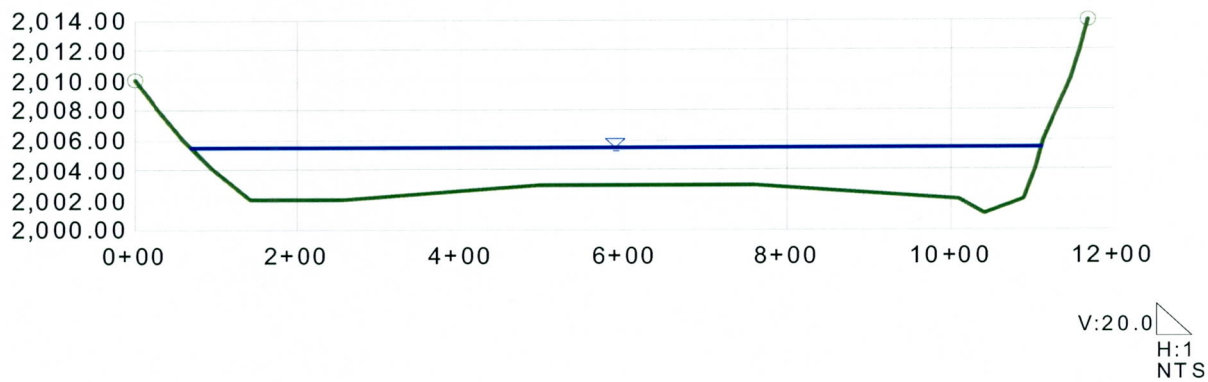

Max Depth (ft)	Flow Area (ft²)	Froude Number	Velocity (ft/s)	Top Width (ft)
4.00	1,938.8	0.54	4.81	796.50

© Haestad Methods, Inc. 37 Brookside Road Waterbury, CT 06708 USA (203) 755-1666

Indirect Discharge Estimates

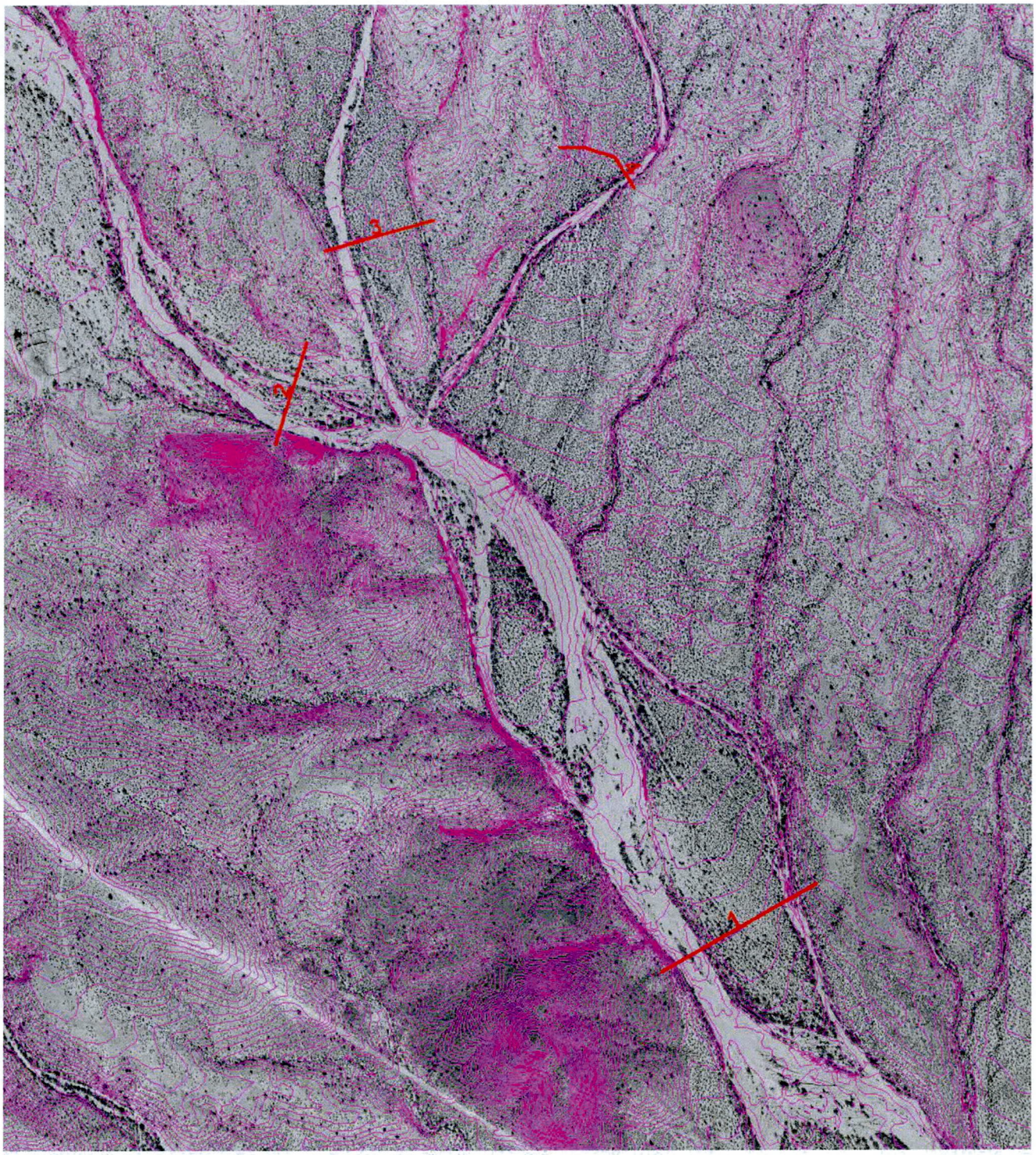

Jackrabbit Wash near Wildcat Well

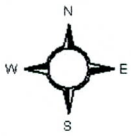

1 Cross-Section Location and ID

0 500 1000 Feet

Contour Interval = 2 ft.

Indirect Discharge Estimates

Project Description	
Worksheet	100
Flow Element	Irregular Channel
Method	Manning's Formula
Solve For	Discharge

Section Data		
Mannings Coefficient	0.040	
Slope	0.010000	ft/ft
Water Surface Elevation	1,972.00	ft
Elevation Range	1,968.00 to 1,978.00	
Discharge	3,459.22	cfs

Jackrabbit Wash near Wildcat Well Cross-Section 4

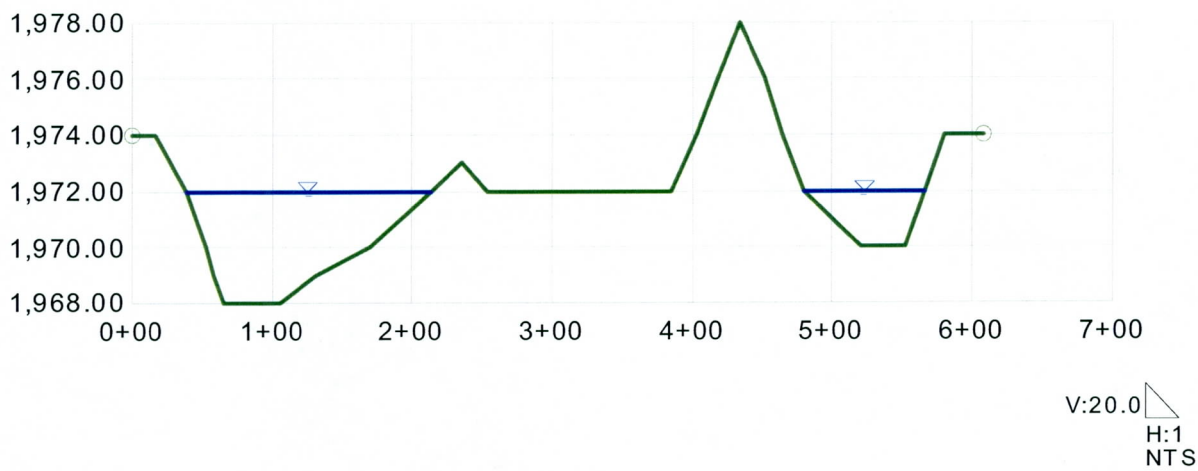

Max Depth (ft)	Flow Area (ft²)	Froude Number	Velocity (ft/s)	Top Width (ft)
4.00	559.5	0.74	6.18	260.00

© Haestad Methods, Inc. 37 Brookside Road Waterbury, CT 06708 USA (203) 755-1666

Indirect Discharge Estimates

Project Description	
Worksheet	100
Flow Element	Irregular Channel
Method	Manning's Formula
Solve For	Discharge

Section Data		
Mannings Coefficient	0.040	
Slope	0.010000	ft/ft
Water Surface Elevation	1,962.00	ft
Elevation Range	1,960.00 to 1,967.00	
Discharge	1,623.98	cfs

Jackrabbit Wash near Wildcat Well Cross-Section 3

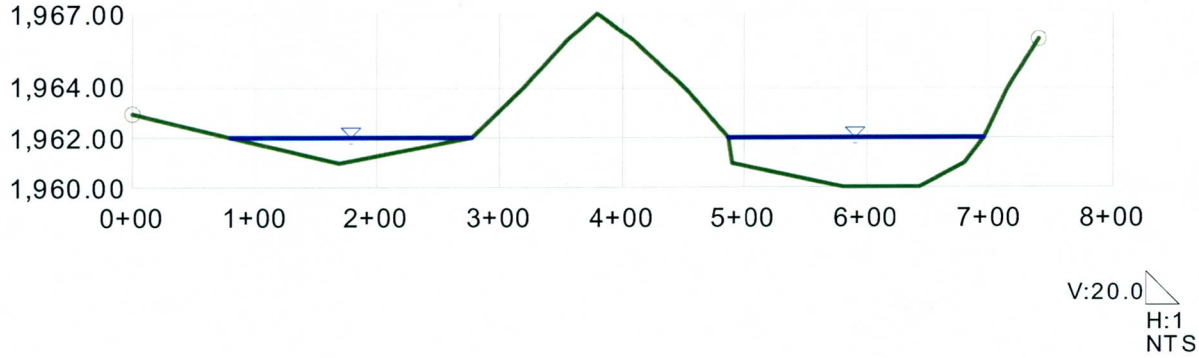

Max Depth (ft)	Flow Area (ft²)	Froude Number	Velocity (ft/s)	Top Width (ft)
2.00	424.5	0.66	3.83	406.00

© Haestad Methods, Inc. 37 Brookside Road Waterbury, CT 06708 USA (203) 755-1666

Indirect Discharge Estimates

Project Description	
Worksheet	600
Flow Element	Irregular Channel
Method	Manning's Formula
Solve For	Discharge

Section Data		
Mannings Coefficient	0.036	
Slope	0.006000	ft/ft
Water Surface Elevation	1,957.00	ft
Elevation Range	1,950.20 to 1,962.00	
Discharge	17,675.90	cfs

Jackrabbit Wash near Wildcat Well Cross-Section 2

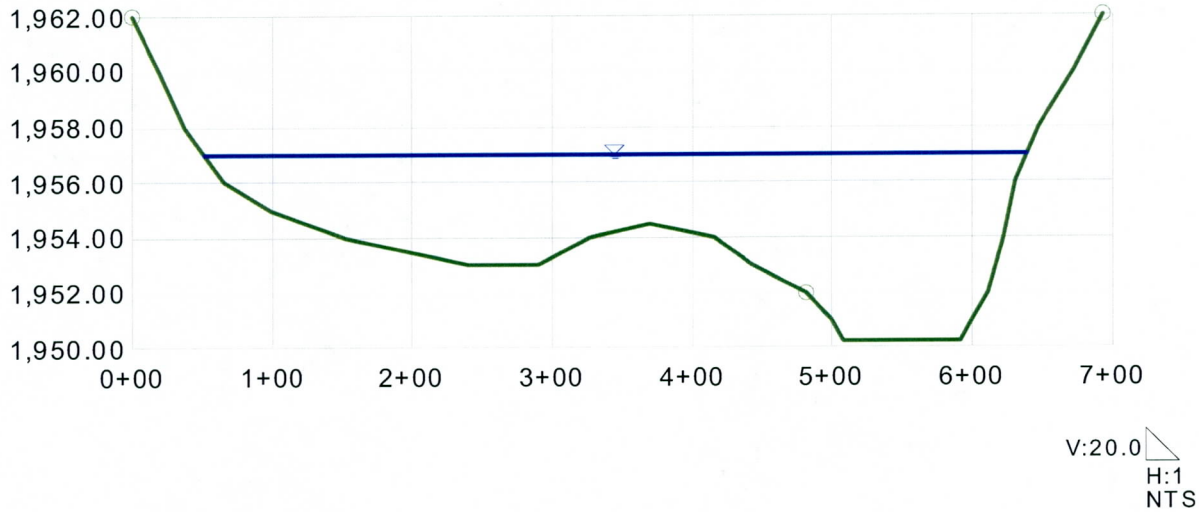

Max Depth (ft)	Flow Area (ft²)	Froude Number	Velocity (ft/s)	Top Width (ft)
6.80	2,240.8	0.71	7.89	587.50

© Haestad Methods, Inc. 37 Brookside Road Waterbury, CT 06708 USA (203) 755-1666

Indirect Discharge Estimates

Project Description	
Worksheet	350
Flow Element	Irregular Channel
Method	Manning's Formula
Solve For	Discharge

Section Data		
Mannings Coefficient	0.037	
Slope	0.008000	ft/ft
Water Surface Elevation	1,923.00	ft
Elevation Range	1,915.00 to 1,926.00	
Discharge	21,119.57	cfs

Jackrabbit Wash near Wildcat Well Cross-Section 1

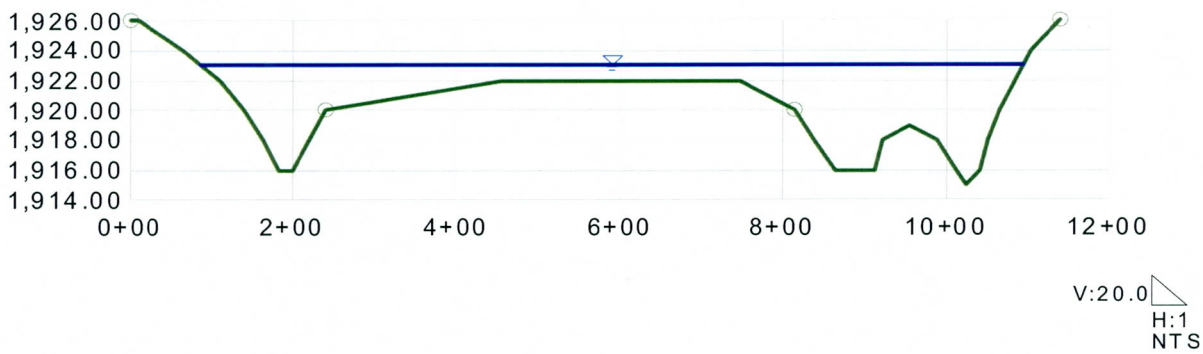

Max Depth (ft)	Flow Area (ft²)	Froude Number	Velocity (ft/s)	Top Width (ft)
8.00	2,917.0	0.75	7.24	1,006.00

© Haestad Methods, Inc. 37 Brookside Road Waterbury, CT 06708 USA (203) 755-1666

Indirect Discharge Estimates

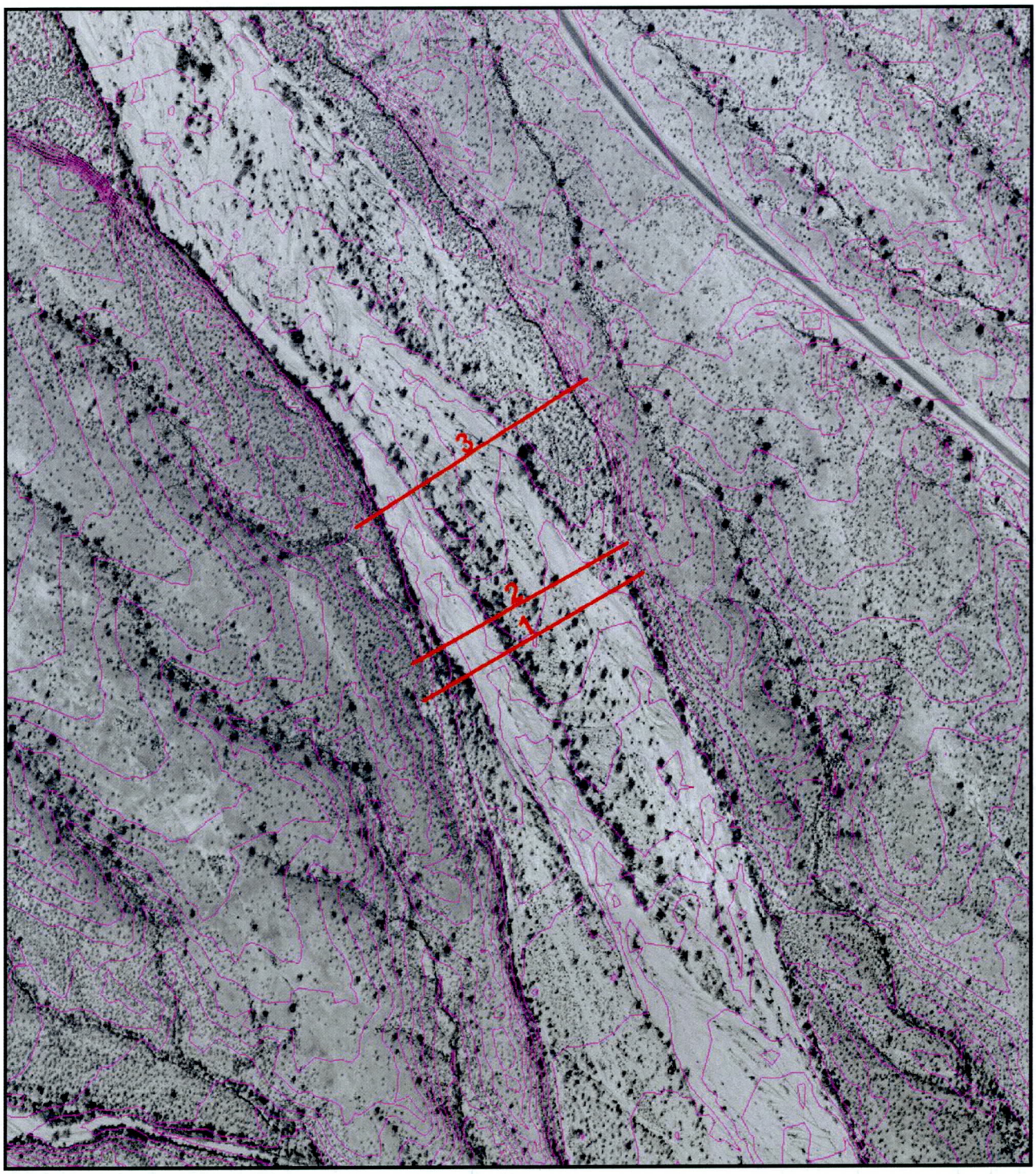

Jackrabbit Wash near FCDMC Gage Site

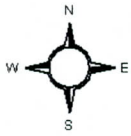

1 Cross-Section Location and ID

0 200 400 Feet

Contour Interval = 2 ft.

Indirect Discharge Estimates

Project Description	
Worksheet	300
Flow Element	Irregular Channel
Method	Manning's Formula
Solve For	Discharge

Section Data		
Mannings Coefficient	0.035	
Slope	0.007000	ft/ft
Water Surface Elevation	1,681.50	ft
Elevation Range	1,674.50 to 1,689.00	
Discharge	26,450.67	cfs

FCDMC Gage Site Cross-Section 3

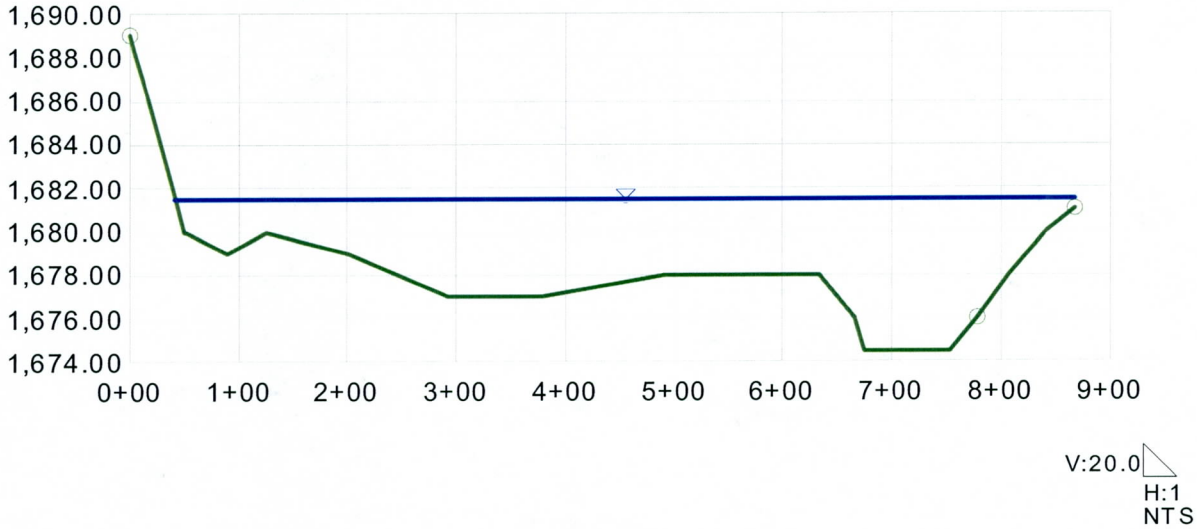

Max Depth (ft)	Flow Area (ft²)	Froude Number	Velocity (ft/s)	Top Width (ft)
7.00	3,116.3	0.77	8.49	827.00

© Haestad Methods, Inc. 37 Brookside Road Waterbury, CT 06708 USA (203) 755-1666

Indirect Discharge Estimates

Project Description	
Worksheet	200
Flow Element	Irregular Channel
Method	Manning's Formula
Solve For	Discharge

Section Data		
Mannings Coefficient	0.037	
Slope	0.007000	ft/ft
Water Surface Elevation	1,678.00	ft
Elevation Range	1,671.50 to 1,681.00	
Discharge	24,729.09	cfs

FCDMC Gage Location Cross-Section 2

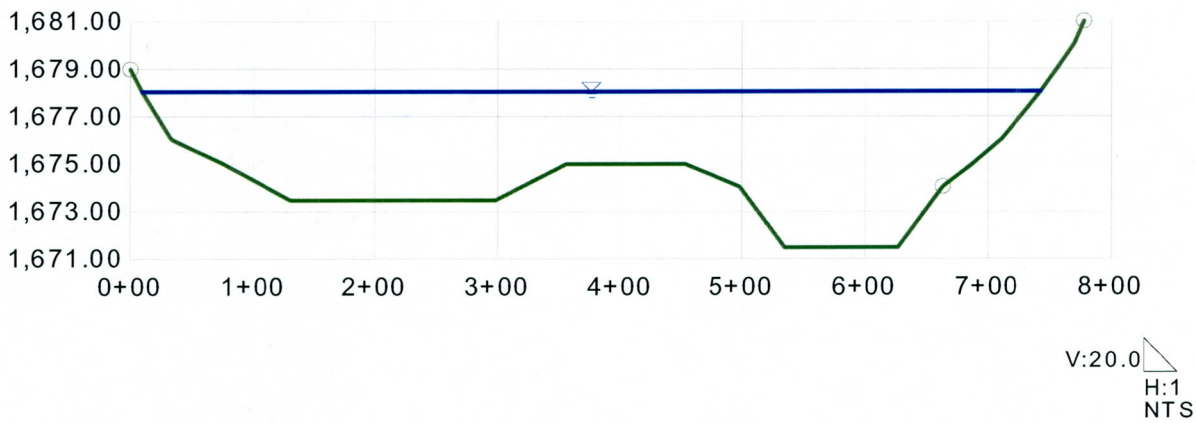

Max Depth (ft)	Flow Area (ft²)	Froude Number	Velocity (ft/s)	Top Width (ft)
6.50	2,918.0	0.75	8.47	734.00

© Haestad Methods, Inc. 37 Brookside Road Waterbury, CT 06708 USA (203) 755-1666

Indirect Discharge Estimates

Project Description	
Worksheet	100
Flow Element	Irregular Channel
Method	Manning's Formula
Solve For	Discharge

Section Data		
Mannings Coefficient	0.035	
Slope	0.007000	ft/ft
Water Surface Elevation	1,677.00	ft
Elevation Range	1,670.20 to 1,680.00	
Discharge	26,128.05	cfs

FCDMC Gage Location Cross-Section 1

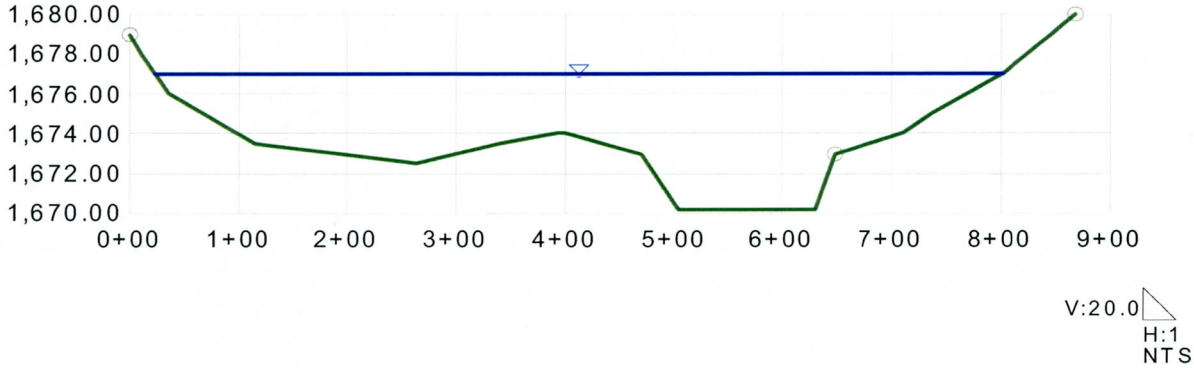

Max Depth (ft)	Flow Area (ft²)	Froude Number	Velocity (ft/s)	Top Width (ft)
6.80	3,007.3	0.78	8.69	779.00

© Haestad Methods, Inc. 37 Brookside Road Waterbury, CT 06708 USA (203) 755-1666

APPENDIX B

Landsat based flood detection in the Jackrabbit Wash Area, Maricopa County, Arizona

by

Dr. Larry Mayer

August 1, 2001

Landsat based flood detection in the Jackrabbit Wash Area, Maricopa County, Arizona

Larry Mayer, Ph.D.

Report for JE Fuller/Hydrology & Geomorphology, Inc.

ABSTRACT

Landscape change detection using Landsat ETM+ sensor data and image processing methods based on band orthogonalization are used for initial mapping of flood inundation along Jackrabbit Wash, in Maricopa County. Results indicate that image processing of Landsat data, which has a nominal 30 m pixel size spatial resolution, can provide a direct method to document flooding in remote areas of Arizona. This study analyzes a portion of two Landsat scenes covering part of Maricopa County, west of Phoenix, Arizona. The study finds that Jackrabbit Wash, in contrast to many of the adjacent streams, has a spectral signature that indicates there was detectable landscape modification associated with the October, 2000 flood. The area of flooding is clearly indicated on the processed satellite image as a band of yellow. Field validation consisting of checking several reaches of Jackrabbit Wash around Vulture Mine Road, corroborated the evidence from the satellite change image. Ubiquitous evidence for very significant flooding was found. The performance of the change detection on a regional basis appears strong. On the local basis, not every pixel which showed evidence for inundation in the field, was highlighted as changed on the change image. A significant finding is that the flooding affected the upstream portions of Jackrabbit Wash and therefore must be related to storm precipitation in the headwaters area.

INTRODUCTORY STATEMENT

Satellite change detection imaging is a process that consists of data selection, pre-processing, and image processing. The satellite change image is then checked through field validation. Landsat satellites acquire data from the visible, infrared, and thermal infrared bands, representing brightness across several electromagnetic wavelengths from descending orbits about 700 km above the Earth's surface. The brightness values are represented as Digital Numbers (DN) for each pixel that vary from 0 to 255. The relative brightness of the pixels is related to the reflectance characteristics of the materials on the surface (see Appendix).

Landsat revisits the same area every 16 days, which defines the smallest period of time over which change can be documented. The information for the non-thermal portion of the electromagnetic spectrum is collected in six bands. Landsat 7 has an additional panchromatic band. The spatial resolution of the visible and near infrared bands of Landsat satellites 4, 5, and 7 is about 30 meters.

Detecting the effects of flooding on the landscape from Landsat satellite data is based on a methodology referred to as *change detection*. The concept behind this methodology is simple. If a flood changes some aspect of the land surface, it should be detectable if the change (1) is large enough spatially, and (2) is reflected in a significant change in the brightness of a ground pixel in any of the sampled bands. Pixels may get either darker or brighter depending on the change, and a single pixel may get darker in one band and brighter in another band. The application of change detection to a landscape is based on the careful comparison of precisely co-registered multi-temporal satellite images. The change image is presented by making a Red-Green-Blue (RGB) color model.

Data Selection

The first step in the use of Landsat 7 data for flood inundation is the selection of scenes according to their dates relative to flooding and the Quality Assurance of the sensor data. There are several known problems with both Thematic Mapper (TM) and Enhanced Thematic Mapper (ETM+) data that relate either to the sensor or to conditions at the time of scene acquisition. If any known problems appear in the dataset, that scene is rejected. In order to provide a meaningful explanation of the process of scene selection, these issues are reviewed.

ETM+ ARTIFACTS

NASA reports that several image artifacts are known for Landsat 7, or ETM+ data. Artifacts represent faulty data acquisition which may or may not actually be present. They are scan-correlated shift, memory effect, coherent noise, dropped lines, and striping. Normally these artifacts are eliminated from data products by Level 1 processing by the Eros data center. However, remnants of these artifacts may reappear following statistical processing of Landsat 7 data. The following summary was extracted from the Landsat 7 Science Users Data Handbook .

Scan Correlated Shift is a sudden change in bias that occurs in all detectors simultaneously. The bias level switches between two states. Not all detectors are in phase, some are 180 degrees out of phase (i.e. when one detector changes from low to high, another may change from high to low). All detectors shift between two states that are constantly time varying, or slowly time varying on the order of days to months.

Memory Effect (ME) is manifested in a noise pattern that commonly appears as banding on an image. Each eastbound and westbound sweep of if the Thematic Mapper can mirror acquires 16 lines of data for the detector array for each spectral band. Thus ME is seen as alternating lighter and darker horizontal stripes that are 16 pixels wide in data that has not been geometrically corrected. These stripes are most intense near a significant change in brightness in the horizontal (along scan) direction, such as a cloud/water boundary. ME can cause significant error in calibration efforts because its effect is scene

dependent. ME is present in Bands 1 through 4 of the Primary Focal Plane, and nearly absent in Bands 5 through 7.

In TM reflective band data, coherent noise (CN), manifests itself in various ways. The power of this component varies strongly even within a scan, with a maximum amplitude of 1 DN. Random noise can be suppressed by applying a moving average filter to the data. Random noise can affect the statistics used for image classification and therefore represents an important artifact.

Dropped lines occur due to errors in the raw data stream ingested by the Landsat Processing System. They are flagged during Level 1 processing and can be restored by replacing the missing pixel with the average of the DN values for the adjacent pixels in the preceding and subsequent scan lines

Striping is a line-to-line artifact phenomenon that appears in individual bands of radiometrically corrected data that can be traced to individual detectors that are miscalibrated with respect to one another. The application of the calibration coefficients to the ETM+ data, i.e. the generation of the level 1R data, is intended to remove the detector to detector variations in gain and offset, effectively de-striping the data. As detector to detector variations are already explicitly taken into account through the generation of relative gains and bias from histograms, and these are included in the process of generating the applied gains and biases, the striping characterization and correction should not be required in routine processing.

In addition to the artifacts discussed above, the data must also be examined for clipping or cropping of the entire data range due to saturation of the sensors. Saturation is evidenced by a truncation of DN distributions at the high end of the brightness histogram.

ATMOSPHERIC SCATTERING

Scattering of electromagnetic radiation in the atmosphere, specifically in the Landsat 7 spectral bands, alters the amount of radiation that reaches the sensor from a target. Scattering is caused by interaction with both gases and particles in the atmosphere. The thicker the atmospheric blanket between the target and the sensor, the greater the amount of scattering. Selective scattering, due to the interaction with atmospheric gases, causes the shorter wavelengths of ultraviolet and blue light to be more intensely scattered than the longer wavelengths of red and infrared light energy. Nonselective scattering, due to the interaction with particles including water particles, and aerosols, causes scattering in all wavelengths equally. One of the effects of atmospheric scattering is that dark objects, such as areas of shade, which should appear black, appear lighter and bluer than they should. Another way to view atmospheric scattering is as a noise component, because the addition of atmospheric scattering to a pixels brightness value actually contains no information about the pixel. Atmospheric scattering reduces the contrast of the image by dampening out the real differences between the brightness values between adjacent pixels.

The effects of selective atmospheric scattering on image data can be estimated by comparing the DNs of band 1, or blue light, with that of band 7, or infrared light. The easiest way to do this is by constructing a scattergram of band 1 on the x-axis and band 7 on the y-axis. If there is no selective scattering, the correlated band data should form a cloud that intersects with the graph origin. However, selective scattering causes a shift of the

DNs of band 1 to higher values. The amount of this shift is an estimate of the magnitude of the scattering effect, and will be different for each band, with a maximum in band 1.

SCENE SELECTION

Scene selection for the Jackrabbit Wash flood inundation study requires several steps. First, the catalog of all Landsat 7 images in the Eros Data Center catalog covering the row path of the study area for period of about one year is extracted. From this catalog, a list of all cloud free scenes is produced and the image previews for these scenes are ordered using the online preview system. These low-resolution image previews are examined to evaluate the data. Specifically, these are examined for clouds and data coherence. Ideally, for flood inundation studies, we would like to bracket the time of flooding as tightly as possible. When this is not feasible, other criteria are included, such as time of year and data quality.

The list of cloud free scenes for the row paths covering the study area included:

```
15 Dec 2000 037037
13 Nov 2000 037037
24 Jul 2000 037037
15 Jul 2000 038037
06 Jun 2000 037037
17 Sep 2000 038037
21 May 2000 037037
23 Jan 2000 038037
27 Nov 1999 037037
```

Second, the scene dates were reviewed with Dr. Philip Pearthree of the Arizona Geological Survey and JE Fuller/ H&G Inc . Based on the requirement to bracket the flood date as closely as possible, we selected the 13 November 2000 scene, representing the post-flood condition, and the 06 June 2000 scene, representing the pre-flood condition. Third, the data were ordered through customer service at the Eros Data Center with the following specifications.

CORRECTION LEVEL: Terrain (highest level of geometric correction)

```
FORMAT: NLAPS Revision 2 (latest version of USGS format)
PIXEL_SPACING=28.5000,28.5000; (size of a pixel in meters)
RESAMPLING=NN; (nearest neighbor)
ORIENTATION=0.000000; (map north)
MAP_PROJECTION_NAME=UTM; (type of geographic projection)
USGS_PROJECTION_NUMBER=1; (USGS code)
USGS_MAP_ZONE=12; (UTM zone)
HORIZONTAL_DATUM=WGS84; (Geoid)
PIXEL_FORMAT=BYTE; (data format)
DATA_FILE_INTERLEAVING=BSQ; (each band in a separate file)
```

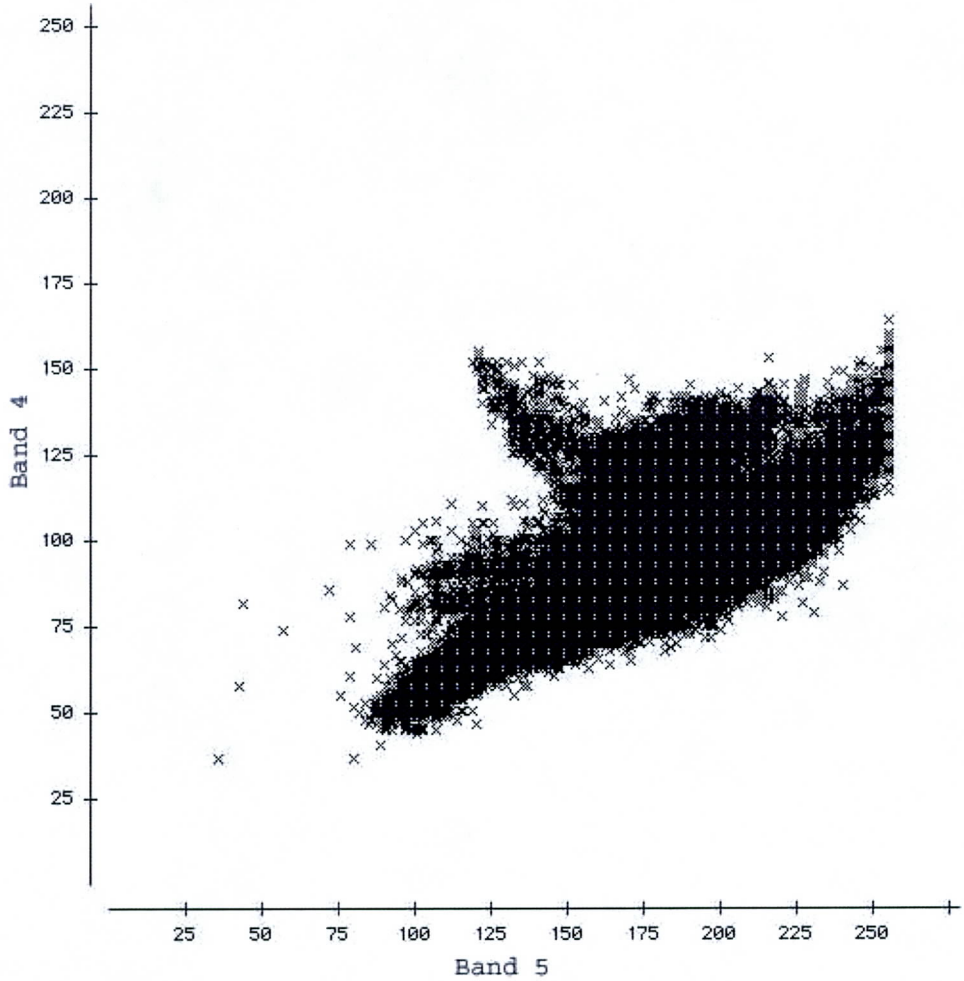

FIGURE 1. Scattergram of Band 5 versus Band 4 for the June 2000 Landsat 7 scene candidate. The scattergram consists of about 500,000 points extracted from the scene for Quality Assurance. The scattergram is scaled to show the entire range of potential DN values, from 0 to 255. Note that the data in Band 5 appear truncated at values of 255, indicating that they are saturated. This characteristic in the data is reason for rejecting the scene.

Each scene was evaluated by first producing RGB images of band combinations 7/4/1 and looking for obvious problems such as native ETM+ image artifacts, clouds, and jet trails. Both scenes passed the first level of Quality Assurance. Next, a region of interest is selected, centered on the confluence of Jackrabbit wash and the Hassayampa river, in order to extract the actual DNs for further examination. These data files are formatted into tab-separated ASCII files containing about 500,000 data points. Then band 5 versus band 4 scattergrams were made from the extracted data for each scene to examine the

actual data distributions in these two important spectral bands. Figure 1 shows the scattergram of band 5 versus band 4 for the June 2000 scene and illustrates a problem with the data in band 5. Note that the data are truncated at the higher DNs. This truncation means that the DNs are saturated and are not reliable for statistical analysis. Finally, band 1 versus band 7 scattergrams were done to examine the effects of atmospheric scattering.

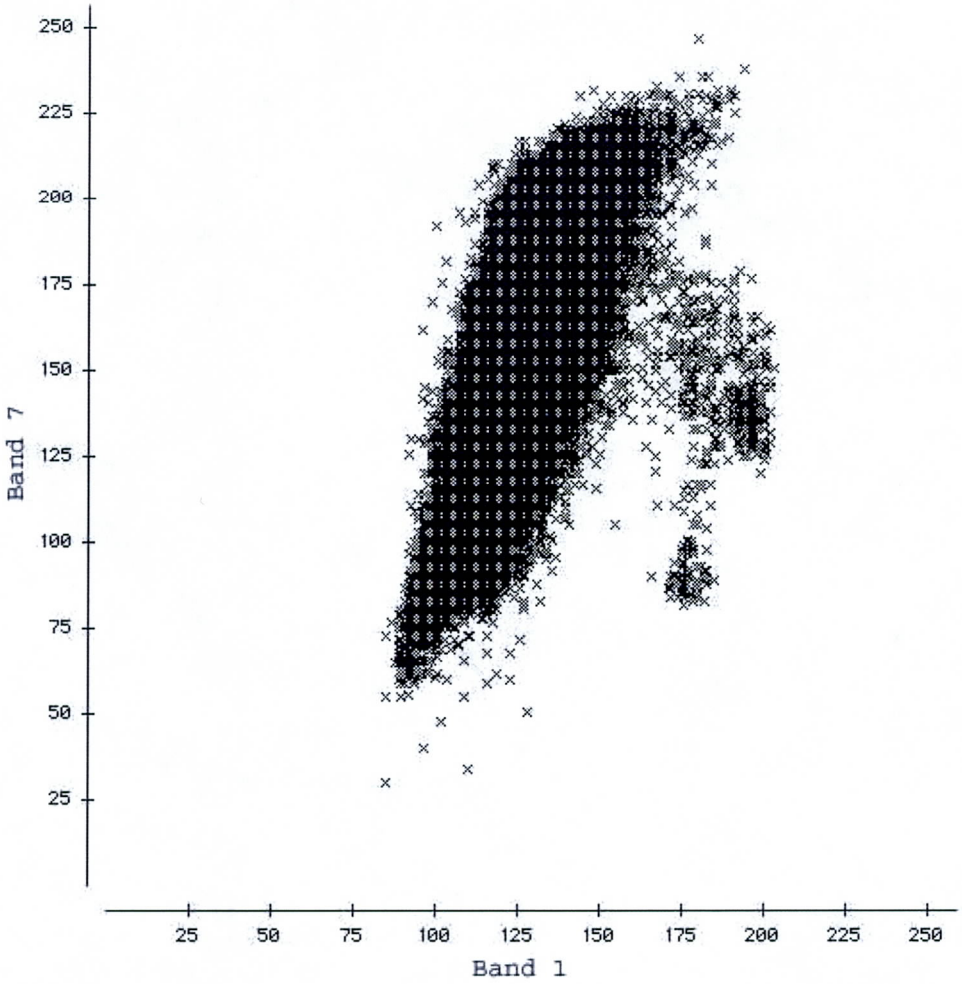

FIGURE 2. Scattergram of Band 1 versus Band 7 illustrating the effect of selective atmospheric scattering. Note that the DNs for Band 7 extend down to about 30, whereas the corresponding DNs for Band 1 are greater than 75. This shift in the DNs of Band 1, or blue light, results from selective scattering. The remaining shift may be the result of nonselective scattering.

The truncation of the DNs in the June 2000 scene is reason for rejecting the scene. In addition, we examined the data to determine the affect of scattering on the data quality. Figure 2 shows the scattergram of band 1 versus band 7 for the June 2000 scene. Note

that the shift of the band 1 values indicates a strong scattering from atmospheric sources. The June 2000 scene did not pass the second level of Quality Assurance and was returned to the Eros data center. Because it was not possible to closely bracket the flooding with a cloud free pre-flood scene, we decided to examine a cloud free scene from the previous year to minimize seasonal differences between the scenes. The scene would still be valid if there was no significant flooding in the intervening period. Another advantage is that it would be possible to evaluate the method of using annual images to detect changes that occurred over that year.

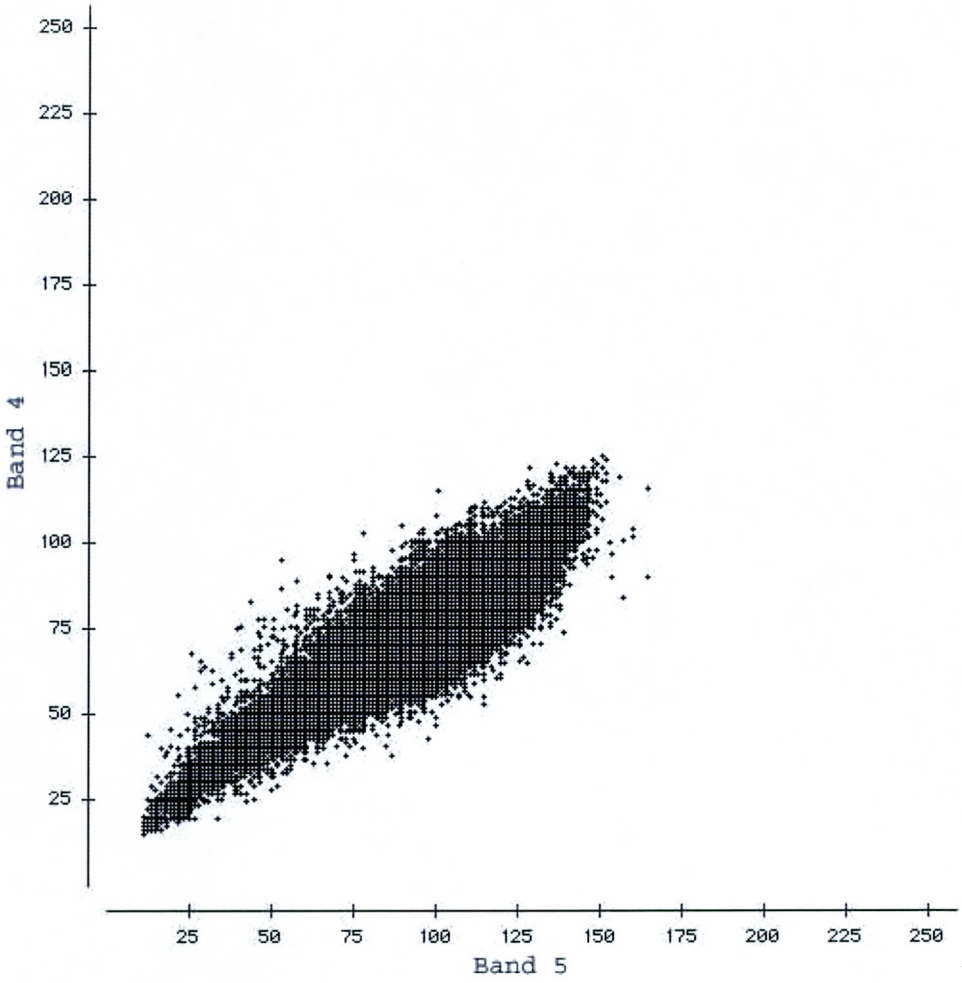

FIGURE 3. Scattergram of Band 5 versus Band 4 for the November 1999 Landsat 7 scene candidate. The scattergram consists of about 500,000 points extracted from the scene for Quality Assurance. The scattergram is scaled to show the entire range of potential DN values, from 0 to 255.

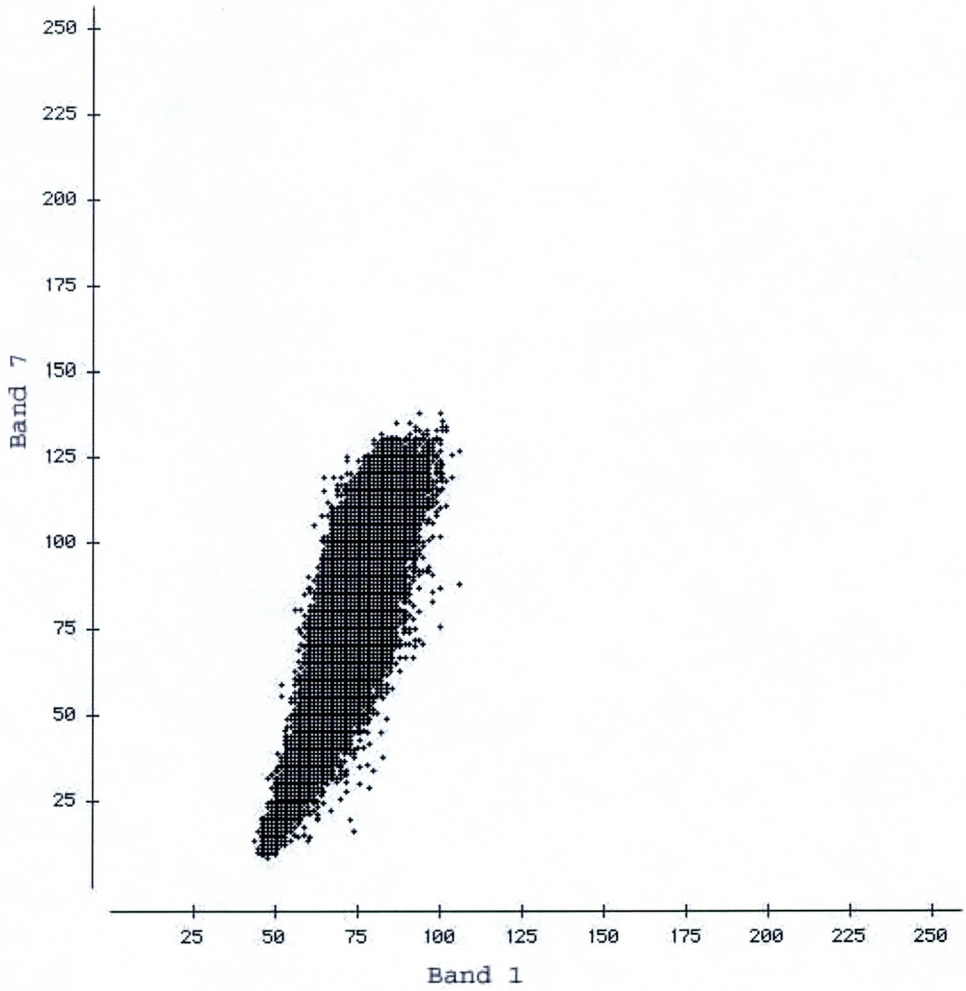

FIGURE 4. Scattergram of Band 1 versus Band 7for the November 1999 scene illustrating the effect of selective atmospheric scattering. Note that the DNs for Band 7 extend down to about 15, whereas the corresponding DNs for Band 1 are greater than 40. This shift in the DNs of Band 1, or blue light, results from selective scattering. Compare this scattergram with Figure 3.

The scattergram of band 5 versus band 4 for the November 1999 scene (Figure 3) shows that the data are not truncated, although the range of the data are not as great as for the June 2000 scene. These data combined with less atmospheric scattering (Figure 4) indicates that the November 1999 data are acceptable. Thus the two scenes used for the flood inundation study are the ones acquired 27 November 1999 and 13 November 2000.

Each scene was shipped on two CD-ROMs containing the following files.

27 November 1999: Before Flood

```
LE7037037009933150.H1 -- Product header #1
LE7037037009933150.H2 -- Product header #2
LE7037037009933150.H3 -- Product header #3
LE7037037009933150.I1 -- ETM+ band 1
LE7037037009933150.I2 -- ETM+ band 2
LE7037037009933150.I3 -- ETM+ band 3
LE7037037009933150.I4 -- ETM+ band 4
LE7037037009933150.I5 -- ETM+ band 5
LE7037037009933150.I6 -- ETM+ band 6, low
LE7037037009933150.I7 -- ETM+ band 7
LE7037037009933150.I8 -- ETM+ band 8
LE7037037009933150.I9 -- ETM+ band 6, high
LE7037037009933150.WO -- Job report file
LE7037037009933150.HI -- Job history file
LE7037037009933150.DH -- DEM header (optional)
LE7037037009933150.DD -- DEM data (optional)
```

13 November 2000: After Flood

```
LE7037037000031850.H1 -- Product header #1
LE7037037000031850.H2 -- Product header #2
LE7037037000031850.H3 -- Product header #3
LE7037037000031850.I1 -- ETM+ band 1
LE7037037000031850.I2 -- ETM+ band 2
LE7037037000031850.I3 -- ETM+ band 3
LE7037037000031850.I4 -- ETM+ band 4
LE7037037000031850.I5 -- ETM+ band 5
LE7037037000031850.I6 -- ETM+ band 6, low
LE7037037000031850.I7 -- ETM+ band 7
LE7037037000031850.I8 -- ETM+ band 8
LE7037037000031850.I9 -- ETM+ band 6, high
LE7037037000031850.WO -- Job report file
LE7037037000031850.HI -- Job history file
LE7037037000031850.DH -- DEM header (optional)
LE7037037000031850.DD -- DEM data (optional)
```

Preprocessing

Landsat data require a few basic preprocessing steps prior to change analysis. The preprocessing steps are: registration of the multitemporal scenes, image area selection by subsetting the analysis area from the multitemporal scenes, and corrections for atmospheric path radiance.

REGISTRATION

Registration of the images is important because bands from two different image acquisition dates are used to form a composite image. Registration of images to one another is usually accomplished using an image to image registration technique where ground control points are matched on each image. Ground control points are commonly road intersections, and other features that can be located on each image with the precision of at least one pixel. Then one image is warped to match the other by a polynomial method and the fit is estimated by a root mean square error. The images used in this study were already within acceptable registration limits, according to the Eros Data Center's processing level.

IMAGE AREA SELECTION

The image area was selected to include the Jackrabbit Wash watershed and excluded the remaining parts of the Landsat scene. The reasons for subsetting the data are: to reduce the amount of data required for analysis; to focus the statistics on the study area; keep the file sizes manageable. The dimensions of the resulting data subset is 1551 samples by 2234 lines (Figure 5). All 12 bands, 6 from each scene, for this area were placed in a single file for further processing.

CORRECTING FOR ATMOSPHERIC SCATTERING

The effect of atmospheric scattering may be estimated by comparing the DNs of band 1 with the DNs of band 7 on a bivariate scattergram (Figure 4). The apparent shift in the band 1 histogram to higher DNs than for corresponding band 7 suggests atmospheric scattering. Dark object subtraction is a method that subtracts that part of the path radiance that is atmospheric in source (Sabins, 1996; Vincent, 1997). The dark object can be defined manually by specifying a dark object DN, automatically by using the lowest DN in the band, or empirically by collecting DNs for dark objects using regions of interest. The DN of the dark object is then subtracted from all bands, based on the lowest DN for that band. Usually, the largest corrections are in band 1. The automatic dark object subtraction method was applied to the data for this study and used for all subsequent analyses. Unlike a display histogram stretch which only changes the appearance of the image in the display, the dark object correction, permanently changes the DNs in the data file, and therefore, these corrected data are stored in a new file. The effect of the dark object correction is shown on Figure 6. Note for example, that the shape of the data cloud is unchanged, because the correction consists of a simple subtraction. Also note that prior to the correction, the band 1 intercept was about 44 DN. Following the dark object correction the band 1 intercept is about 0. No other corrections were applied to the data.

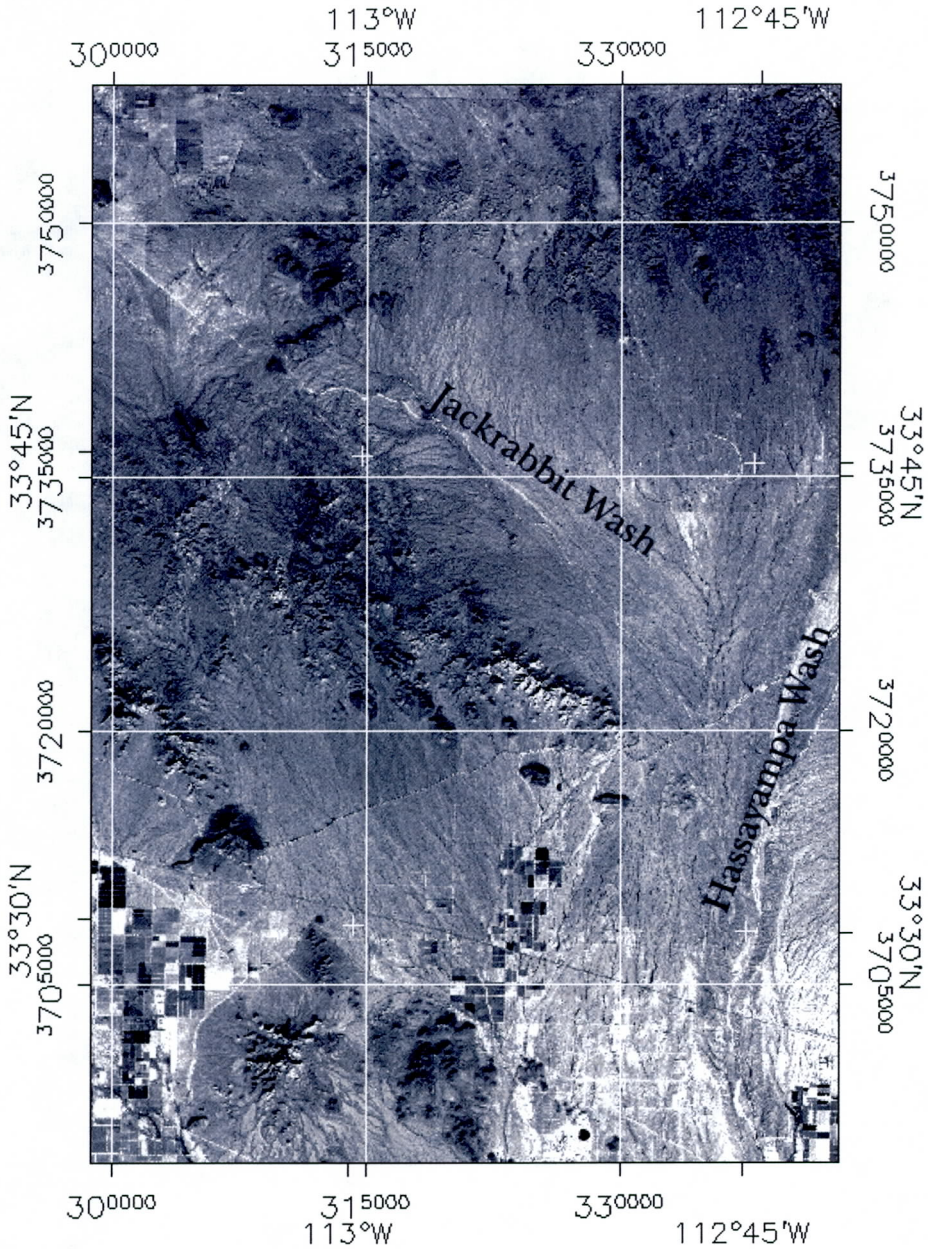

FIGURE 5. Study area portion of the Landsat scene. The image dimensions are 1551 samples by 2234 lines. The data are in a UTM projection

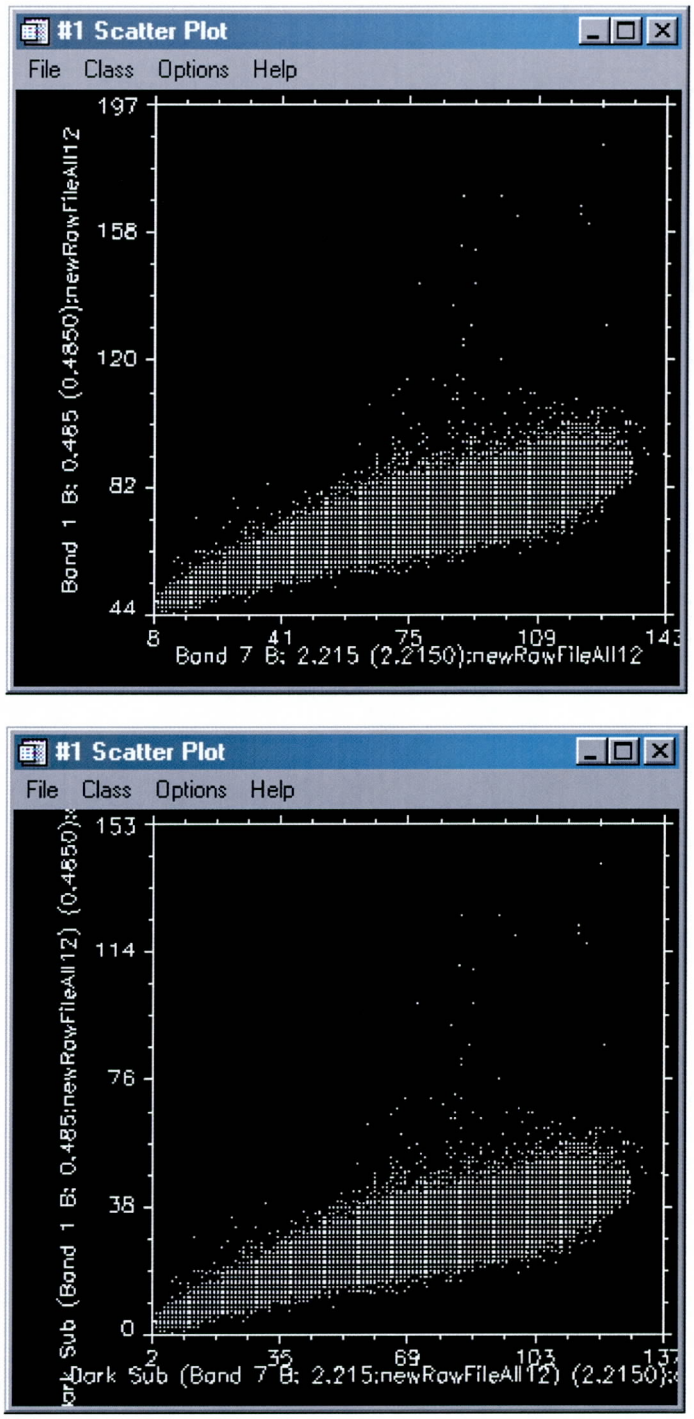

FIGURE 6. Scattergrams showing band 7 versus band 1 before the dark object subtraction (top) and after (bottom).

Image Processing

This analysis is based on the comparison of two Landsat ETM+ scenes for path-row 037-037. The first scene was recorded 27 November 1999 and represents the ground condition before the passage of the runoff producing storm(s). The second scene was recorded 13 November 2000 and represents the ground condition after the storm. These scenes were ordered through the Eros Data Center, in the UTM projection, and had terrain-level corrections applied. The pixel resolution is 28.5 m. Due to the difference in the time that the scenes were acquired, there is an inherent difference in the solar illumination.

Three image-processing methods can be used to document flood inundation in the Jackrabbit Wash area: 1) band to band comparisons of before and after scenes; 2) linear-regression radiometric residual mapping of before and after scenes; and 3) orthogonalization of bands using a decorrelation stretch using bands from before and after the flood event. These three methods are highly complementary and provide first order remotely sensed data to delineate landscape change related to flooding.

BAND TO BAND

A direct method to make landscape comparisons is to examine pairs of bands, representing the same band before and after a flood event. For example, one could compare band 4 before and after a flood event to look for vegetation changes. The before image can be mapped into the Red channel and the after image into the Green channel of an RGB color image (Figure 7). Then any pixel that is brighter in the before image shows up as red and any pixel that is brighter in the after image shows up as green. If the brightness is roughly equal, or unchanged from before to after, then the pixel shows up as yellow.

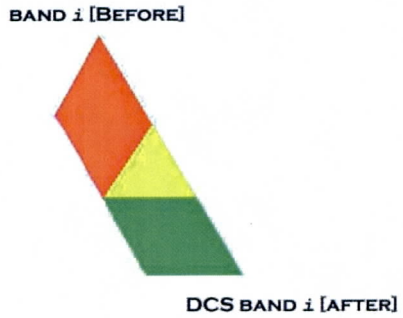

FIGURE 7. RG image space. A two band, or Red-Green, comparison using only the Red and Green channels of the RGB color space is a convenient way of comparing single bands, before and after an event. Pixels that appear red on a RG image are brighter in the before image of that band. Pixels that appear green on a RG image are brighter in the after image of that band.

LINEAR REGRESSION

An inherent difficulty in change detection is that factors other than actual change of the land surface can also cause differences between multi-temporal images. For example, atmospheric conditions, haze, or the thickness of the atmosphere may be sufficiently different between the times the images were acquired that the brightness values are different between them. Other sources of non-land surface change include differences in source illumination at different times of day or times of year, dust in the atmosphere, or sensor calibration. Often, even cursory examination of multi-temporal images indicates that they are not radiometrically equivalent. In other words, they appear different even though they are not. The correction of these differences in radiometric response is called radiometric normalization (*Schott et al.*, 1988; *Elvidge et al.*, 1995) or radiometric rectification (*Hall et al.*, 1991). Many of the radiometric differences not related to land-surface changes could be corrected if targets with known spectral characteristics were deployed and used to adjust the responses. Lacking these installed targets, other, mostly empirical, methods are used to apply corrections to one or more of the multi-temporal images in order to make them radiometrically comparable to the others. In the case of two images, one image can be adjusted or normalized to the other in order to correct for non-land surface change differences between the two images. One can easily think of this correction as a linear transformation function

$$Y = B_0 + B_1 X \qquad \textbf{(EQ 1)}$$

where Y is the estimator of corrected or normalized image DNs based on a linear transformation of the original BVs in X. This operation assumes that there are clearly identifiable pixels that have not changed from one image to another. The regression is done for each band using a relatively small number of pixels. The regression coefficients are used for the coefficients of the radiometric transform operation. The pixels represent two kinds of objects in the images; the lightest and also the darkest objects. All other objects are linearly transformed to the radiometric response of the other image by means of the regression coefficients (*Hall et al.*, 1991). Operationally, the linear transformation function (1) is estimated using linear regression. This method produces results comparable to histogram matching (*Schott et. al.*, 1988). Other methods of radiometric normalization do not require the selection of only dark and bright objects, but assume that no change pixels can be identified throughout the brightness histograms of the bands (*Yuan and Elvidge*, 1996). After the data are radiometrically normalized, image differencing, which subtracts the spectral response of one image from another, can identify significant changes between images. Alternatively, one examine the residuals from a least-squares fit between two bands. Positive residuals mean the DN is brighter than predicted and negative residuals mean the DN is darker than predicted.

ORTHOGONALIZATION

An alternative to direct and explicit radiometric normalization is orthogonalization of selected bivariate band pairs from before and after the flood (*Mayer and Pearthree*, in press). This method relies on the correlation structure between spectral bands of the image. The spectral responses in Landsat TM bands are highly correlated to one

another. Principal components analysis can be used to determine the correlation structure and by use of the covariance matrix, calculate a new set of axes that minimize this correlation to produce a new orthogonal reference frame. The principle components procedure used is derived by Richards (1993). A related technique, also used to enhance the color model, is de-correlation stretching (*Rothery and Hunt*, 1990). To perform a de-correlation stretch, one first calculates the principal components of the image, then stretches each of the bands in principal component space, and finally re-projects the data back into the original band coordinate system. The re-projection back to the original coordinate system allows the investigator to make interpretations from the spectral responses rather than from the more abstract principal components.

The strategy for selecting the input bands for orthogonalization is based on the kinds of changes expected from flooding. Band 4, which is excellent for detecting vegetation cover, is a good choice because it is likely that greening or growth of vegetation following a flood will be evident on floodplains and along stream channels. Band 7 or band 5 can be used to look for non-vegetation changes, for example reworking of sediment in channels and other areas of relatively deep flow. We elected to use bands 5 and 4 as comparison bands, and we used band 5 for normalization. In this paper, we refer to band number and its timing relative to the change; band 4 [before] refers to band 4 on the image before the storm. The RGB color model used to portray change between images is composed of de-correlation stretched bands

Red channel – band 5 [after]
Green channel – band 4 [after]
Blue channel – band 5 [before]

If a region in the change image is any one of the primary channel colors, i.e., red, green, or blue, then the brightness is mostly coming from the corresponding orthogonalized band (Figure 8). For example, if an area shows up as green on the change image, then the pixels are bright only in band 4 (the vegetation band) and therefore dark in the other channels. These areas likely had substantially more vegetation cover in the second satellite image. Regions that are simultaneously bright in the red and green channels (bands 5 [after] and 4 [after]) show up as yellow areas. In their study of the 1997 flooding from Hurricane Nora in Tiger Wash, Arizona, Mayer and Pearthree (in press) found that these areas, typically located in or near stream channels, appear to represent the deposition of fresh sediment and some vegetation growth. Regions that are simultaneously bright in the green and blue channels (bands 4 [after] and 5 [before]) show up as cyan. Cyan areas in channels and floodplains appear to represent the greening of vegetation following the storm. Areas that appear blue on the change image are darker in band 5 after the flood. This may result from moist sediment or extensive dead vegetation (*Mayer and Pearthree*, in press). Regions that are simultaneously bright in the red and blue channels (bands 5 [after] and 5 [before]) show up as purple or magenta.

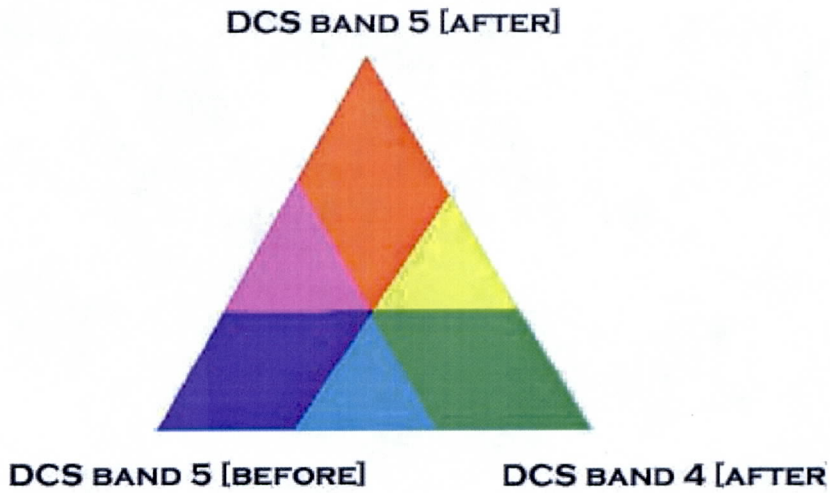

FIGURE 8. RGB Color space for mapping decorrelation stretch bands. Each vertex of the triangle represents saturation in that band, while the line opposite to the vertex represent zero saturation. This triangle is similar to a triangular mixing diagram. Pixels that are simultaneously bright in band 4 and bright in band 5 after a storm event may represent fine sediment because if the vegetation present is not bright in band 5, or a particular type of vegetation that is bright in band 5 as well as band 4. Notice that this diagram does not show intermediate values of mixing. Increasing the contrast on the intermediate values shows their end-member mixing values.

DISCUSSION

Overall change in scene brightness within a single band can be assessed using RG image space (as in Figure 7). An example of a single channel comparison for the Jackrabbit Wash area is shown in Figure 9, which shows the relative brightness in band 4 (near infrared) in the before and after scenes. Areas that are red represent areas that were brighter in the before scene. Areas that are green represent areas that were brighter in the after scene. To emphasize the change, the raw RG image (Figure 9 left) was imported into Adobe Photoshop, posterized sequentially to remove the dark areas (Figure 9 right). The effect of this procedure is to reduce the number of tones to show only the brightest pixels representing the strongest changes. Note that Jackrabbit wash shows up as a ribbon of green, above its confluence with the Hassayampa river.

Figure 9 emphasizes the importance of relative changes in brightness. For example areas in yellow are about the same brightness in the before and after scenes. From a process point of view, anything that increases the reflectance of a pixel, can result in the pixel showing up as green in the RG comparison. This might be the growth of vegetation or the deposition of fine silt or sand. Similarly, a pixel will show red if a process darkened the area, such as the wetting of a region.

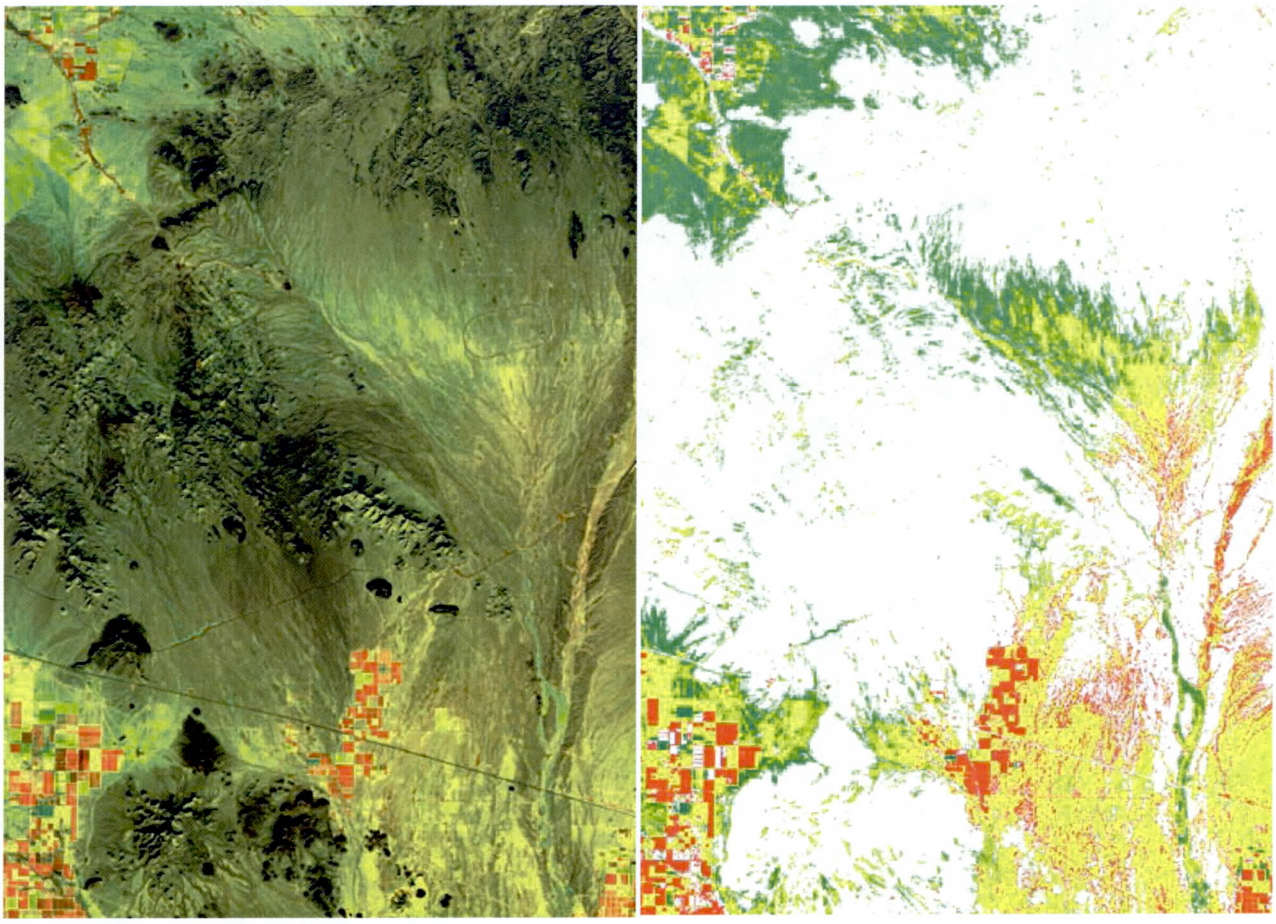

FIGURE 9. Before and after comparisons of band 4 in RG Space. The before image is in the Red channel and the after image is in the Green channel. The panel on the left shows the raw RG image. The panel on the right shows only the strongest changes in the scene (see text for discussion).

For the purpose of detecting all change, we return to the method of orthogonalization where the interpretation of the color model follows Figure 8. The decorrelation stretch image consists of three bands of data which have been stretched in an orthogonal reference frame. Figure 10 illustrates the combination of these bands and the resulting colors in RGB space.

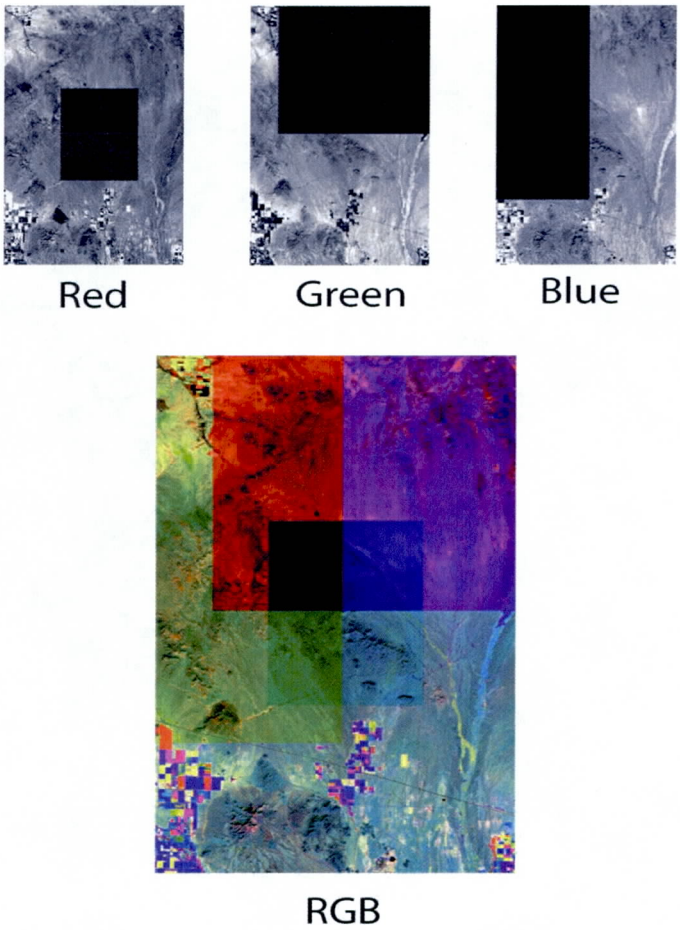

FIGURE 10. Interpreting the RGB Model of decorrelation stretch data. Each channel has a region zeroed data shown as black boxes. The RGB model of these three bands of data is a type of Venn diagram that shows the union of the data. For example the portion of the scene with no blue, shows up as a RG image in the RGB composite.

The change image, representing areas that appear different between the before and after scenes is shown in Figure 11. To interpret this image, it is useful to again refer to Figure 8 and Figure 10. Pixels that show up blue represent areas that were made darker in the after scene. Pixels that show up green represent areas that were bright in band 4 after, and probably band 4 before as well.

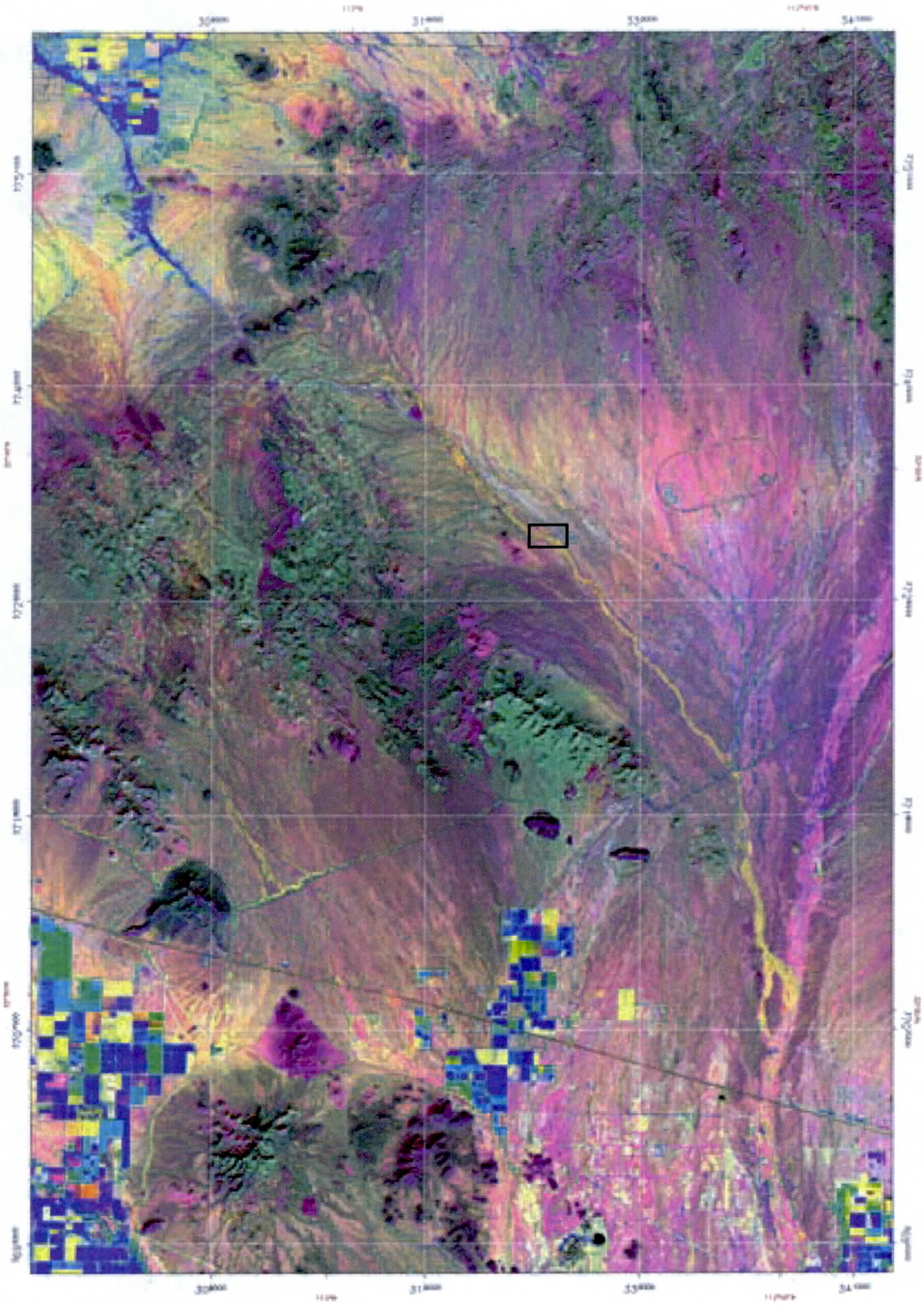

FIGURE 11. Decorrelation stretch image of the Jackrabbit wash area. Jackrabbit wash shows up as a very clear yellow ribbon from the upper part of the basin to the confluence with the Hassayampa river. Small box shows area of field validation.

Field Validation

The goal of validation is to determine, based on direct observation in the field, the nature of landscape changes that accompanied the October 2000, flood and how these changes relate to the satellite change image. The satellite change image (Figure 11), produced prior to any knowledge of what occurred on the ground, indicated that Jackrabbit Wash had experienced detectable change between the two image dates. This change shows up as a yellow ribbon that highlights Jackrabbit Wash. The primary question is whether or not the areas highlighted, by the color yellow in particular, truly represented areas of flood inundation. In addition, there are several other questions that are relevant, including: What changes are being detected? What changes are not being detected? At what scale can this method be used?

On July 16th, Mayer, along with Phillip Pearthree and Ann Youberg of the Arizona Geological Survey, examined the effects of flooding on the upper portion of Jackrabbit Wash adjacent to Vulture Mine Road (Figure 12; also see black rectangle on Figure 11). On July 17th, Ted Lehman of JE Fuller/H&G Inc. joined us and we had the opportunity to examine flood evidence in the headwaters of Jackrabbit Wash and several tributaries to Jackrabbit Wash.

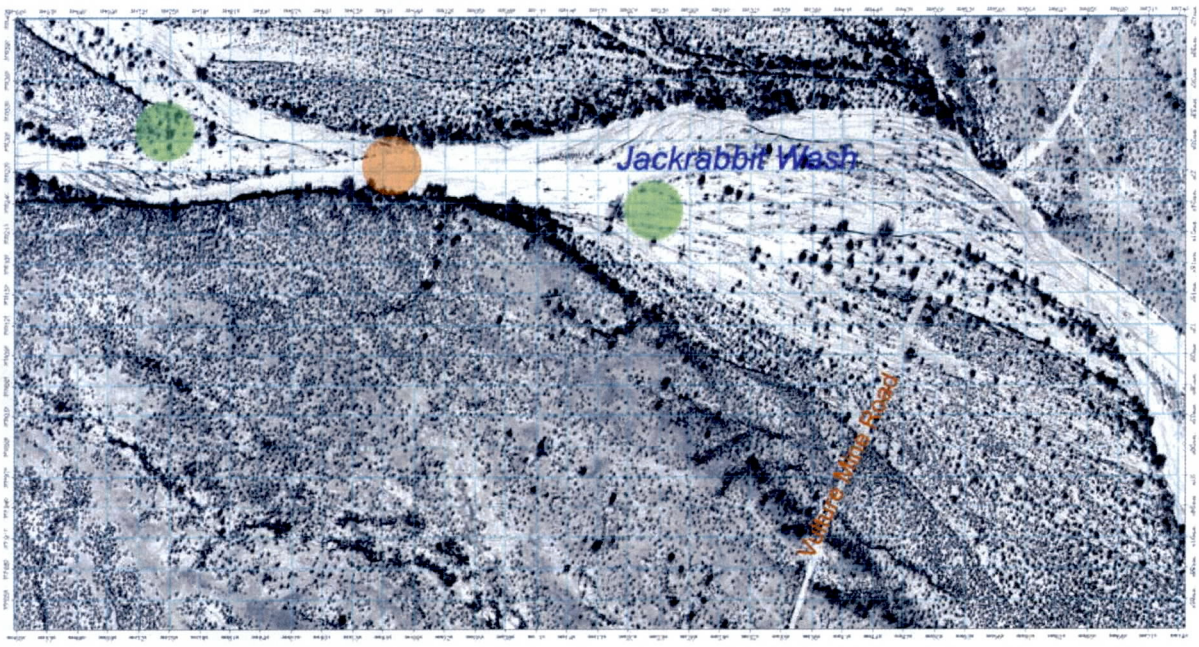

FIGURE 12. Airphoto of Jackrabbit Wash at Vulture Mine Road taken after the October 2000 flooding. The cyan grid marks 30 m cells that are approximately the same size as the resolution of Landsat 7 spectral bands. The green dots indicate expansion reaches and the red dot indicates a contraction or constricted reach of Jackrabbit Wash. Notice that vegetation grows throughout this portion of the channel. Vegetation is especially clear along and east of Vulture Mine Road. Also see black rectangle on Figure 11 for location in scene.

Jackrabbit Wash varies in width from about 60 m to about 200 m as it alternates between constriction and expansion reaches near Vulture Mine Road (Figure 12). The characteristics of these reaches are very different, which have implications for flood inundation detection. The constricted reach is wider than the nominal 30 m resolution for Landsat and therefore this reach is covered by two pixels. Assuming that registration is better than one pixel, the data represented by these pixels should be real. The constricted reach is characterized by a homogeneous cover of poorly-sorted gravel. In contrast, the expansion reach bars that represent overbank flooding areas for smaller floods and the main floodway for larger floods. Particle sizes are more variable in the expansion reach, ranging from silt to coarse gravel and cobbles. Vegetation in the expansion reach is also quite varied, consisting of dominantly desert broom on the lowest areas of the reach. Paloverde and desert broom are also found in low areas, and creosote dominates the higher parts of the reach. Field observation and examination of airphotos suggests that desert broom can reclaim the less active parts of the channel very quickly.

FLOODED AREAS AND CHANGE IMAGE

The evidence for flooding is ubiquitous in Jackrabbit Wash and consists of fresh bank erosion, morphologically fresh coarse sediment lobes, vegetation removal and damage, sediment deposition, overbank deposition of sand, silt and gravel, overbank erosion and channeling, and fresh high water flotsam. Our examination suggests that along Vulture Mine Road, Jackrabbit Wash inundated at least up to a higher terrace (marked by the "e" in Mine on Figure 12).

To facilitate some basic comparisons between the satellite change image and field observations for this area, the change image was merged with the airphoto (Figure 13, Top). The merging process alters the colors so they do not exactly coincide with those of Figure 11, however, the actual data are also shown in Figure 13, Bottom. A well known illusion of merging low resolution data with high resolution data is that the merged data appears to be higher resolution than it actually is. The registration between the two data sets is approximate because we have no ground control points for the satellite image and airphoto. Comparison of Figure 13 Top and Bottom illustrates the apparent increase in resolution clearly.

The reach downstream of Vulture Mine Road coincides with yellow and yellow-orange areas on the satellite change image and some yellow extends into the constriction reach itself. The brightest yellow is located immediately downstream of the constriction reach. Farther downstream, the yellow is mixed with red and turns distinctly orange in what is normally overbank areas. In addition to the yellow color, there are also magenta, green, and the occasional blue pixel in the channel, green being by far the most common of this latter group.

The areas outside of the channel are dominated by reddish-magenta colors south of Jackrabbit Wash. North of Jackrabbit Wash the colors are more complicated and intricately mixed, including green, magenta, and blue (Figure 13). This more complex pattern may result primarily from vegetation patterns developed on the dissected old gemorphic surface.

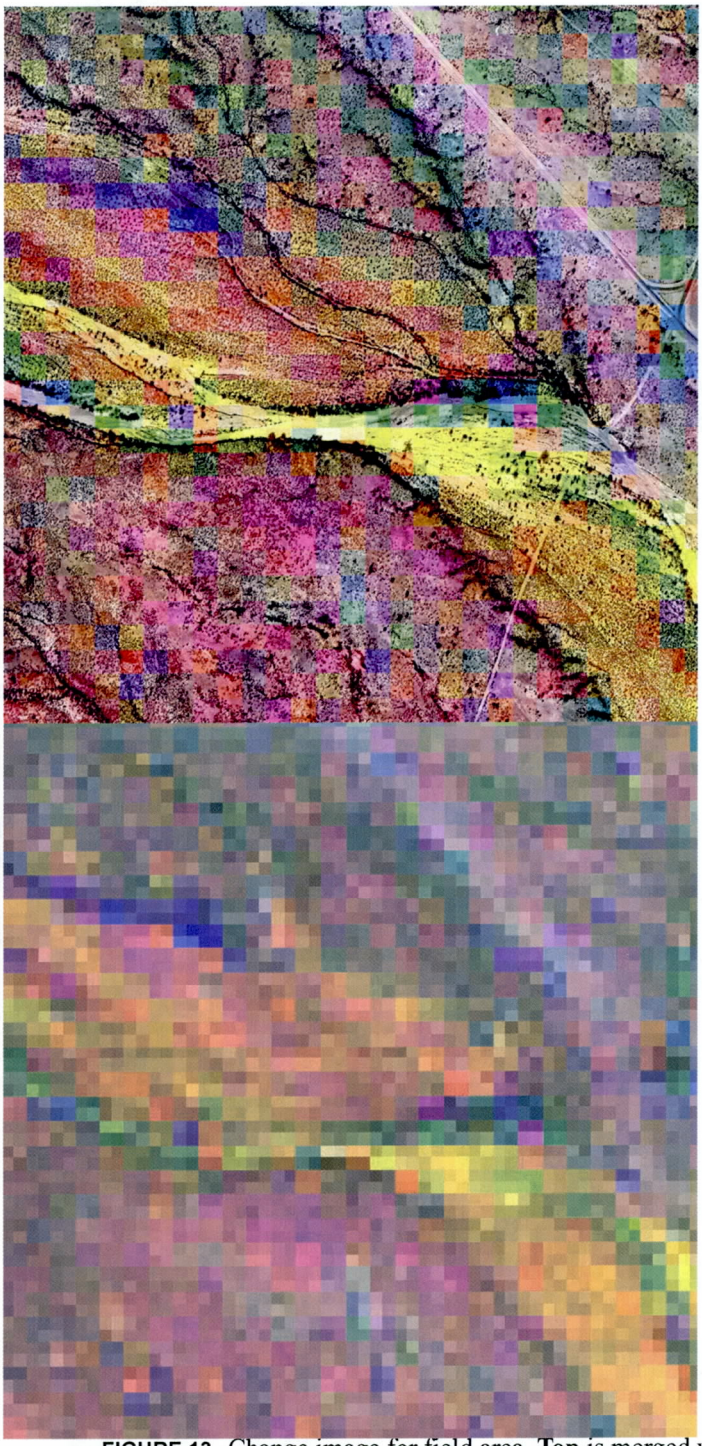

FIGURE 13. Change image for field area. **Top** is merged with airphoto from part of Figure 12. **Bottom** is raw data from Figure 11. Pixel size is 28.5 m. Registration with airphoto is approximate. See text for discussion.

In the field the flooded area just downstream of Vulture Mine Road may be broken down into four very broad landform categories: the main channel thread, secondary channels, and highly vegetated bars and the overbank. The highly vegetated bars have fresh sediment clearly deposited on them, and also have flotsam in topographically higher positions (see "A" Figure 14). Secondary channels were probably vegetated prior to the flood and thus radiometrically, these would indicate a simultaneous reduction in vegetation and increase in sediment. The position "B" in Figure 14 marks an example of this condition. Finally, the main channel will have fresh sediment, especially immediately below the constriction where hydraulic conditions change rapidly ("C" and "D" in Figure 14).

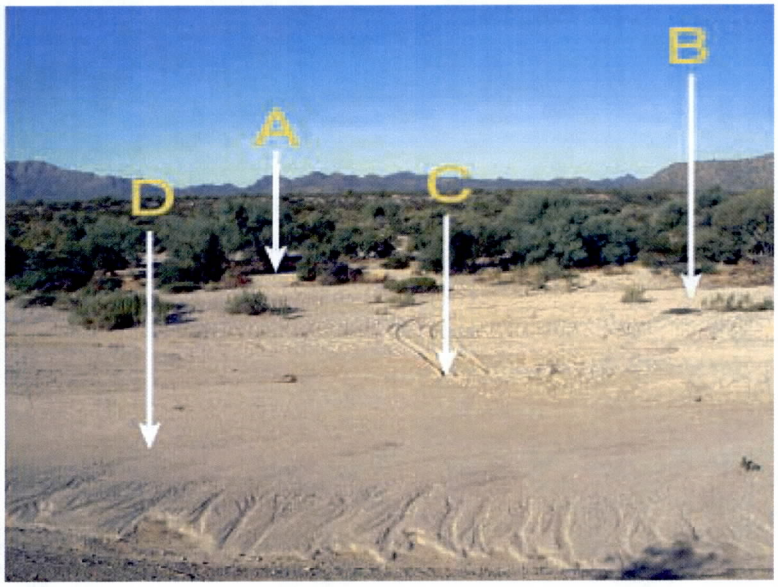

FIGURE 14. Photograph of Jackrabbit Wash about 100 m downstream of Vulture mine road. "A" points to recent deposition found between vegetation in the channel bar position. This area receives deposition in larger floods. A secondary channel at location "B" is only active in larger floods. This is evidenced by existence of tire tracks in the channel "C", which were destroyed by a small flood in July, 2001 that flowed in the channel at "D".

Thus in this area, there is clear evidence that regions, which show up as yellow were indeed flooded, and we can to some extent explain the cause of the radiometric changes. In the area above the constriction, the yellow is less distinct and again, oranges dominate, except for the vegetated bank, where green dominates. Within the upstream expansion reach, we have found that in areas that we expected to see change, we see such change and in other places, the evidence is not unambiguous. We believe, for example that overbank deposition in the constriction reach is visible on the change image despite the fact that the areal extent borders on the resolution limit of the data (Figure 15).

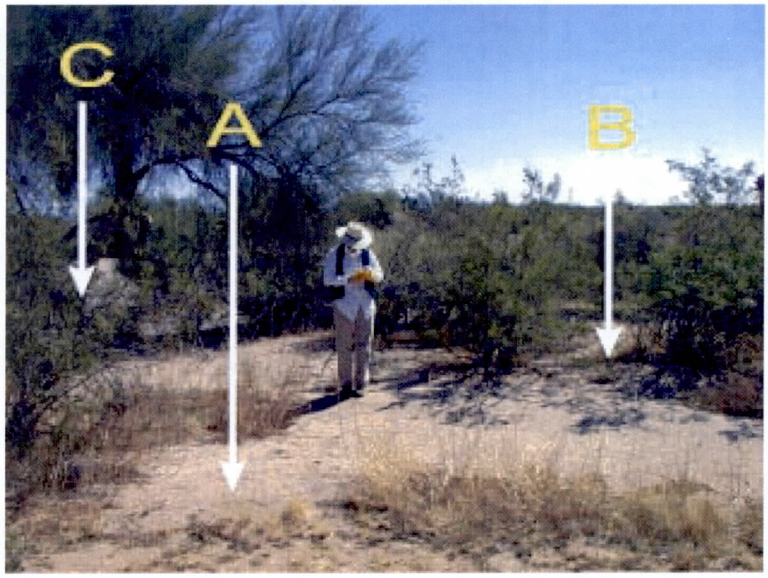

FIGURE 15. Photograph of overbank deposits adjacent to Jackrabbit Wash on the south side of the constriction reach. These deposits are found in a small gulley that drains into the main channel. During very the peak stages of large floods, this channel is in a slackwater position and collects finer sediments of the flood. In location "A", these deposits are clearly visible from above, and presumably from satellites, but in position "B" which represents most of the surface, creosote vegetation obstructs the view of the ground. Jackrabbit Wash is behind the paloverde tree at "C".

LIMITATIONS

Several circumstances clearly limit the resolution of flood inundation mapping using Landsat data. We find that in areas of overbank flooding where the vegetation is relatively dense so that the relative contribution to total radiometric reflection is high, the vegetation and not the underlying sediment will dominate the signal. If the main landscape change in an area was the deposition of sediment under a canopy or in the exposed patches of ground between the vegetation, it could be very difficult to detect. In the extreme case, a canopy of bushes, shrubs, trees, etc., could completely mask detection.

Another limitation in exposed areas centers on the nature of the flood induced changes. In the main thread of a channel that is always dominated by alluvium with the same particle size distribution and same chemical composition, flood detection is difficult. Width-restricted sections of a channel may represent this environment. Basically, each flood may bring fresh sediment into a channel reach, but because it looks identical to the sediment that was there before the flood, it can't be used to indicate the extent of flooding induced change. However, if fine sediments are deposited on top of coarser sediments, it is likely that these will differ not only in particle size, but also in chemical

composition. These areas would result in good detection of flood inundation. In channel reaches that are constricted and where flood flow is restricted to a single channel, change detection may rely on changes in the position of coarse channel bars, and the removal of vegetation in the channel itself.

A similar situation may also occur in the overbank areas. Overbank areas along Jackrabbit Wash receive a variety of sediment caliber, depending on the hydraulics of the flow. In those areas that receive fine sand during large floods, pre-flood and post-flood conditions may not differ radiometrically because the fine sands deposited after the flooding may not be distinctly different from the fine sands, which were already there. However, if the recurrence interval between floods is large, the surface may accumulate wind blown silts, that could make the pre-flood surface distinct from the post-flood surface.

Conclusions

The methodology for making change images for detecting flooding discussed in this report is a single step procedure that requires little operator training. Pre-processing and interpretation of the images may require trained operators. The methodology has been validated for alluvial fan flooding for Tiger Wash (Mayer and Pearthree, in press). Our satellite change image which covered a very large area, clearly indicated that Jackrabbit Wash had undergone landscape change between the November 1999 and 2000. Landscape change was indicated by the color yellow on the change image. Based on field checking in the area of Jackrabbit Wash near Vulture Mine Road, we find that wherever yellow occurs in a stream, that significant flooding is indicated.

The procedure outlined in this report indicates that band orthogonalization is an effective method for finding areas of flood inundation in remote regions of Arizona, and that much of the data are significant even at the resolution of individual pixels (Figure 13). Overbank deposition may not be detectable in areas that are not visible from space because of vegetation cover .

References

Eldvidge, C.D., Yuan, D., Weerackoon, R.D. and Lunetta, R.S., 1995. Relative radiometric normalization of Landsat multispectral scanner (MSS) data using an automatic scattergram controlled regression. Photogrammetric Engineering & Remote Sensing, 61: 1255-1260.

Hall, F.G., Strebel, D.E., Nickeson, J.E. and Goetz, S.J., 1991. Radiometric rectification: Toward a common radiometric response among multidate multisensor images. Remote Sensing of Environment, 35: 11-27.

NASA, Landsat 7 Science Users Data Handbook , http://ltpwww.gsfc.nasa.gov/IAS/handbook/handbook_toc.html

Mayer, L. and Pearthree, P.A., in press. Mapping Flood Inundation in Southwestern Arizona using Landsat TM Data: A Method for Rapid Regional Flood Assessment Following Large Storms. American Geophysical Union.

Richards, J., 1993, Remote Sensing Digital Image Analysis, An Introduction, 2nd Edition, Springer-Verlag.

Rothery, D.A. and Hunt, G.A., 1990. A simple way to perform decorrelation stretching and related techniques on menu-driven image processing systems. International Journal of Remote Sensing, 11: 133-137.

RSI, 1999. ENVI User's Guide. Research Systems Inc., 842 pp.

Sabins, F.F., 1996. Remote Sensing: Principles and Interpretation. W.H. Freeman and Company, New York, 469 pp.

Schott, J.R., Salvaggio, C. and Volchok, W.J., 1988. Radiometric scene normalization using pseudoinvariant features. Remote Sensing of Environment, 26: 1-16.

Song, C., Woodcock, C.E., Seto, K.C., Lenney, M.P. and Macomber, S.A., 2001. Classification and Change Detection Using Landsat TM Data: When and How to Correct Atmospheric Effects? Remote Sensing of Environment, 75: 230-244.

Vincent, R.K., 1997. Fundamentals of Geological and Environmental Remote Sensing. Prentice Hall, Upper Saddle River, New Jersey, 338 pp.

Yuan, D. and Eldvidge, C.D., 1996. Comparison of relative radiometric normalization techniques. Journal of Photogrammetry & Remote Sensing, 51: 117-126.

Appendix

LIST OF FILES ON CD

The following files are on the CD included with this report. The *.hdr files are text header files describing the contents of the datafile. The *.jgw files are text geography or world files, the equivalent of geoTiff headers but for jpeg files. All figures are also included on the CD as well as the pdf of this report.

1) alldark, alldark.hdr: these are the 12 bands of data for the study area after the dark object subtraction.

2) data fro Jun. 2000, data for Nov. 1999: tab delineated text files for a section of the data that were used to evaluate the quality of the scenes.

3) DCS Pan merge, DCS Pan merge.jgw: Change image merged with the Landsat 7 Panchromatic band using HSV sharpening.

4) DCS5a4a5b, DCS5a4a5b.jgw: the full scale change image shown in Figure 11.

5) dcs4atif,dcs5atif,dcs5btif: the individual orthogonal bands in Tiff format for viewing and use in interpretation of Figure 11.

6) dcs5a4a5b,dcs5a4a5b.hdr: The data file containing the orthogonalized bands.

LIST OF PAPER MAPS

1) The satellite change image at 1:100,000 scale.

2) The airphoto, change image merge for the field validation area. Note as explained in the text, the registration is only approximate.

INTERPRETING SPECTRAL RESPONSES

Reference spectra are required to interpret the responses measured by Landsat satellites and to decide which bands to use for analysis Direct comparisons between laboratory spectra and satellite data are only possible after all atmospheric path effects have been accounted for. Relative comparison are possible after dark object corrections. Reference spectra are available from the United States Geological Survey, http://speclab.cr.usgs.gov/.

Figure 16 shows the portions of the electromagnetic spectrum, or bandwidths, acquired by Landsat 7. The bands are chosen to coincide with wavelengths that are able to be transmitted through the atmosphere. Bands 3, 2, 1 approximately coincide with the visible colors red, green, and blue, respectively. Laboratory spectra are shown to indicate which bands will record a particular surface cover (Figure 16). For example, note that the reflectance of lawn grass is much brighter in the near infrared band 4 than in the visible band 2 (green). Hematite has more reflectance in band 5 than in the visible band 3 (red). Quartz has high reflectance throughout the sensor range and therefore appears bright in all bands. If vegetation such as grass is removed and replaced by quartz, for example, an image that was bright in band 4 will now be bright in band 5.

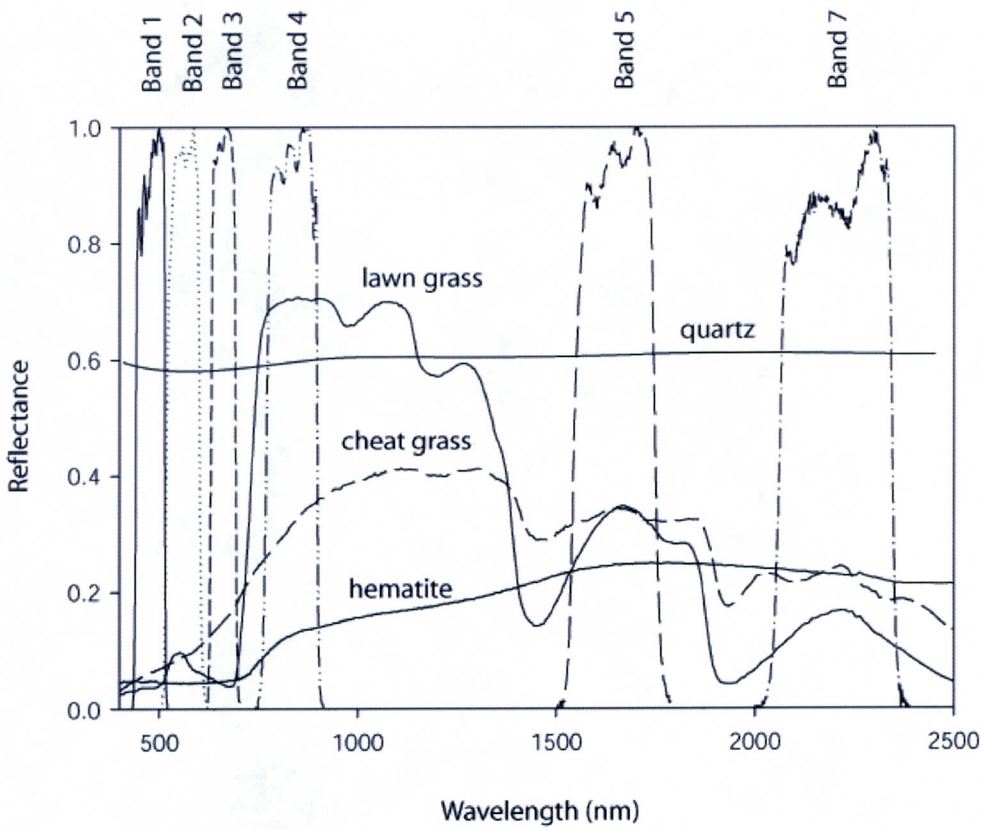

FIGURE 16. Graph showing the performance of Landsat 7 sensors and the laboratory spectra of reference materials (spectra from USGS).

SOFTWARE USED FOR ANALYSIS

ENVI was used for all image analysis in this report (RSI, 1999). Comparable products include ER Mapper, and ERDAS Imagine.

Color Copies of Pages with Color Figures

Page 13

Page 16

Page 17

Page 18

Page 19

Page 20

Page 22

Page 23

Page 24

APPENDIX C

Geomorphologic Assessment of the October 2000 Flood on Jackrabbit Wash, Maricopa County, Arizona

by
Ann Youberg and Dr. Philip A Pearthree

Geomorphologic Assessment of the October 2000 Flood on Jackrabbit Wash, Maricopa County, Arizona

by

Ann Youberg and Philip A Pearthree

Arizona Geological Survey

Draft Report to the Flood Control District of Maricopa County

February, 2002

Arizona Geological Survey
416 W. Congress, Tucson, AZ 85701

Includes 24 pages of text, two 1:24,000 scale geologic maps, and one 1:36,000 plate

Research supported by Flood Control District of Maricopa County and the Arizona Geological Survey. Work done in cooperation with JE Fuller Hydrology & Geomorphology and Larry Mayer.

INTRODUCTION

Current populations trends and 2000 Census data indicates Arizona's population will increase 48% by 2020, with Maricopa County's population increasing by a similar amount (Arizona DES, 2001). Expansion of urban development onto piedmont areas that are currently remote from the metropolitan area, like those of western Maricopa County, should be expected to accommodate growth in the future. Flood hazard management in these broad, relatively low-relief areas can be challenging, but it will become increasing important as development continues.

Managing flood hazards requires estimates of flood frequency and magnitude, channel stability and potential erosion hazards, and expected extent of inundation during floods. Flood hazard management in arid regions is difficult due to a limited understanding of fluvial processes on arid streams and limited data (Parker, 1995). Streams in arid and semiarid regions may not experience any flow for many years. When floods do occur, there may be severe lateral bank erosion and changes in channel location and geometry (Pearthree and others, 1992, Parker, 1995; Klawon and Pearthree, 2000). Most piedmont areas of southern and western Arizona remain remote with limited accessibility and instrumentation. Although Maricopa County is at the forefront in developing a comprehensive network of rain and streamflow gages, they are still fairly widely spaced or have short records. Floodplain managers need rapid and efficient methods for detecting flooding in these remote areas, and for extracting data for regional flood assessments.

Mayer (2000) developed a new method to detect landscape change from flooding by quantitatively comparing two Landsat 7 satellite data scenes taken before and after a flooding event. Mayer and Pearthree (2002) first evaluated this method on Tiger Wash fan, a large distributary system in western Maricopa County. They found a strong correlation between the detected changes from remote-sensing data and extent of flood inundation from field mapping. This change detection methodology was applied to Jackrabbit Wash, which experienced a very large flood in October 2000. The goal of this study is to assess how well this method detects flood inundation and extent on a piedmont tributary system like Jackrabbit Wash. This report compares extent of flood inundation derived from the satellite change image with field data.

Geologic and geomorphic information can also provide invaluable information of flood hazards in piedmont areas (Field and Pearthree, 1992; Hjalmarson and Kemna, 1991; Pearthree and others, 1992; Field, 1994a and 1994b; Hjalmarson, 1994; Klawon and Pearthree, 2000). Mapping surficial geologic deposits based on surficial characteristics such as surface color, soil development, accumulation of calcium carbonate, development of desert varnish and desert pavement, drainage patterns and entrenchment, local topography, and vegetation provides information about the age of the deposit and potential inundation from flooding. Analyzing evidence of flood extent and flow characteristics provides information about potential erosion hazards and channel changes (Klawon and Pearthree, 2000). Surficial geologic mapping and channel change analysis of Jackrabbit Wash was conducted at Vulture Mine Road crossing.

Jackrabbit Wash is located in northwestern Maricopa County, Arizona, approximately 20 miles southwest of Wickenburg (Figure 1). The headwaters of Jackrabbit Wash are located on the western piedmont of the Vulture Mountains and the northern flank of the Big Horn Mountains. Jackrabbit Wash flows southeast over the Hassayampa Plain to its confluence with the Hassayampa River. The drainage area of Jackrabbit Wash above the confluence with Star Wash, the study area for this project, is approximately 140 square miles. Jackrabbit Wash is a tributary system with the upper piedmonts of the Hassayampa Plain providing most of the contributing area. Below Vulture Mine Road, Jackrabbit and other nearby washes are well entrenched into the piedmont and tend to flow parallel to each other, limiting additional contributing areas to adjacent slopes. The next major tributary that joins Jackrabbit Wash is Star Wash, which is at the downstream end of our study area. Topographic relief in the Jackrabbit Wash watershed is

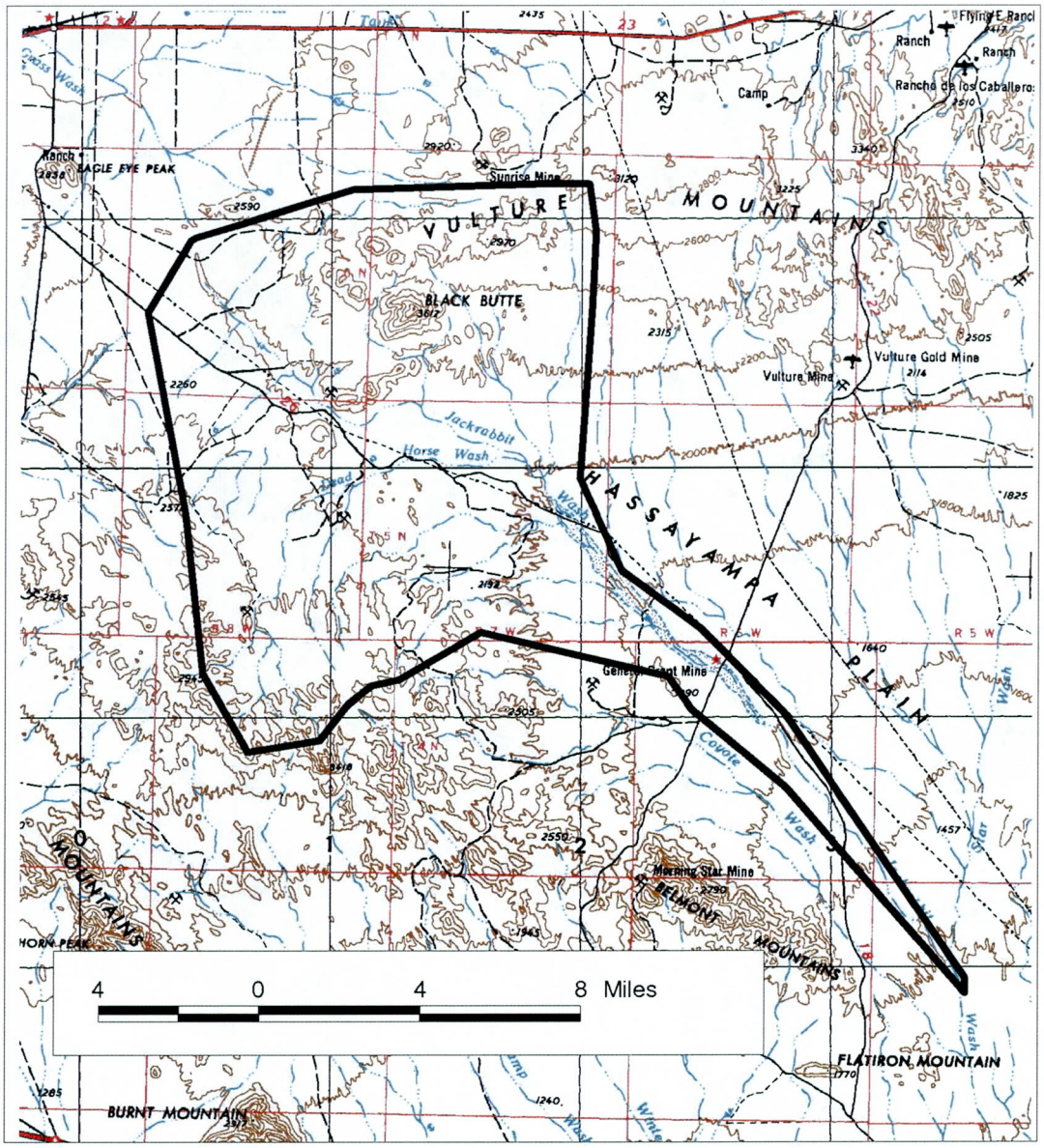

INDEX MAP SHOWING LOCATION OF STUDY AREA

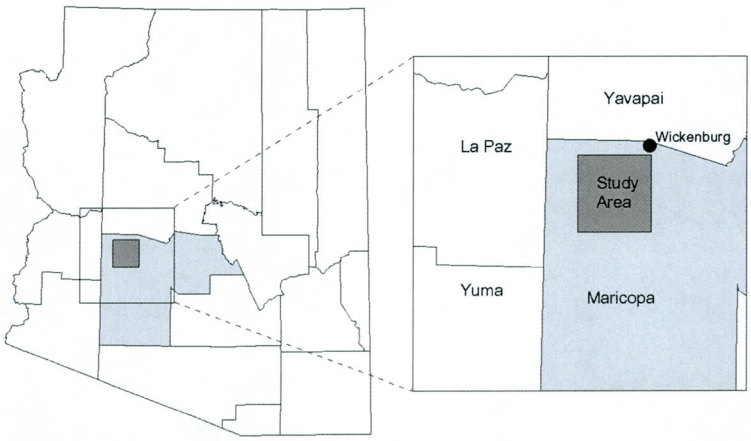

Figure 1. Jackrabbit Wash drainage basin in west-central Arizona. Solid line on main map shows the approximate extent of the watershed above the confluence with Star Wash. Inset map shows the location of Jackrabbit Wash in northwestern Maricopa County.

modest, with a maximum elevation difference of 2,252 feet between the top of Black Butte in the western Vulture Mountains and the confluence of Jackrabbit and Star washes, at the Central Arizona Project canal crossing. Elevation differences between the upper piedmonts and the CAP canal are about 1000 feet.

Magnitude of Rainfall and Flooding

The principal Jackrabbit Wash flood occurred in the latter half of October 2000, near the end of an unusually wet period associated with a persistent low-pressure trough. The month of October featured a series of Pacific low-pressure frontal systems that tapped tropical moisture in northern Mexico as they passed through Arizona, resulting in heavy widespread rain with numerous embedded thunderstorms (Waters and others, 2001). Much of western and northern Maricopa County was impacted by these storms. Coincidentally, the area affected most by the late October 2000 storm systems and dissipating Hurricane Nora in September 1997 was quite similar, although the storm systems were quite different. The first storm system affected this area on October 20 and 21. It caused serious flooding along Centennial Wash in the Wenden area in La Paz County and a moderately large flood on Tiger Wash in westernmost Maricopa County. The heaviest precipitation associated with this storm was north and west of the Jackrabbit Wash drainage basin (Waters and others, 2001). A second storm on 10/27 caused more flooding on Tiger Wash and Centennial Wash, although on both of these washes the second peaks were not as large as the 10/21 flood peaks. The most intense rainfall associated with the second storm was concentrated in a north-south-trending band across the upper part of the Jackrabbit Wash watershed. This precipitation generated a very large flood on Jackrabbit Wash.

A number of FCDMC Alert System precipitation gages around the margins of the Jackrabbit Wash drainage basin recorded large rainfall amounts for the late October storms. Many gages received about 2.5 to 3.5 in of precipitation in the 10/21 event, but the largest rainfall amounts stretched through McMullen Valley to the western edge of Wickenburg (Waters and others, 2001). Rainfall totals in the Jackrabbit drainage were generally less than 1 in. Precipitation estimates based on radar reflectivity are consistent with the rain gage data (Waters and others, 2001). Rainfall amounts recorded at most FCDMC Alert gages for the 10/27 storm were less impressive, with a maximum total of less than 3 inches. However, the rainfall estimates based on radar reflectivity were substantially higher, ranging up to at least 4 in. for the storm total. Indeed, the radar-based estimates indicate that the heaviest precipitation was concentrated in a north-south-trending band across the upper Jackrabbit watershed. In addition, the ground was probably wet before the second storm, and this most likely served to increase runoff.

The Jackrabbit flood of October 2000 was clearly very large. This relative size of the flood may be evaluated in a number of ways. The FCDMC reported a peak discharge estimate of 32,400 cubic feet per second at the site of their stream gage, which was installed just after the 2000 flood (Waters and others, 2001). The peak discharge record for Jackrabbit Wash as reported by the U.S. Geological Survey stretches back intermittently to 1964. The largest previous peak was 13,000 cfs in September 1983, so the 10/27 flood discharge is more than twice as large as any previously reported peak for this drainage. Prior to the 10/27 flood, the U.S. Geological Survey estimated that the 100-yr discharge for this drainage was 33,000 cfs (Pope and others, 1998), so by that measure the 2000 flood was essentially the 100-yr flood. The 100-yr flood estimate for the FCDMC gage site developed by rainfall-runoff modeling is about 21,000 cfs, so in that framework the 10/27 flood was an extreme event.

We may also evaluate the 10/27 flood on Jackrabbit Wash by comparing it with other floods in the lower Colorado River region. Plots of peak discharge vs. drainage basin area are a useful framework in which to consider the relative sizes of floods over a broad region, essentially using a large number of sites over a reasonably homogeneous region in order to better evaluate the sizes

of the largest floods in a region (Enzel and others, 1993; House and Baker, 2001). In this context, it is clear that the 10/27 flood was exceedingly large. While it is somewhat below the envelope that encompasses the most extreme floods reported for this region, it is about the largest flood that has been reported for this particular size drainage basin (Figure 2).

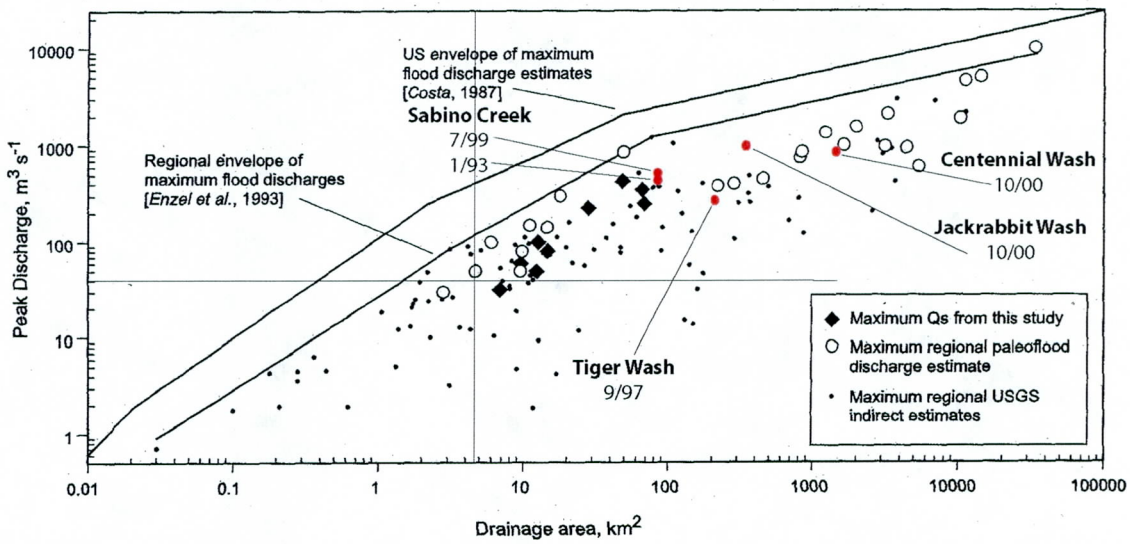

Figure 2. Comparison of maximum flood peak discharges to the regional envelope curve of maximum peak discharge versus drainage area in the lower Colorado River Basin and to the envelope curve for the largest floods in the conterminous United States (from House and Baker, 2001).

LANDSAT CHANGE IMAGE

A major objective of the field investigations in this study was to ground-truth the extent of inundation derived from the satellite change image. To meet this objective, the primary goals in the field were to (1) determine the extent of inundation along Jackrabbit Wash; (2) document changes that occurred in the landscape and which changes were detected on the image; and (3) evaluate the scale at which the satellite change detection method is useful.

Extent of flood inundation was mapped on the satellite change image at a scale of 1:24,000 in a GIS framework. On the satellite change image of Tiger Wash, Mayer and Pearthree (2002) identified yellow, cyan, and green as the colors representing landscape change, and shades of magenta as representing no change. For a complete discussion of the change image analysis please see Mayer (this report), and Mayer and Pearthree, (2002). On the Jackrabbit Wash change image, yellow, green and blue colors appear along the probable path of inundation. Orange was also prominent along the wash and also appeared to represent change. Based on fieldwork, areas in orange appeared to be shallow inundation on vegetated terraces and were included within extent of inundation.

Field verification of the Landsat change image was conducted on July 16-17, 2001, and November 1-2, 2001. On July 16, 2001, Philip Pearthree, Larry Mayer, and Ann Youberg compared extent of flood inundation from the Landsat change image with evidence along Jackrabbit Wash at Vulture Mine Road (county gage site) and at the confluence with Star Wash. On July 17, 2001, Ted Lehman of JE Fuller joined us and we field checked flood inundation at several locations on Jackrabbit Wash upstream from Vulture Mine Road, and at the road crossing

on Dead Horse Wash. During the November field trip, Pearthree and Youberg mapped inundation and surficial geologic units along Jackrabbit Wash approximately 1 mile above and below Vulture Mine Road. Eighteen transects were traversed to map in detail extent of inundation and depth and character of flow.

Abundant evidence of inundation was left by the October 2000 flood. A ubiquitous clay layer, and locally fine flotsam (floating organic material), marked the edge of inundation in quieter waters (Figure 3). In some areas, deposits of sand, fine gravel, or larger flotsam marked the edge of inundation where flow broke out of steep, high banks. Approximate depth and character of flow was mapped based on evidence such as scouring and deposition, sand, gravel or boulder bar deposits, character of channels, bars and terraces, presence or absence of vegetation, size of flotsam, and height of vegetation/debris piles. Flow depths were broken into six categories; no flow, less than 20 cm, 20-50 cm, 0.5-1 m, 1-1.5 m, and greater than 1.5 m (Figure 4).

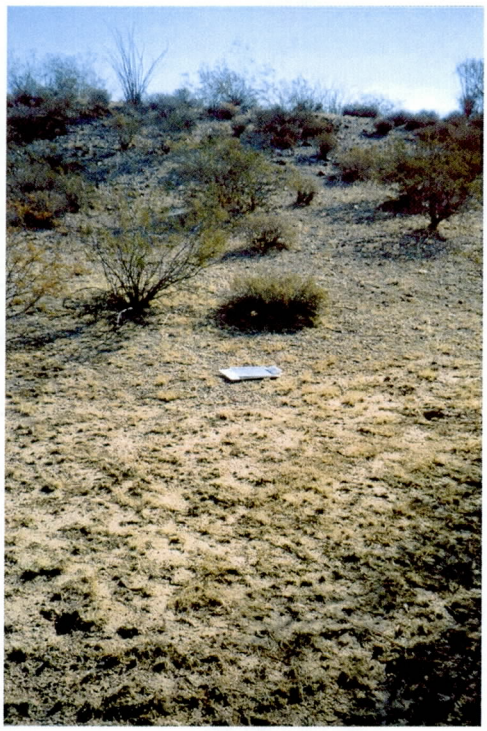

Figure 3. Fine clay deposits mark the extent of flood inundation. Notebook is above flood deposits.

Flow less than 20 cm was composed of shallow sheetflow on terraces or bars relatively high above the main channels. These areas had the lowest velocities as evidenced by clay deposits and very fine flotsam (Figure 5). Within these areas of shallow sheetflow, some isolated portions of

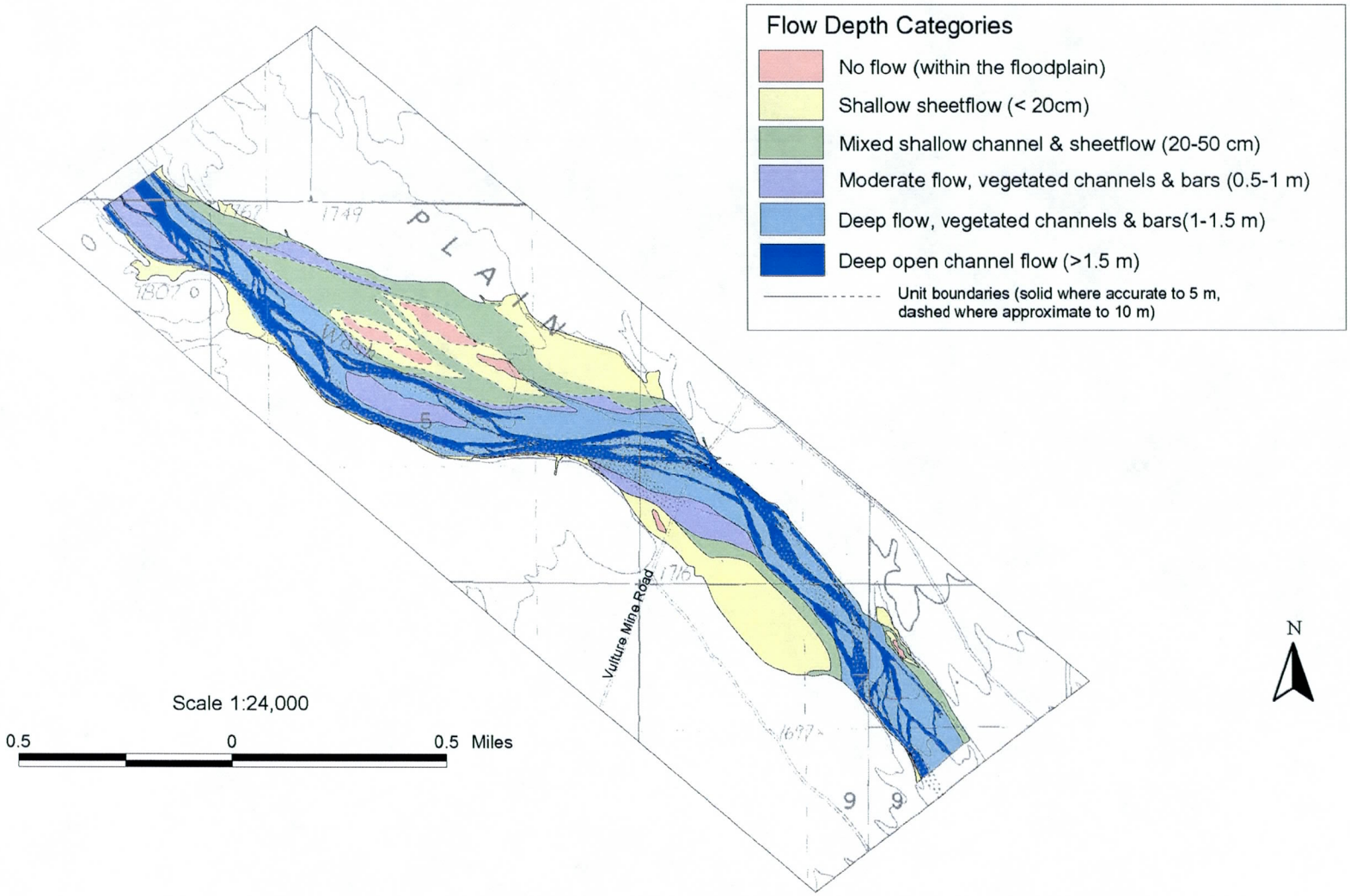

Figure 4. Approximate flow depths of October 2000 flood on Jackrabbit Wash at Vulture Mine Road

Figure 5. Fine Flotsam and clay deposits in areas with flow depths less than 20 cm.

the terraces were just high enough to avoid inundation. Flow depths of 20-50 cm were a mixture of shallow sheetflow and shallow channels, and involved some local scour and deposition (Figure 6). These areas typically were vegetated terraces closer to channels and slightly lower than the highest

Figure 6. Limited scouring and deposition in areas with flow depths from 20 to 50 cm.

terraces. Flow depths of 0.5-1 m were composed mainly of flow in shallow vegetated channels and bars, with some deeper sheetflow; there was evidence of substantial scour and deposition in these areas (Figure 7). Flow depths of 1-1.5 m were deep, high velocity flows over vegetated channels, bars and some lower overbank areas. In these areas, deposits typically were fairly thick (up to 1.5 m), and there was substantial disturbance, removal and deposition of vegetation (Figure 8). Flow depths greater than 1.5 m were composed of deep open channel flow. These areas have no to very little vegetation and received the deepest flows with the highest velocities (Figure 9).

Figure 7. Scouring and deposition in areas with flow depths from 0.5 to 1 m.

Figure 8. Vegetated channels and bars with flow depths from 1 m to 1.5 m.

Figure 9. Open channels with flow depths greater than 1.5 m.

Comparison of Landsat change image to field-based inundation mapping

Extent of flood inundation on Jackrabbit Wash, based on the satellite change image, reflects ground conditions very well with a few exceptions. The Landsat change image with flood extent for all of Jackrabbit Wash is shown on Plate 1. The following figures illustrate some of the findings from this study. In each of these figures, black lines represent extent of flooding based on the Landsat change image. White lines represent extent of flooding modified from the Landsat change image based on high-resolution TIFF images taken after the October 2000 flood and field data.

Three sets of figures compare inundation extent along Jackrabbit Wash. The first set of figures shows Jackrabbit Wash just upstream from the USGS gage (Figures 10a and 10b). In this area the wash is well entrenched and floodwaters were confined within steep, high banks. Both sets of lines representing extent of flooding are in good agreement.

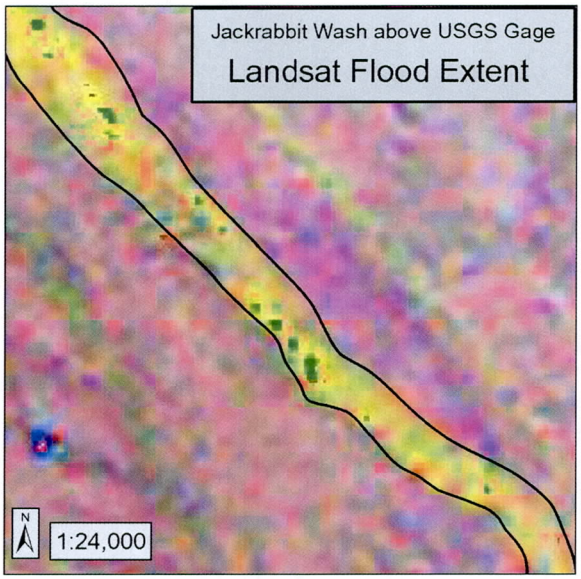

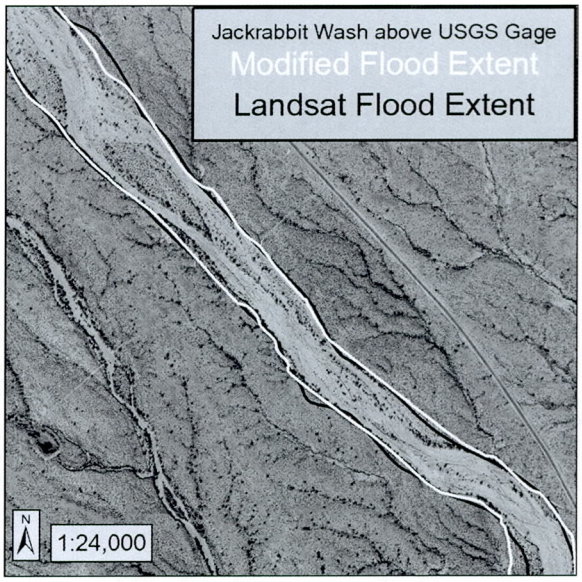

Figures 10a and 10b. Jackrabbit Wash just upstream from the USGS gage. Figure 10a shows flood extent based on the Landsat change image. Figure 3b shows modified (white line) flood extent from 2000 TIFF images. Scale 1:24000.

The second set of figures show the Vulture Mine Road crossing where we mapped in detail (Figures 11a and 11b). In general there is good correlation with the exception of a few areas where overbank flow occurred. Colors on the change image in these areas of discrepancy are variable and subject to interpretation. This may be a resolution issue or a training issue. A comparison of these images to the depth of flow (Figure 4) shows that the deepest flows are represented in yellow, while shallower flows are represented in orange, and a combination of orange and magenta. The dark green was identified by Mayer and Pearthree (2002) as increase in vegetation size or density after the flood. The dark blue or purple bands may also be vegetation or a combination of vegetation and sediment changes.

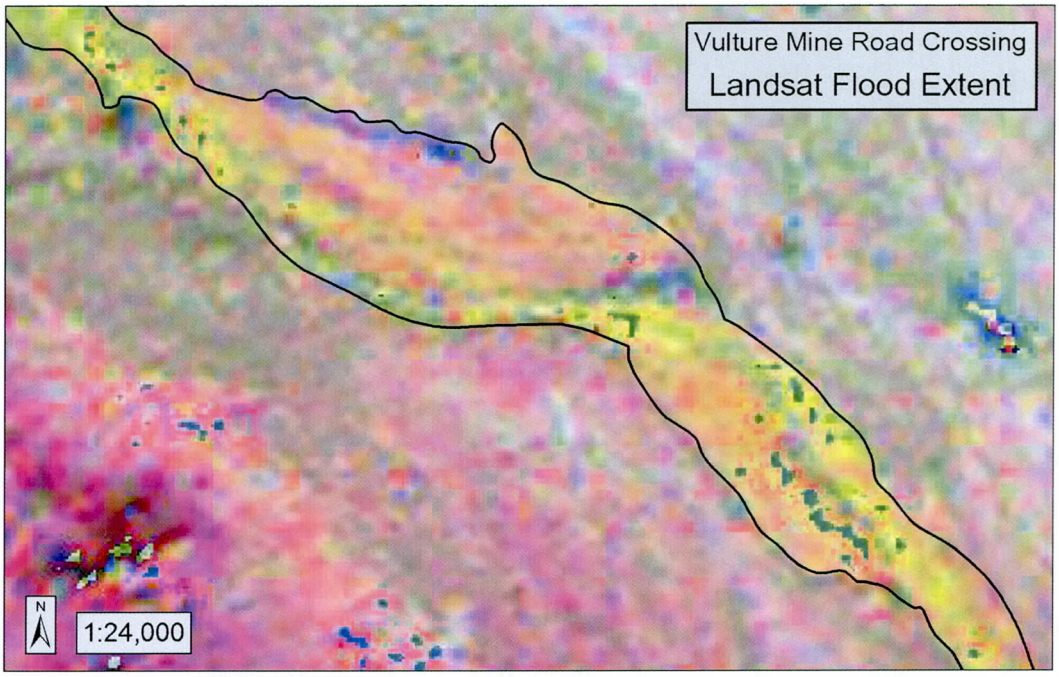

Figure 11a. Jackrabbit Wash at the Vulture Mine Road Crossing. Figure 11a shows flood extent based on Landsat change image. Scale 1:24000.

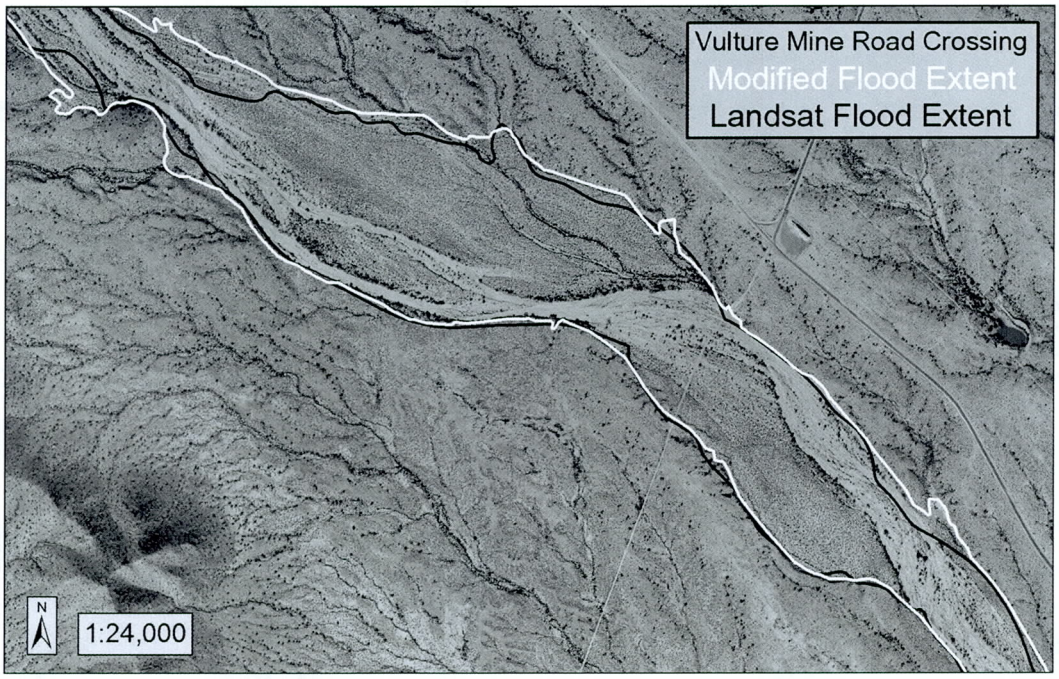

Figure 11b. Jackrabbit Wash at the Vulture Mine Road Crossing. Figure 11b shows modified flood extent (white line) from 2000 TIFF images. Scale 1:24000.

Dead Horse Wash is a major tributary to Jackrabbit Wash and accounts for a large portion of contributing area in the upper watershed (Figure 1). During fieldwork in July, evidence of the October 2000 flood was observed in Dead Horse Wash at the road crossing. Above the confluence of Jackrabbit and Dead Horse washes, the change image shows landscape changes along both channels but not as strongly as below the confluence. As contributing area increases, flow becomes deeper and the signature of landscape changes becomes stronger on the image. Conversely, near the headwaters of flow, the change signature will not be as strong. The third set of figures are from Dead Horse Wash, between the confluence with Jackrabbit Wash and the road crossing (Figure 12a and 12b). Although there is agreement between the two sets of lines, the black lines appear to be shifted south on the eastern half of this image. A review of the TIFF image shows the black lines from the change image miss the main channel and are located high on the southern ridge. There may be several explanations for this discrepancy, including a weaker signal, resolution of the image, and registration. Since the signal is not as strong above the confluence, extent of flooding is subject to greater interpretation. Resolution of Landsat images are 30 m pixels. The width of Dead Horse Wash floodplain varies from approximately three to eight pixels (100 to 250 m) so landscape changes may not be as evident. Flood extent based on the Landsat image appears to be shifted south of the TIFF image. This is probably due to registration problems. Overall, there is excellent agreement between the flood extents based on the change image and modified from photos, and field observations.

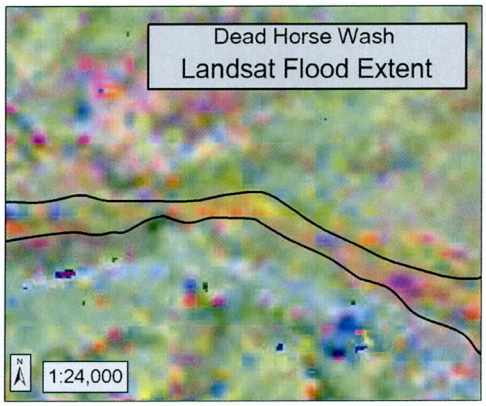

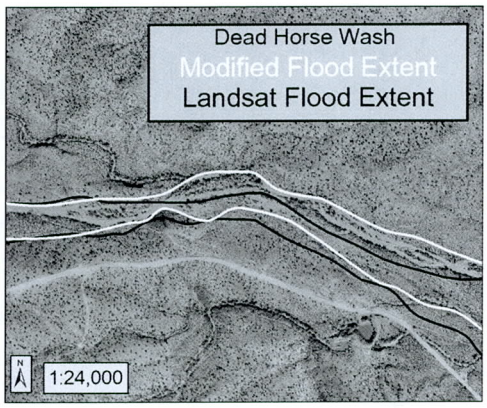

Figures 12a and 12b. Dead Horse Wash between the road crossing and the confluence with Jackrabbit Wash. Figure 12a shows flood extent based on Landsat change image. Figure 12b shows modified flood extent (white lines) from 2000 TIFF images. Scale 1:24000.

SURFICIAL GEOLOGIC FRAMEWORK OF JACKRABBIT WASH

Surficial geologic mapping provides information about the long-term behavior of fluvial systems. Alluvial deposits provide a record of the character and extent of fluvial activity. Surficial characteristics such as surface color, soil development, accumulation of calcium carbonate, development of desert varnish and desert pavement, drainage patterns and entrenchment, and local topography provide information about the age of the deposit.

Alluvial surfaces of similar age have a distinctive appearance and soil characteristics because they have undergone similar post-depositional modifications. Terraces and alluvial fans that are less than a few thousand years old still retain clear evidence of the original depositional topography, such as bars of gravel deposits, swales (troughlike depressions) where low flows passed between bars, and distributary channel networks, which are characteristic of active alluvial fans. Young alluvial surfaces have little rock varnish on surface clasts, little soil development,

and are minimally dissected. Very old fan surfaces, in contrast, have been isolated from substantial fluvial deposition or reworking for hundreds of thousands of years. These surfaces are characterized by strongly developed soils with clay- and calcium-carbonate-rich horizons, well-developed tributary stream networks that are entrenched below the fan surface, and where surfaces are well preserved, smooth, closely packed, strongly varnish desert pavements. The ages of alluvial surfaces in the southwestern United States may be roughly estimated based on these surface characteristics, especially soil development (Gile and others, 1981; Bull, 1991).

Surficial geology of Jackrabbit Wash above and below the Vulture Mine Road crossing was mapped using 1979 color aerial photographs (1:24,000), and high resolution, georeferenced digital black and white aerial photographs taken after the October 2000 flood and supplied by Maricopa County Flood Control District. Surficial units were identified during the November 2001 fieldwork; unit boundaries were delineated from the aerial photographs and images (Figure 13). Initial unit boundaries were based on 1979 aerial photos, then adjusted using the 2000 TIFF images. Physical characteristics of Quaternary alluvial surfaces (channels, alluvial fans, floodplains, stream terraces) evident on aerial photographs and in the field were used to differentiate their associated deposits by age.

Table 1. Selected properties of surficial geologic units in Jackrabbit Wash study area.

Unit	Drainage characteristics	Sedimentology	Surface topography	Soils
Qy_c modern channels	single thread and braided channels	very poorly sorted sand, gravel, cobbles and boulders	flat-bottomed channels, some low bars	depositional layering, essentially no soil development
Qy_2 bars and low terraces adjacent to channels	poorly defined, transitional and discontinuous small channels to moderately entrenched distributary channels	bars are coarse with poorly sorted sand, gravel, cobbles, and boulders; low terraces are finer-grained with mostly sand and gravel	undulating bar and swale topography to fairly smooth channel bottoms	depositional layering, no to very little soil development
Qy_1 higher terraces, typically not part of active system	moderately entrenched tributary channels, and small local channels and swales	generally finer-grained, poorly sorted silt, sand and gravel	undulating bars and swales to fairly smooth where silt and sand dominate	some soil structure, fine, open, unvarnished, gravel lags
Ql moderately old relict alluvial fans and terraces, not part of active system	local tributary channels slightly entrenched	poorly sorted gravels, cobbles and sand	bars and swales preserved on higher surfaces, lower terraces may be scoured	weak soil development, slight reddening, weakly varnish on gravel lags
Qm old relict alluvial fan deposits	local tributary channels slightly to moderately entrenched	poorly sorted gravels, cobbles, sand, and boulders	planar between channels and swales, rounded adjacent to entrenched drainages	moderately developed soil structure with reddened clay zones, carbonate cementation, well developed, darkly varnished desert pavements

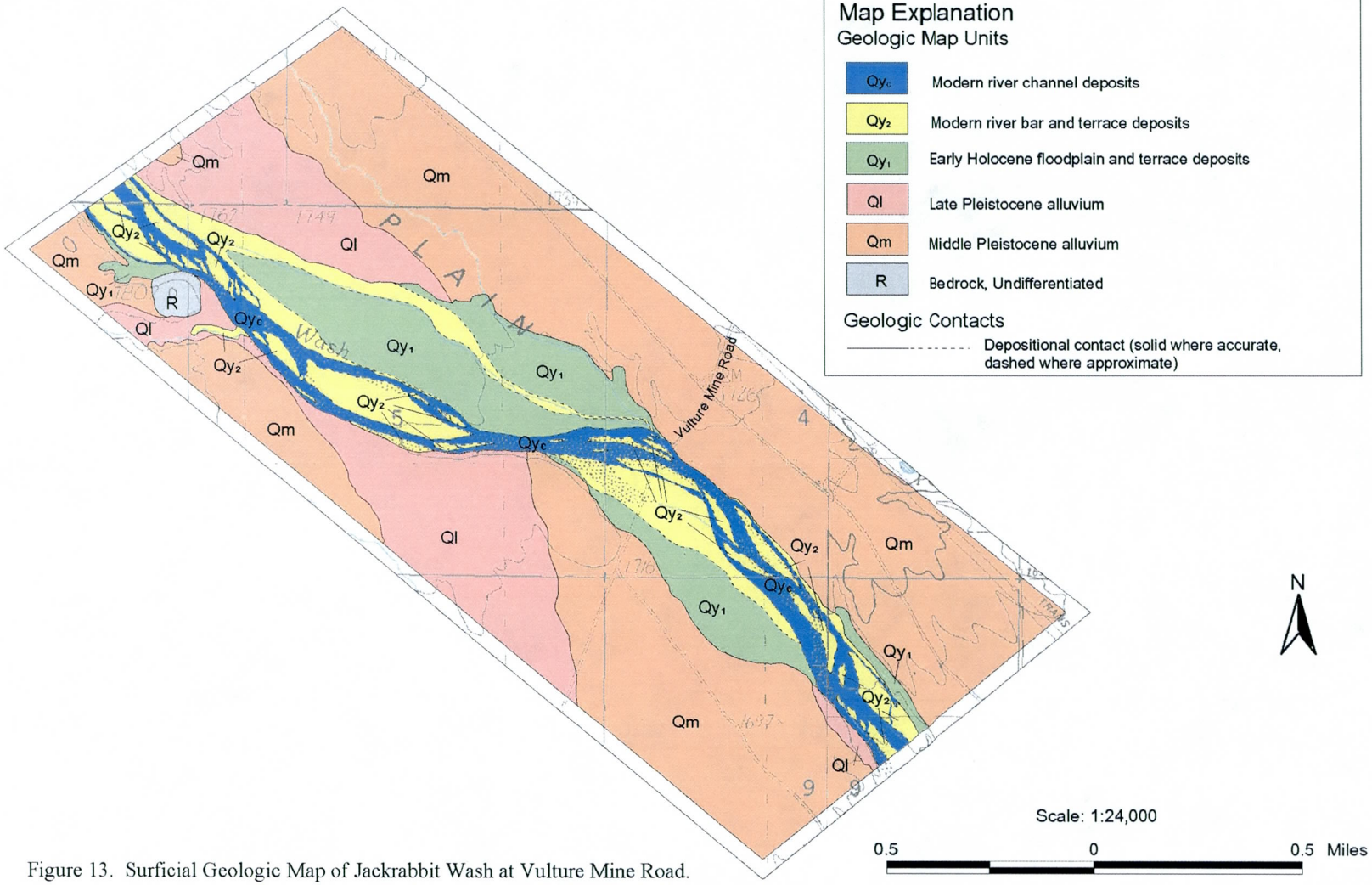

Figure 13. Surficial Geologic Map of Jackrabbit Wash at Vulture Mine Road.

Surficial Geologic Map Units

The surficial geologic map provides some insight into the long-term behavior of Jackrabbit Wash. Five surficial units were delineated and can be grouped into Holocene or Pleistocene ages. For a description of each unit please refer to Table 1. Holocene units are located within the geologic floodplain of Jackrabbit Wash and include channel deposits (Qy_c), bars and low terraces (Qy_2), and slightly higher terraces and bars (Qy_1). Units Qy_c and Qy_2 are part of the active alluvial system. Unit Qy_1 is older, slightly higher, and is probably not part of the active system during most flow events. The fact that Qy_1 surfaces were mostly inundated during the October 2000 flood attests to the relative size of this event. These units are inset below the oldest Pleistocene surface (Qm) by three to five meters.

Unit Qy_c consists of modern river channel deposits and correlates to the deep open channel flow unit of the flow depth map (Figures 4 and 9). Within the map area, channels are typically entrenched 0.5 to 2 m below adjacent bars and young terraces (unit Qy_2). These channels are extremely flood prone and are subject to deep, high velocity flow in moderate to large flood events. During the 2000 flood, flow was typically deeper than 1.5 meters. There is no to very little vegetation with the channels. Channel banks are unprotected and are subject to severe lateral erosion during floods.

Unit Qy_2 consists of vegetated bars, and low terraces adjacent to unit Qy_c. Bar deposits are typically coarser than terrace deposits. Unit Qy_2 correlates to several flow depth units. During the October 2000 flood, bars and terraces closest to the main channels experienced deep flow (1-1.5 m). The higher terraces or overbank areas were not as deeply inundated and experienced moderate flow depths (0.5-1 m) with shallow channel scouring and gravel bar deposition mixing and shallow sheetflow towards the outer edges (20-50 cm). Most of unit Qy_2 is vegetated but may be subject to deep flow during floods, with high velocities resulting in channel scouring, removal of vegetation, and gravel bar deposition (Figure 8). Banks are subject to severe lateral erosion during flooding. This unit appears to have been the most modified by the October 2000 flood.

Unit Qy_1 consists of early Holocene terrace and floodplain deposits found within the geologic floodplain of Jackrabbit Wash. Qy_1 surfaces are slightly higher and less subject to inundation than adjacent Qy_2 and Qy_c surfaces. During the October 2000 flood, inundated Qy_1 surfaces within the map area had mostly shallow sheetflow (<20 cm) with mixed shallow channel flow (20-50 cm) near larger incised channels. Clay and fine flotsam were deposited in areas of shallow sheetflow (Figure 5), while shallow scouring and fine-gravel bar deposition occurred where there was deeper flow (Figure 6). The surfaces of unit Qy_1 were relatively undisturbed, but channel change analyses indicate that Qy_1 terrace edges experience substantial local bank erosion. Qy_1 surfaces are vegetated and support mainly creosote bush. These areas of inundation typically appeared orange on the Landsat change image.

The Pleistocene units mapped in this area are above and outside of the geologic floodplain and have not been subject to deep inundation for thousands of years. Unit Ql consists of slightly to moderately dissected relict alluvial fans and terraces found approximate three to four meters above the active channels of Jackrabbit Wash. Floodwaters from the 2000 flood were generally confined below Ql surfaces, however, in some locations floodwaters flowed onto Ql surfaces (Figures 4 and 13). Inundated Ql surfaces typically had very shallow sheetflow and fine sediment deposition. Unit Qm consists of moderately to highly dissected relict alluvial fans and terraces with strong soil development. Qm surfaces are four to five meters above the active channels of Jackrabbit Wash. Within the map area, floodwaters did not inundate Qm surfaces. Ql and Qm surfaces form high steep banks. Both units experienced some minor bank erosion (Figures 14 and 15) in the map area, but changes were not large enough to map at this scale.

Figure 14. Scouring of late Pleistocene bank deposits. Surficial geologic unit Ql.

Figure 15. Scouring of mid-Pleistocene bank deposits. Surficial geologic unit Qm.

CHANNEL CHANGE ANALYSIS

A channel change analysis was conducted investigate how channels and floodplain areas changed over time, how the system responded to the October 2000 flood, and to relate surficial geologic units with potential erosion hazards. The same reach was studied as in the inundation and surficial geologic mapping components of this study. Aerial photographs from 4 different years were used to delineate areas of channels, bars and discontinuous or distributary channels, and overbank, or terrace, deposits. Resolution of the photographs varied, as did contrast. Black and white aerial photographs from 1953 (scale 1:60,000) were scanned at 1200 dpi. Color photographs from 1979 (scale 1:24,000) were scanned as black and white images at 600 dpi. All images were adjusted in Photoshop to equalize contrast. Aerial photos from 1998 and 2000 were provided by MCFCD. Images from 1998 had to be re-rectified using the Erdas Imagine program prior to analysis. Images from 2000 were very high resolution and georectified, which allowed for more detailed delineation of flow types as compared to 1953, 1979, or 1998.

Different flow areas were vectorized using ArcInfo and attributed in ArcView. The brightest, or lightest gray, areas were delineated as main channels (channels), medium or stippled gray areas as bars and discontinuous channels (bars), and dark gray areas as terraces or overbank deposits (overbank). Attribute tables were exported from ArcView into Excel to extract area information for each flow type. Total floodplain area did not change from year to year, as the limits of the geologic floodplain are defined by the extent of Holocene deposits and this did not change measurably through the period recorded by the photographs. Observable changes within the Holocene units included locations of channels and bars, extent of overbank areas, and the proportional area that each occupied. On the following figures, channels are shown as a stippled pattern, bars as horizontal lines, and overbank areas as vertical lines. All figures are shown at a scale of 1:24,000 unless otherwise noted.

Changes to channels, bars and overbank areas over time are evident in Figures 16 through 19, which show the extents of each flow type in each of the four years. A more detailed example of changes to flow areas is shown on Figure 20. There are several things to note on this figure. First, it illustrates quite well resolution differences between images from each year. This probably accounts for some flow area differences between years, particularly between channel and bar areas. Second, there are fewer bars within the channel in 1953. Bars increase and channel areas decrease in 1979. This trend continues based on 1998 photos, until 2000 when bars are scoured during the flood. Another point to note is the significant bank erosion that occurred between 1953 and 1979, shown at the north end of the double arrow. USGS gage data (Figure 21) show some flow events between these dates (USGS, 2002). Due to limited data and aerial photographs, it is not possible to determine during which event, or events, the erosion occurred. Erosion at this location, on the outside edge of a bend, is not unexpected. What is interesting is that further erosion does not seem to occur in this particular area in the following decades, including the 2000 flood.

A comparison of proportional flow areas (Figure 22) show channel areas were similar in 1953 and after the 2000 flood. Proportional flow areas in 1979 and 1998 are approximately the same with channel and overbank areas slightly less than those in 1953, and bar areas slightly greater. Although channel areas in 2000 are only slightly greater than 1953, overbank areas decreased from 1953 while bar areas increased. These trends and figures indicate that, in addition to the active fluvial system (surficial units Qy_c and Qy_2), major bank erosion also occurred along the edges of Qy_1. This is significant for floodplain managers as it shows that although Qy_1 deposits are not typically part of the active fluvial system, they are subject to flooding and bank erosion hazards.

This analysis at Vulture Mine Road did not identify Pleistocene bank erosion (units Ql and Qm) at a scale of 1:24,000. A comparison between 1979 and 2000 aerial photographs of the banks along Jackrabbit Wash, from the confluence with Star Wash upstream to the stock tank above the confluence with Dead Horse Wash, also did not indicate significant Pleistocene bank erosion. Based on field observations, some scouring of Pleistocene banks did occur during the flood (Figures 14 and 15). A larger scale comparison of the bank at the county gage (Figure 15) between 1979 and 2000 did not reveal significant erosion from the 2000 flood (Figure 23). Pleistocene surfaces are not part of the active alluvial system. Some Pleistocene surfaces adjacent to Jackrabbit Wash were slightly inundated, and scouring of Pleistocene banks did occur during this extreme event, however significant lateral erosion did not occur.

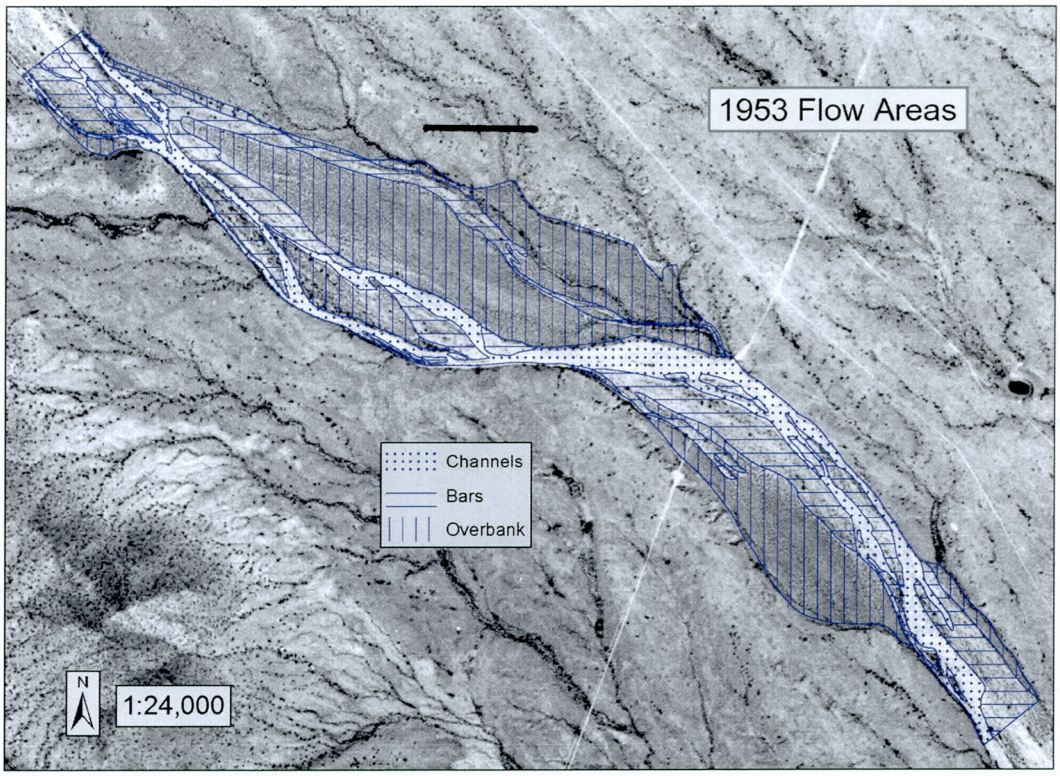

Figure 16. Delineated flow areas from 1953 aerial photographs, scanned and rectified. Jackrabbit Wash at Vulture Mine Road.

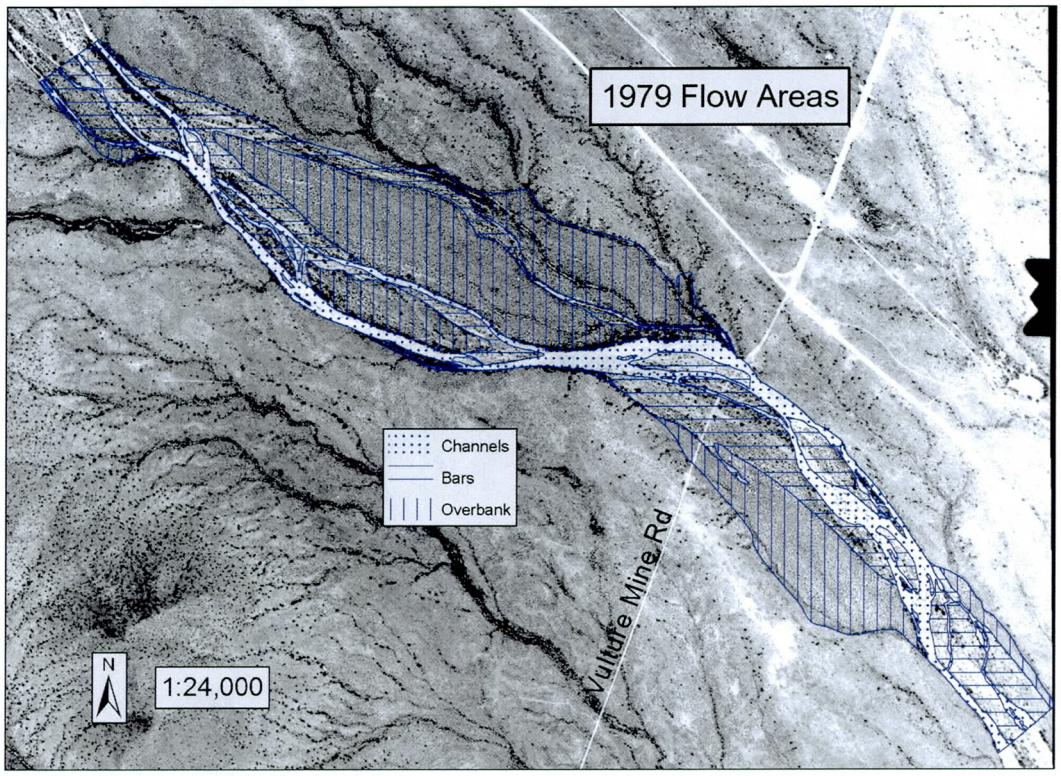

Figure 17. Delineated flow areas from 1979 aerial photographs, scanned and rectified. Jackrabbit Wash at Vulture Mine Road.

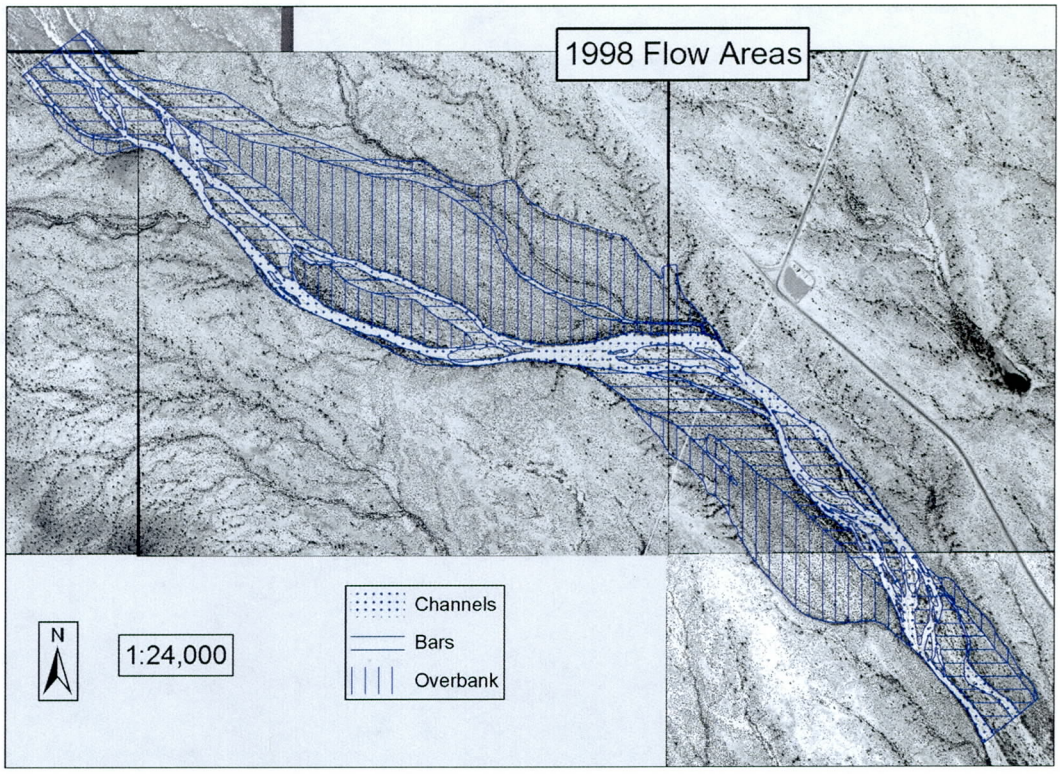

Figure 18. Delineated flow areas from 1998 TIFF images, re-rectified in ERDAS Imagine. Jackrabbit Wash at Vulture Mine Road.

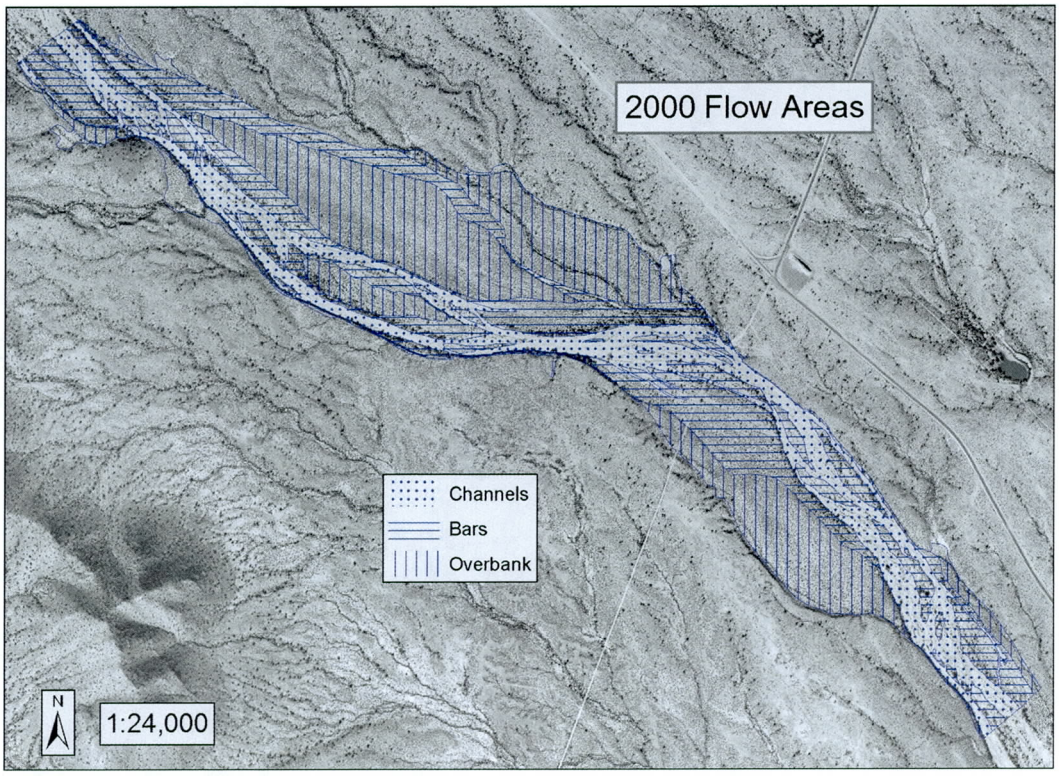

Figure 19. Delineated flow areas from high resolution, geo-rectified 2000 TIFF images. Jackrabbit Wash at Vulture Mine Road

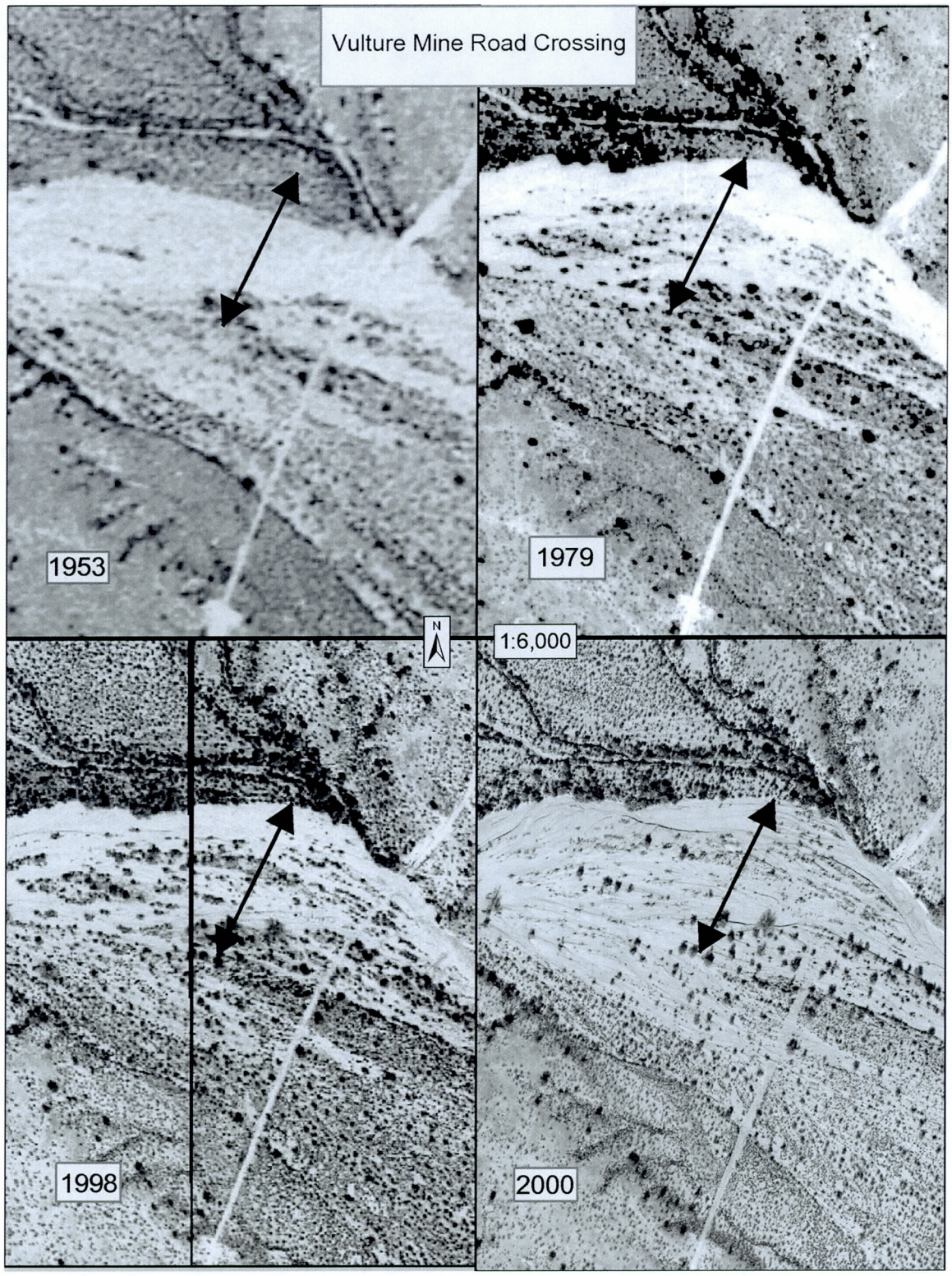

Figure20. Larger scale comparison of Jackrabbit Wash at Vulture Mine Road (light line in lower right corner of each photograph). The black double arrow is the same size, and in the same location, in each photo.

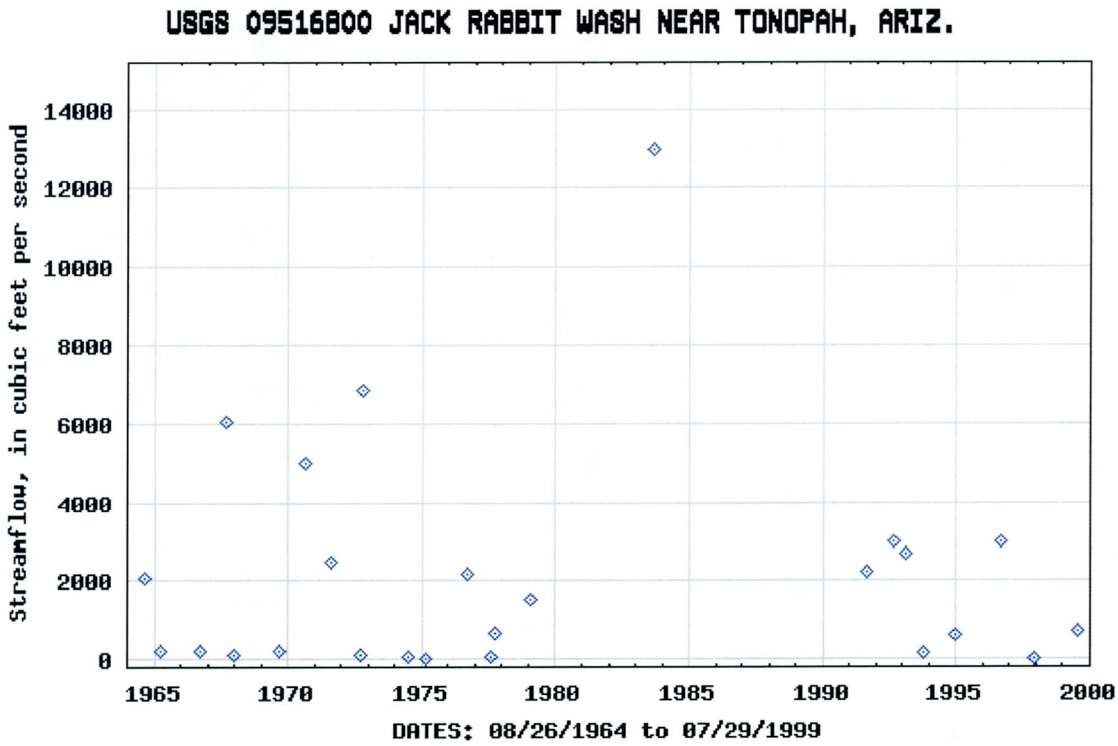

Figure 21. USGS gage peak streamflow data from Jackrabbit Wash. Data was not collected from late 1980 to 1990, with the exception of 1983 (from USGS, 2002).

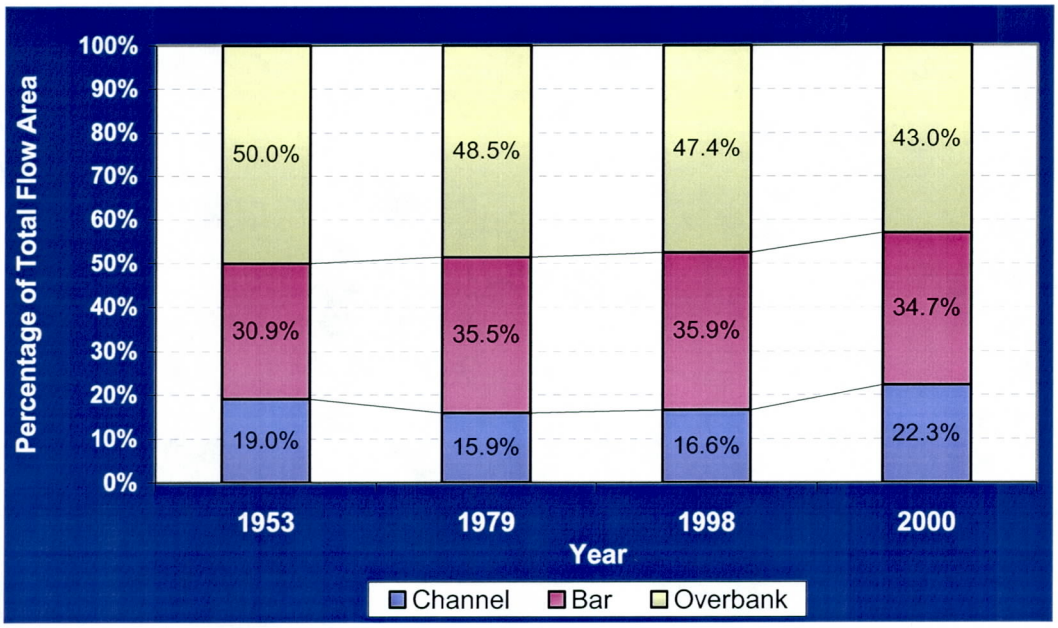

Figure 22. Proportional flow areas within Jackrabbit Wash floodplain at Vulture Mine Road.

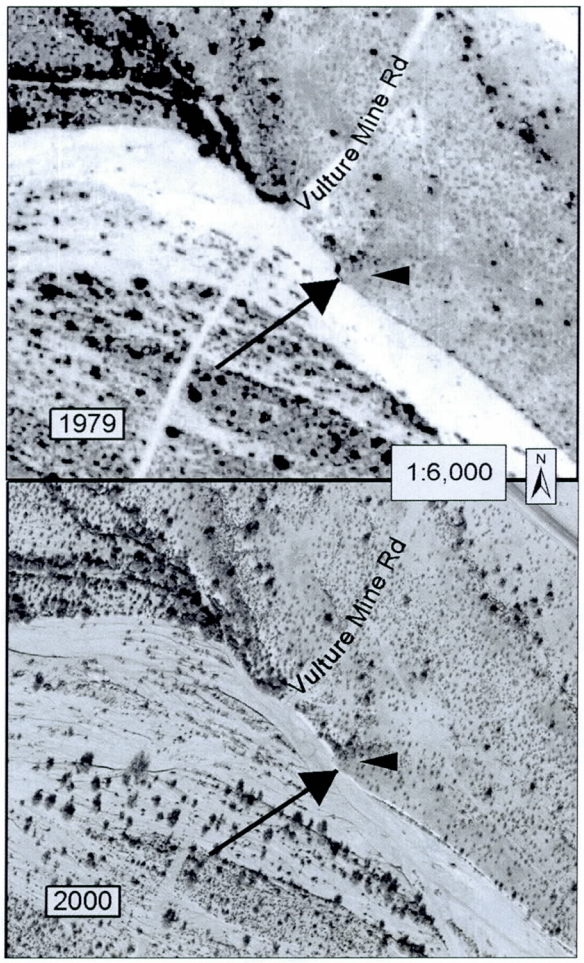

Figure 23. Larger scale (1:6,000) comparison of a mid-Pleistocene bank (surficial geologic unit Qm) at FCDMC gage (arrowhead) between 1979 and 2000. Black arrow is same size and in same location in each frame. Resolution of images from 1953 and 1998 prevented comparisons at this scale and location.

CONCLUSIONS

Geomorphologic investigations of Jackrabbit Wash following the large flood of October 2000 provide information on the extent and character of inundation in that flood, the usefulness of satellite change detection methods in delineating the extent of flood inundation, and the value of geologic and geomorphic information in delineating flood corridors. Reconnaissance field investigations were conducted at a number of sites along Jackrabbit Wash to evaluate the extent and character of inundation in the October 2000 flood. These observations were compared with the data derived from analysis of changes in satellite images from before and after the flood. The fit between the field observations and the extent of colors reflecting various kinds of changes was found to be very good, with the greatest uncertainties being in areas of very shallow inundation and less-than-perfect georectification of the satellite data. High-resolution, georectified aerial images provided by the FCDMC were used to improve the accuracy of the delineation of the extent of inundation along 25 miles of Jackrabbit Wash.

More detailed field investigations were conducted along a 2-mile-long reach of Jackrabbit Wash on either side of the Vulture Mine Road crossing. The extent and depth of inundation in the 2000 flood was mapped in detail, and inundation was subdivided into several depth categories ranging from very shallow flow up to deep channel flow. We found that colors on the satellite change image that are suggestive of change correlated very well with the overall extent of

inundation, and various colors on the satellite change image correlated fairly well with different flow depths. We mapped the surficial geology of this reach using pre-flood aerial photos and field observations. The distribution of Holocene channel and terrace deposits along Jackrabbit Wash defines the areas that have been subject to substantial erosion or deposition over the past few thousand years. Higher Pleistocene terraces provide the topographic constraints for this geologic floodplain. We found that nearly all of the geologic floodplain along this part of Jackrabbit Wash was inundated in the 2000 flood, and locally the youngest Pleistocene terraces were subject to very shallow inundation. The extent of inundation in the 2000 flood attests to the relatively extreme nature of this flood. Comparison of the size of the peak discharge in the 2000 flood on Jackrabbit Wash with floods from drainages of similar size in the lower Colorado River region also indicates that it was an extreme event. Analysis of historical aerial photos of this reach documented changes in the extent of channels, bars and terraces over the past 50 years or so. Channel areas were most extensive in 1953 and in late 2000, which suggests that Jackrabbit Wash experienced a large flood sometime shortly before 1953. Extensive changes in channel position and associated bank erosion occurred at the expense of Holocene bars and terraces through the historical record, but no detectable erosion into banks formed by Pleistocene deposits occurred during that interval.

ACKNOWLEDGEMENTS

Many people contributed to the development of this report. Funding for this research was provided by the Flood Control District of Maricopa County and the Arizona Geological Survey. The work was conducted in cooperation with JE Fuller Hydrology/Geomorphology and Larry Mayer. The FCDMC provided TIFF images from 1998 and 2000. Ted Lehman of JE Fuller and Larry Mayer provided field assistance and feedback.

REFERENECES

Arizona Department of Economic Security, 2001, July 1, 1997 to July 1, 2050 Arizona County Population Projections, in Population Statistics Projections, ADES Web Page.

Bull, W.B., 1991, Geomorphic Response to Climatic Change, New York: Oxford University Press, 326 p.

Enzel, Y., Ely, L.L., House, P.K., Baker, V.R., and Webb, R.H., 1993, Paleoflood evidence for a natural upper bound to flood magnitudes in the Colorado River Basin: Water Resour. Res., 29, 2287-2297.

Field, J.J., 1994a, Surficial processes on two fluvially dominated alluvial fans in Arizona: Arizona Geological Survey Open-File Report 94-12, 31 p.

Field, J.J., 1994b, Processes of channel migration on fluvially dominated alluvial fans in Arizona: Arizona Geological Survey Open-File Report 94-13, 40 p.

Field, J.J., and Pearthree, P.A., 1992, Geologic mapping of flood hazards in Arizona: An example from the White Tank Mountains area, Maricopa County: Arizona Geological Survey Open-File Report 91-10, 16 p, 4 plates, scale 1:24000.

Gile, L.H., Hawley, J.W., and Grossman, R.B., 1981, Soils and geomorphology in the basin and range area of southern New Mexico -- guidebook of the Desert Project: New Mexico Bureau of Mines and Mineral Resources Memoir 39, 222 p.

Hjalmarson, H.W., 1994, Potential flood hazards and hydraulic characteristics of distributary-flow areas in Maricopa County, Arizona: U.S. Geological Survey Water-Resources Investigations Report 93-4169, 56 p.

Hjalmarson, H.W., and Kemna, S.P., 1991, Flood hazards of distributary-flow areas in Southwestern Arizona: U.S. Geological Survey Water-Resources Investigations Report 91-4171, 58 p.

House, P.K., and Baker, V.R., 2001, Paleohydrology of flash floods in small desert watersheds in western Arizona: Water Resour. Res., 37, 1825-1839.

Klawon, J.E., and Pearthree, P.A., 2000, Field guide to a dynamic distributary system: Tiger Wash, Western Arizona: Arizona Geological Survey Open-File Report 00-01, 34 p.

Mayer, L., 2000, Satellite remote sensing of flood related landscape change resulting from hurricanes in Baja California and the southwestern United States, *in* Hassen, M. and others, eds, The Hydrology-Geomorphology Interface: Rainfall, Floods, Sedimentation, Land Use: International Association of Hydrological Sciences Publication 261, pp 201-214.

Mayer, L., and Pearthree, P.A., 2002, Mapping flood inundation in southwestern Arizona using Landsat TM data: a method for rapid regional flood assessment following large storms, *in* House, P.K. and others, eds., Ancient Floods, Modern Hazards: Principles and Applications of Paleoflood Hydrology, Water Science and Application Volume 5: Washington, DC, American Geophysical Union, pp 61-75.

Parker, J.T.C., 1995, Channel change and sediment transport in two desert streams in central Arizona, 1991-92: U.S. Geological Survey Water-Resources Investigations Report 95-4059, 42 p.

Pearthree, P.A., Demsey, K.A., Onken, J., Vincent, K.R., House, P.K., 1992, Geomorphic assessment of flood-prone areas on the southern piedmont of the Tortolita Mountains, Pima County, Arizona: Arizona Geological Survey Open File Report 91-11, 31 p, 4 sheets, scale 1:1,000.

Pope, G.L., Rigas, P.D., and Smith, C.F., 1998, Statistical summaries of streamflow data and characteristics of drainage basins for selected streamflow-gaging stations in Arizona through Water Year 1996: U.S. Geological Survey Water-Resources Investigations Report 98-4225, 907 p.

U.S. Geological Survey , 2001, Jack Rabbit Wash near Tonopah, Arizona, in Peak Streamflow for the Nation, Water Resources Data, National Water Information System Web Site (NWISWeb).

Waters, S.D., Perfrement, E.J., and Gardner, D.E., 2001, Storm report on the late August/October 2000 storms in the Centennial Wash and Wickenburg areas, in ALERT Publications, Flood Control District of Maricopa County, Arizona, FCDMC Web site.

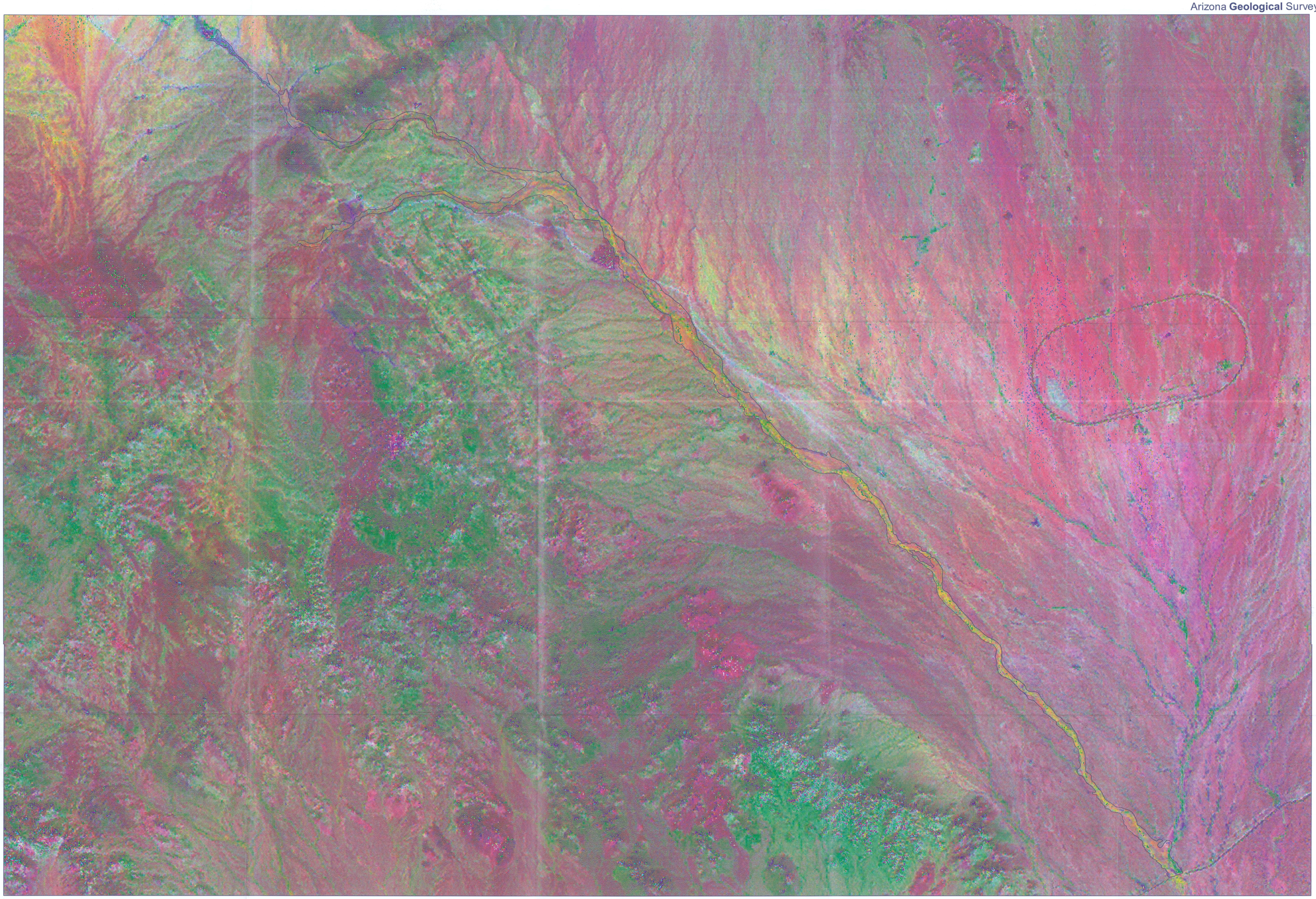

Arizona **Geological** Survey

Plate 1 - Landsat Change Image of Jackrabbit Wash, Western Maricopa County, Arizona

February, 2002

by

Ann Youberg, Philip A Pearthree

Landsat Change Image created by Larry Mayer

Map Explanation

Flood Extent Based on Landsat Change Image

N

0 4,800 9,600 19,200 28,800 38,400 Feet

APPENDIX D

FLDFRQ3 Input and Output

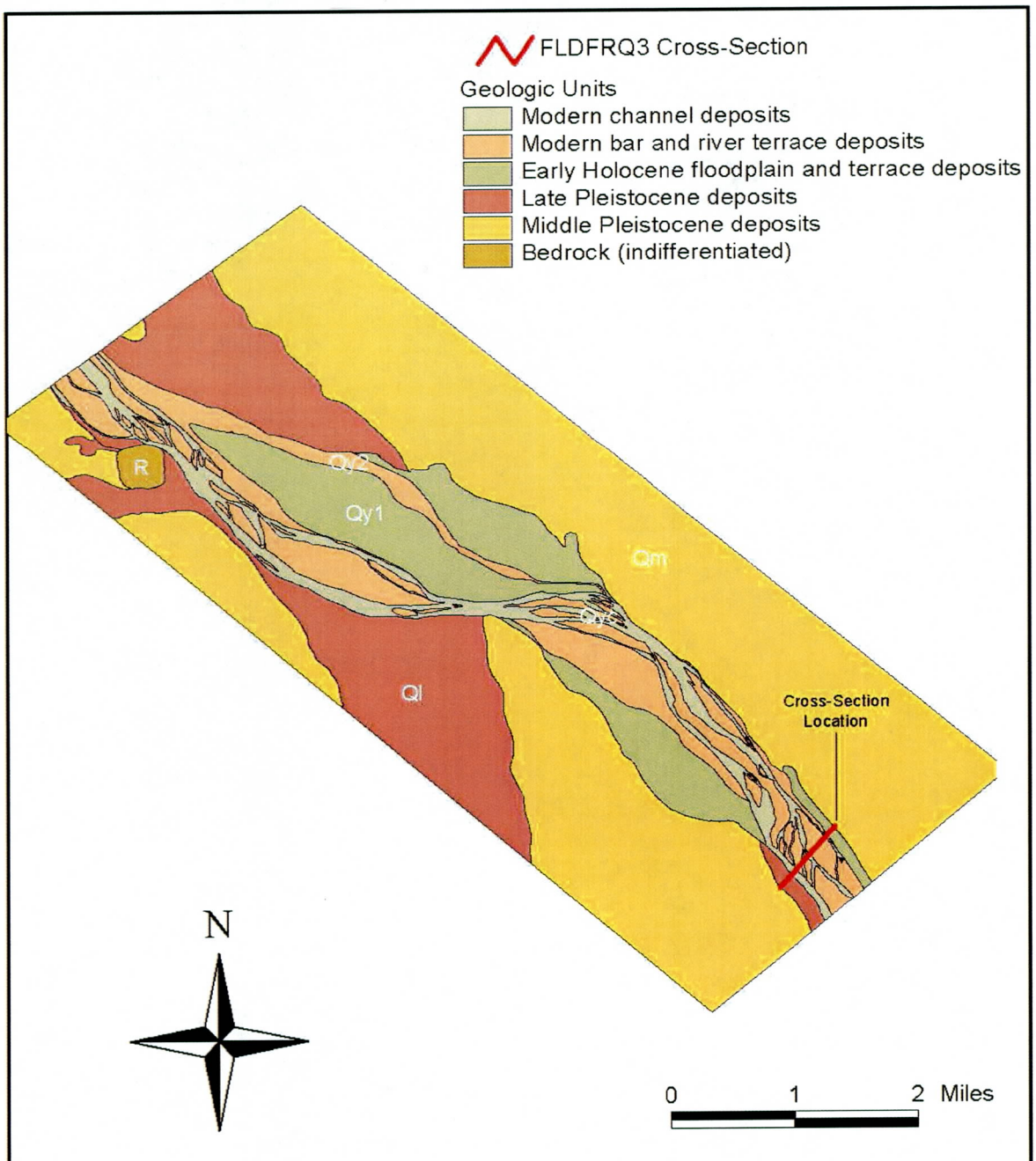

Location of Cross-Section Used to Determine Non-Exceedence Discharge Estimate for Ql Surface

Project Description	
Worksheet	100
Flow Element	Irregular Channel
Method	Manning's Formula
Solve For	Discharge

Section Data		
Mannings Coefficient	0.036	
Slope	0.007000	ft/ft
Water Surface Elevation	1,686.00	ft
Elevation Range	1,674.60 to 1,695.80	
Discharge	45,726.71	cfs

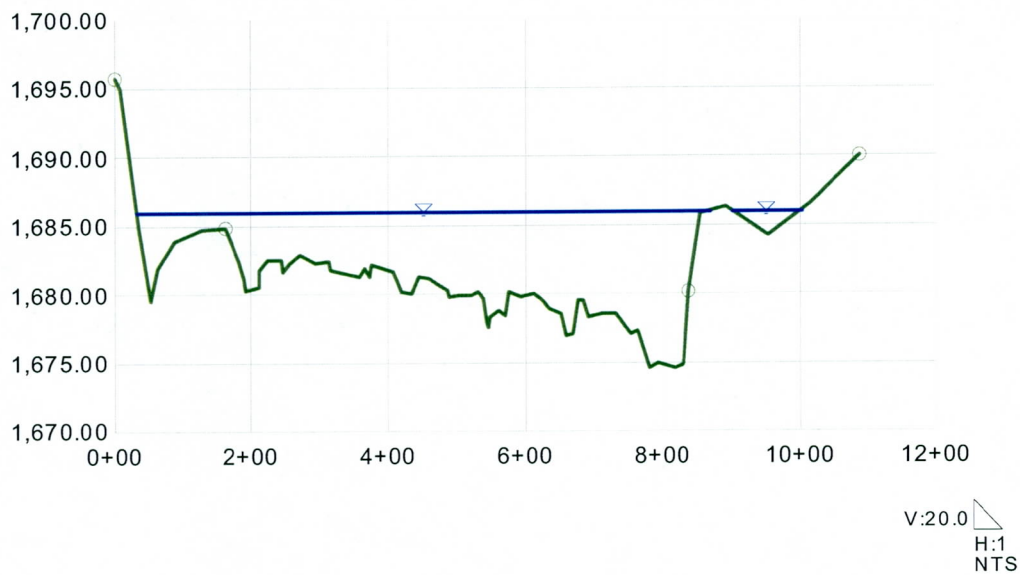

FlowMaster Output for Non-exceedence analysis – geometry data from FCDMC December 2000 survey of cross section 7.

Note: Small right overbank area not hydraulically connected to channel. It is a tributary to Jackrabbit Wash

FLDFRQ3 Input File: fcdmc.in

```
Systematic error threshold with fractional error below and above value, date datum
3000. 0.10 0.25 2001
Number of Systematic record followed by that many values
28
2070 1964
200 1965
200 1966
6040 1967
105 1967
200 1969
5000 1970
2500 1971
100 1972
6840 1972
75 1974
6 1975
2200 1976
80 1977
650 1977
1510 1979
13000 1983
2250 1991
2960 1992
2670 1993
191 1993
617 1994
3000 1996
9700 1997
34 1998
706 1999
180 2000
32400 2001
number of Nonexceedence thresholds followed by flow and duration info
1
34295.0 1.0 57159.0 1.0 45727.0 7500 12500 10000 0.8 'QI surface'
number of paleofloods followed by min, max, most likely, and fraction @ min-max
0
number of exceedence bounds (no upper limit) followed by flow information
0
run mode, frequency function, df, initial distribution parameters
2    7         100.0    0. 0. 0.
number of return periods to calculate probability regions
6
list of returns periods
5.0 10.0 50.0 100.0 500.0 427350.
number of peak discharges to estimate annual probability regions
6
list of peak discharges
13000. 17736. 25074. 27000. 32400. 45700.
nnm, tfac, rt, eps, ns, nt, maxevl, seed1, seed2
2   5.0  0.8 1e-8  20  50   0    1    2
maxit, ratio, nv[3], nprobs
400000  1e-7   4 60 60 5
probs
0.025 0.16 0.50 0.84 0.975
spreadsheet output file
fcd_lp3.out
bfile
fcd_lp3.bin
```

FLDFRQ3 Primary Output File: fcdmc.out

Systematic record error peak discharge threshold = 3000.000000
Fractional 2 sigma error below 3000.000000 = 0.100000
Fractional 2 sigma error above 3000.000000 = 0.250000

Date Datum = 2001
Number of systematic peak discharges = 28
Sorted Peak Discharge Observations

Year,	-2*sigma,	Observed,	+2sigma
1975	5.400	6.000	6.600
1998	30.600	34.000	37.400
1974	67.500	75.000	82.500
1977	72.000	80.000	88.000
1972	90.000	100.000	110.000
1967	94.500	105.000	115.500
2000	162.000	180.000	198.000
1993	171.900	191.000	210.100
1969	180.000	200.000	220.000
1965	180.000	200.000	220.000
1966	180.000	200.000	220.000
1994	555.300	617.000	678.700
1977	585.000	650.000	715.000
1999	635.400	706.000	776.600
1979	1359.000	1510.000	1661.000
1964	1863.000	2070.000	2277.000
1976	1980.000	2200.000	2420.000
1991	2025.000	2250.000	2475.000
1971	2250.000	2500.000	2750.000
1993	2403.000	2670.000	2937.000
1992	2664.000	2960.000	3256.000
1996	2250.000	3000.000	3750.000
1970	3750.000	5000.000	6250.000
1967	4530.000	6040.000	7550.000
1972	5130.000	6840.000	8550.000
1997	7275.000	9700.000	12125.000
1983	9750.000	13000.000	16250.000
2001	24300.000	32400.000	40500.000

Number of Nonexceedence Discharge Bounds = 1

low	prob	high	prob	mlh b	low y	high y	mlh y	eprob
34295.00	1.000	57159.00	1.000	45727.00	7500	12500	10000	0.8

Number of Non-Gaussian peak discharges = 0

Number of Exceedence bounds = 0

Option = (0) Print input and plotting positions.

Option = (1) Also calculate MLH model.

Option = (2) Also calculate probability regions with grid integration.

You have selected distribution number 7 which corresponds
to a Log Base 10 Pearson type III frequency distribution

Discrete peak discharge integration interval (df) = 100.000000

Starting Log Base 10 Pearson type III parameters are
m = 0.000000, s = 0.000000, g = 0.000000

Number of return periods to calculate estimates = 6
List of return periods and associated annual probabilities
Return Period = 5.000000, Annual Probability = 0.200000
Return Period = 10.000000, Annual Probability = 0.100000
Return Period = 50.000000, Annual Probability = 0.020000
Return Period = 100.000000, Annual Probability = 0.010000
Return Period = 500.000000, Annual Probability = 0.002000
Return Period = 427350.000000, Annual Probability = 0.000002

number of peak discharges to estimate annual probabilities for = 6
List of peak discharges
Peak discharge = 13000.000000
Peak discharge = 17736.000000
Peak discharge = 25074.000000
Peak discharge = 27000.000000
Peak discharge = 32400.000000
Peak discharge = 45700.000000

Nelder Mead parameters
Total number of Nelder Mead optimizations =2

Simulated annealing parameters
Initial misfit multiplier to produce the starting temperature = 5.000000
Temperature reduction factor(RT) = 0.800000
Convergence criteria (EPS) = 0.000000
Number of cycles before step length is adjusted (NS) = 20
Number of iterations before temperature reduction (NT) = 50
Maximum number of function evaluations (MAXEVL) = 0
Randum number generator seeds (ISEED1 and ISEED2) = 1, 2

Grid integration parameters
Maximum number of grid points = 400000
Likelilood ratio for grid trunctionation = 0.000000
MLH parameter divisors for integration steps = 4.000000 60.000000 60.000000
Number of probabilities levels = 5

Requested Probability Levels
0.025000
0.160000
0.500000
0.840000
0.975000

Binary grid integration output file path
fcd_lp3.bin

i = 0 noseey = 10000.000000 noseeyc = 10000.000000

Observed Data Plotting Positions

Peak Discharge	Weibull	Median	Cunnane	Hazen	
a =	(0.00)	(0.32)	(0.40)	(0.50)	
32400.00	0.0344828	0.0240613	0.0212766	0.0178571	0 27
13000.00	0.0689655	0.0593161	0.0567376	0.0535714	0 26
9700.00	0.1034483	0.0945708	0.0921986	0.0892857	0 25
6840.00	0.1379310	0.1298255	0.1276596	0.1250000	0 24
6040.00	0.1724138	0.1650802	0.1631206	0.1607143	0 23
5000.00	0.2068966	0.2003349	0.1985816	0.1964286	0 22
3000.00	0.2413793	0.2355896	0.2340426	0.2321429	0 21
2960.00	0.2758621	0.2708444	0.2695035	0.2678571	0 20
2670.00	0.3103448	0.3060991	0.3049645	0.3035714	0 19
2500.00	0.3448276	0.3413538	0.3404255	0.3392857	0 18
2250.00	0.3793103	0.3766085	0.3758865	0.3750000	0 17

2200.00	0.4137931	0.4118632	0.4113475	0.4107143	0 16
2070.00	0.4482759	0.4471179	0.4468085	0.4464286	0 15
1510.00	0.4827586	0.4823726	0.4822695	0.4821429	0 14
706.00	0.5172414	0.5176274	0.5177305	0.5178571	0 13
650.00	0.5517241	0.5528821	0.5531915	0.5535714	0 12
617.00	0.5862069	0.5881368	0.5886525	0.5892857	0 11
200.00	0.6206897	0.6233915	0.6241135	0.6250000	0 9
200.00	0.6551724	0.6586462	0.6595745	0.6607143	0 10
200.00	0.6896552	0.6939009	0.6950355	0.6964286	0 8
191.00	0.7241379	0.7291556	0.7304965	0.7321429	0 7
180.00	0.7586207	0.7644104	0.7659574	0.7678571	0 6
105.00	0.7931034	0.7996651	0.8014184	0.8035714	0 5
100.00	0.8275862	0.8349198	0.8368794	0.8392857	0 4
80.00	0.8620690	0.8701745	0.8723404	0.8750000	0 3
75.00	0.8965517	0.9054292	0.9078014	0.9107143	0 2
34.00	0.9310345	0.9406839	0.9432624	0.9464286	0 1
6.00	0.9655172	0.9759387	0.9787234	0.9821429	0 0

Estimated L-moments = 2.888897 0.509062 -0.067249

L-moments (modified for distribution)
initial parameter estimates = 2.888897 0.907087 -0.883019

Initial misfit = 130.830934

Nelder misfit =120.529531 after 142 iterations for pass 1

Log Base 10 Pearson type III Solution parameters for pass 1 are
m = 2.989364, s = 0.737444, g = -0.833928

Nelder misfit =120.529531 after 129 iterations for pass 2

Log Base 10 Pearson type III Solution parameters for pass 2 are
m = 2.989353, s = 0.737439, g = -0.833917

Quantile Estimates

Return Period,	Probability,	Peak Discharge
5	0.20000000	4171.25
10	0.10000000	6989.28
50	0.02000000	14434.39
100	0.01000000	17736.09
500	0.00200000	25073.66
427350	0.00000234	45701.88

Peak Discharge Frequency Estimates

Peak Discharge,	Probability,	Return Period
13000.00	0.02701896	37
17736.00	0.01000019	100
25074.00	0.00199985	500
27000.00	0.00127145	787
32400.00	0.00031927	3132
45700.00	0.00000234	426923

Predicted Versus Observed Flood Frequency
Using the Weibull Plotting Position
Probability Plot Correlation Coefficient = 0.930758

Observed	Calculated	Residual	Normalized Residual
32400.00	11843.42	20556.58	3.100
13000.00	8632.07	4367.93	2.687
9700.00	6843.21	2856.79	2.354
6840.00	5634.69	1205.31	1.408

6040.00	4741.02	1298.98	1.717
5000.00	4044.13	955.87	1.526
3000.00	3481.30	-481.30	-1.282
2960.00	3015.32	-55.32	-0.328
2670.00	2622.36	47.64	0.414
2500.00	2286.27	213.73	1.670
2250.00	1995.62	254.38	2.195
2200.00	1742.03	457.97	3.100
2070.00	1519.20	550.80	3.100
1510.00	1322.28	187.72	2.163
706.00	1147.47	-441.47	-3.100
650.00	991.70	-341.70	-3.100
617.00	852.54	-235.54	-3.100
200.00	727.97	-527.97	-3.100
200.00	616.32	-416.32	-3.100
200.00	516.21	-316.21	-3.100
191.00	426.49	-235.49	-3.100
180.00	346.20	-166.20	-3.100
105.00	274.52	-169.52	-3.100
100.00	210.80	-110.80	-3.100
80.00	154.52	-74.52	-3.100
75.00	105.27	-30.27	-3.100
34.00	62.87	-28.87	-3.100
6.00	27.41	-21.41	-3.100

Predicted Versus Observed Flood Frequency
Using the Median Plotting Position
Probability Plot Correlation Coefficient = 0.947055

Observed	Calculated	Residual	Normalized Residual
32400.00	13552.14	18847.86	3.100
13000.00	9317.05	3682.95	2.266
9700.00	7231.31	2468.69	2.035
6840.00	5884.19	955.81	1.117
6040.00	4911.76	1128.24	1.493
5000.00	4164.95	835.05	1.334
3000.00	3568.23	-568.23	-1.510
2960.00	3078.12	-118.12	-0.783
2670.00	2667.40	2.60	0.264
2500.00	2317.91	182.09	1.430
2250.00	2016.96	233.04	1.928
2200.00	1755.36	444.64	3.100
2070.00	1526.24	543.76	3.100
1510.00	1324.36	185.64	2.131
706.00	1145.62	-439.62	-3.100
650.00	986.77	-336.77	-3.100
617.00	845.20	-228.20	-3.100
200.00	718.77	-518.77	-3.100
200.00	605.73	-405.73	-3.100
200.00	504.62	-304.62	-3.100
191.00	414.24	-223.24	-3.100
180.00	333.58	-153.58	-3.100
105.00	261.80	-156.80	-3.100
100.00	198.23	-98.23	-3.100
80.00	142.32	-62.32	-3.100
75.00	93.70	-18.70	-3.100
34.00	52.23	-18.23	-3.100
6.00	18.16	-12.16	-3.100

Predicted Versus Observed Flood Frequency
Using the Cunnane Plotting Position
Probability Plot Correlation Coefficient = 0.952000

Observed	Calculated	Residual	Normalized Residual

32400.00	14138.95	18261.05	3.100
13000.00	9520.71	3479.29	2.141
9700.00	7342.06	2357.94	1.943
6840.00	5953.99	886.01	1.035
6040.00	4958.96	1081.04	1.429
5000.00	4198.09	801.91	1.283
3000.00	3591.93	-591.93	-1.576
2960.00	3095.17	-135.17	-0.880
2670.00	2679.59	-9.59	-0.208
2500.00	2326.44	173.56	1.357
2250.00	2022.70	227.30	1.862
2200.00	1758.93	441.07	3.100
2070.00	1528.13	541.87	3.100
1510.00	1324.91	185.09	2.123
706.00	1145.13	-439.13	-3.100
650.00	985.46	-335.46	-3.100
617.00	843.25	-226.25	-3.100
200.00	716.33	-516.33	-3.100
200.00	602.92	-402.92	-3.100
200.00	501.55	-301.55	-3.100
191.00	411.00	-220.00	-3.100
180.00	330.25	-150.25	-3.100
105.00	258.45	-153.45	-3.100
100.00	194.92	-94.92	-3.100
80.00	139.12	-59.12	-3.100
75.00	90.69	-15.69	-3.100
34.00	49.48	-15.48	-3.100
6.00	15.81	-9.81	-3.100

Predicted Versus Observed Flood Frequency
Using the Hazen Plotting Position
Probability Plot Correlation Coefficient = 0.958511

Observed	Calculated	Residual	Normalized Residual
32400.00	14975.66	17424.34	3.100
13000.00	9784.89	3215.11	1.978
9700.00	7482.54	2217.46	1.828
6840.00	6041.63	798.37	0.933
6040.00	5017.88	1022.12	1.352
5000.00	4239.29	760.71	1.216
3000.00	3621.32	-621.32	-1.651
2960.00	3116.26	-156.26	-1.011
2670.00	2694.63	-24.63	-0.106
2500.00	2336.97	163.03	1.271
2250.00	2029.77	220.23	1.787
2200.00	1763.34	436.66	3.100
2070.00	1530.44	539.56	3.100
1510.00	1325.60	184.40	2.113
706.00	1144.52	-438.52	-3.100
650.00	983.85	-333.85	-3.100
617.00	840.85	-223.85	-3.100
200.00	713.33	-513.33	-3.100
200.00	599.48	-399.48	-3.100
200.00	497.80	-297.80	-3.100
191.00	407.04	-216.04	-3.100
180.00	326.18	-146.18	-3.100
105.00	254.37	-149.37	-3.100
100.00	190.90	-90.90	-3.100
80.00	135.24	-55.24	-3.100
75.00	87.03	-12.03	-3.100
34.00	46.15	-12.15	-3.100
6.00	13.01	-7.01	-3.100

Integration grid step = 0.747338 for parameter 1

Integration grid step = 0.012291 for parameter 2

Integration grid step = 0.013899 for parameter 3

Finished m = 2.989353

Finished m = 2.242015

Probability Region Estimates
Likelihoods were calculated for a total of 329
Log Base 10 Pearson type III models

Parameter quantiles for the Log Base 10 Pearson type III

Quantiles for m

Probability	Value
0.025000	2.98935
0.160000	2.98935
0.500000	2.98935
0.840000	2.98935
0.975000	2.98935

Quantiles for s

Probability	Value
0.025000	0.737439
0.160000	0.737439
0.500000	0.76202
0.840000	0.798892
0.975000	0.835764

Quantiles for g

Probability	Value
0.025000	-0.931207
0.160000	-0.889511
0.500000	-0.833917
0.840000	-0.792221
0.975000	-0.750525

Peak Discharge Quantiles for a return period of 5.000000

Probability	Value
0.025000	2812.5
0.160000	4175.43
0.500000	4375.59
0.840000	4675.54
0.975000	5003.21

Peak Discharge Quantiles for a return period of 10.000000

Probability	Value
0.025000	5509.96
0.160000	7075.03
0.500000	7424.57
0.840000	8037.74
0.975000	8720.95

Peak Discharge Quantiles for a return period of 50.000000

Probability	Value
0.025000	14174.4
0.160000	14867.2
0.500000	15786.1

0.840000 17034.3
0.975000 18342.3

Peak Discharge Quantiles for a return period of 100.000000
Probability Value
0.025000 17689.2
0.160000 18340.6
0.500000 19503.8
0.840000 21123.2
0.975000 22761.6

Peak Discharge Quantiles for a return period of 500.000000
Probability Value
0.025000 25055.1
0.160000 26309.9
0.500000 27953.7
0.840000 30211.3
0.975000 31979.7

Peak Discharge Quantiles for a return period of 427350.000000
Probability Value
0.025000 45417.5
0.160000 47720.7
0.500000 50806.7
0.840000 56517.8
0.975000 65058.1

Annual Probability Quantiles for a Peak Discharge of 13000.000000
Probability Value
0.025000 0.0248796
0.160000 0.0291318
0.500000 0.0334225
0.840000 0.0405825
0.975000 0.0481828

Annual Probability Quantiles for a Peak Discharge of 17736.000000
Probability Value
0.025000 0.00993811
0.160000 0.0112825
0.500000 0.013936
0.840000 0.017711
0.975000 0.022005

Annual Probability Quantiles for a Peak Discharge of 25074.000000
Probability Value
0.025000 0.00199416
0.160000 0.00261159
0.500000 0.00359217
0.840000 0.00499764
0.975000 0.00679282

Annual Probability Quantiles for a Peak Discharge of 27000.000000
Probability Value
0.025000 0.0012692
0.160000 0.00175003
0.500000 0.0024442
0.840000 0.00362685
0.975000 0.00486513

Annual Probability Quantiles for a Peak Discharge of 32400.000000
Probability Value
0.025000 0.00031388

0.160000 0.000489135
0.500000 0.00079037
0.840000 0.0013224
0.975000 0.00186255

Annual Probability Quantiles for a Peak Discharge of 45700.000000
Probability Value
0.025000 2.13542e-006
0.160000 6.28667e-006
0.500000 2.19432e-005
0.840000 6.97554e-005
0.975000 0.00017349

i = 0 npg = 2 val = 1.000000

Grid elements for parameter 1 = 2.000000

i = 1 npg = 29 val = 2.000000

Grid elements for parameter 2 = 14.500000

i = 2 npg = 329 val = 58.000000

Grid elements for parameter 3 = 5.672414

The spreadsheet file fcd_lp3.out
contains a total of 39 columns

APPENDIX E

CD-ROM containing –
HEC-1 models for October 2000 storms
and other digital data from this study